



University of West Bohemia in Pilsen
Faculty of Education
Department of Mathematics, Physics and Technical Education

The physical properties of membranes for fuel cells in teaching in basic university course

Ph.D. THESIS

I declare that the thesis developed independently
using specified literature and information sources.

In Pilsen

.....
signature

For excellent leadership, endless patience and valuable advice in preparing this thesis I thank my supervisor Dr. Jagan Moha Dodda, PhD. I would also like to thank and acknowledge all colleagues from the Engineering of Special Materials at New technologies Research Centre and from the Department of General Physics for their willingness and friendship. This work would also not arise without the support of my family.

Annotation

The primary goal of thesis is to summarize current knowledge about renewable energy sources, especially fuel cells, which will be used in teaching. This topic must be sufficiently detailed and clear at the same time. It must comply with the requirements for topic by teachers and by students as well. The task is therefore to submit the findings of theoretical description of membranes for fuel cells so that they are useful in teaching and also to prepare a study material for those among students who are interested in this topic. The secondary aim is to create a laboratory exercise for physical practicum where students shall investigate properties of polymer membranes for fuel cells using the latest instruments in research centres. These measurements must be easy to understand and must be easily performable by the students themselves. Another objective of this work is to collect knowledge about renewable energy sources from student using a questionnaire survey, which will be later to use result to prepare laboratory tasks and study materials. Another goal of this work is preparation of new composite membranes for fuel cells. The achieved results will be published in impact journals and conference proceedings.

Key words

Fuel cells, membranes, composite, Nafion, polyvinyl alcohol, pedagogy, motivation

Anotace

Hlavním cílem práce je zpracování současného poznání o obnovitelných zdrojích energie, speciálně o palivových článcích, do celku, který bude použitelný ve výuce. Takový celek musí být dostatečně podrobný a zároveň přehledný. Musí splňovat požadavky, které vznášejí učitelé i sami studenti. Cílem je tedy podat poznatky teoretického popisu membrán pro palivové články tak, aby byly použitelné ve výuce a také aby tvořily studijní materiál pro studenty, kteří mají zájem o toto téma. Dílčím cílem je vytvoření laboratorní úlohy pro fyzikální praktikum, kde by mohli studenti zkoumat vlastnosti polymerních membrán pro palivové články za použití nejnovějších měřících přístrojů umístěných ve výzkumném centru. Taková úloha musí být snadno pochopitelná a musí být slehce proveditelná pro samotné studenty. Dalším dílčím cílem práce je shromáždění znalostí o obnovitelných zdrojích energie u studentů za použití dotazníkového šetření, jehož závěry budou použity pro přípravu laboratorních úloh a studijních materiálů. Dalším dílčím cílem je příprava nových kompozitních membrán použitých v palivových článcích. Získané výsledky budou publikovány v impaktovaných časopisech a na konferencích.

Klíčová slova

Palivový článek, membrány, kompozit, Nafion, polyvinyl alkohol, pedagogyka, motivace

TABLE OF CONTENTS

1. Introduction.....	10
1.1. Membrane.....	10
1.2. Historical development of membranes.....	14
1.3. Proton Exchange membranes PEM.....	16
1.3.1. Nafion.....	17
1.3.2. Poly(vinylalcohol) membranes.....	18
1.5. Literature.....	21
2. Pedagogy.....	27
2.1. Didactic.....	27
2.1.1. Motivation.....	27
2.2. Questionnaire survey of knowledge about renewable energy among college students	31
2.3. Tasks for Physical Laboratory practise.....	44
2.3.1. Manual for measurement.....	45
2.4. Literature.....	46
3. Experimental.....	47
3.1. Material.....	47
3.1.1. Solvents.....	47
3.1.2. Monomers.....	47
3.1.3. Tools.....	48
3.2. Membrane preparation.....	48
3.2.1. Modification of Nafion.....	48
3.2.2. Preparation of PVA membranes.....	50
3.3. Experimental technique.....	53
3.3.1. Water uptake measurements.....	53
3.3.2. Thermogravimetric Analysis (TGA).....	54
3.3.3. Dynamic Mechanical Analysis (DMA).....	54
3.3.4. Rheology.....	54
3.3.5. Fourier Transform Infrared Spectroscopy (FTIR).....	55
3.3.6. Dynamic Vapor Sorption (DVS).....	55
3.3.7. SAXS/WAXS.....	56
3.3.8. Electrical impedance.....	56
3.3.9. Raman spectroscopy.....	57

3.3.10.	Atomic force microscopy	57
3.3.11.	Differential scanning calorimetry.....	58
3.4.	Literature	58
4.	Results and discussion	59
4.1.	Modification of Nafion [®] 115 by polyfurfuryl alcohol.....	59
4.1.1.	FT-IR ATR.....	59
4.1.2.	SAXS/WAXS.....	59
4.1.3.	Thermal analysis	61
4.1.4.	Dynamic mechanical properties	63
4.1.5.	Water uptake (W_u).....	66
4.1.6.	Dynamic vapor sorption	68
4.1.7.	Electrical properties.....	68
4.2.	PVA/SiO ₂ and PVA/SiO ₂ /GA membranes.....	72
4.2.1.	Raman spectroscopy.....	72
4.2.2.	Small- and wide-angle X-ray scattering.....	74
4.2.3.	Atomic force microscopy	79
4.2.4.	Water uptake	81
4.2.5.	Thermal analysis	83
4.2.6.	Dynamic mechanical analysis	88
4.3.	PVA/SSA/SiO ₂ membranes.....	90
4.3.1.	FT-IR.....	90
4.3.2.	Rheology	91
4.3.3.	TGA.....	92
4.3.4.	DMA.....	94
4.3.5.	Water uptake	95
4.3.6.	Ion conductivity.....	96
4.4.	Summary.....	99
4.5.	Literature	100
5.	Conclusion	103
	Appendices.....	104

List of abbreviations

PEM	polymer electrolyte membrane
SPE	solid polymer electrolyte
E^0	standard electrode potential
SHE	standard hydrogen electrode
UV	ultraviolet
PEMFC	polymer electrolyte membrane fuel cell
PVA	poly(vinyl alcohol)
PVAc	poly(vinyl acetate)
AA	adipic acid
SA	succinic acid
PFA	polyfurfuryl alcohol
TEOS	tetraethylortosilcate
SSA	sulfosuccinic acid
PET	polyethylene terephthalate
TG	thermogravimetry
N115	Nafion 115
FA	furfuryl alcohol
GA	glutaraldehyde
W_u	water uptake
W_s	weight of swollen membranes
W_d	weight of dry membranes
TGA	thermogravimetric analysis
DMA	dynamic mechanical analysis
E'	storage modulus
E''	loss modulus
T_g	glass transition temperature
E_R	rubbery modulus

FTIR	fourier transform infrared spectroscopy
ATR	attenuated total reflectance
DVS	dynamic vapor sorption
RH	relative humidity
SAXS	small angle x-ray scattering
WAXS	wide angle x-ray scattering
AFM	atomic force microscopy
FOA	free oscillating amplitude
SPA	set point amplitude
DSC	differential scanning calorimeter
W_{vu}	water vapor uptake
DTG	derivative thermogravimetric
T_m	melting transition
US	United States
GFT	german engineering company
FPE	Faculty of Education
FEL	Faculty of Electrical Engineering
FAV	Faculty of Applied Sciences
FF	Faculty of Philosophy
FEK	Faculty of Economics
FST	Faculty of Engineering
FPR	Faculty of Law
FZS	Faculty of Health Studies
NTC	New Technologies - Research Centre
ISM	Engineering of special materials

1. Introduction

1.1. Membrane

Membrane in the broadest sense can be described as a barrier that separates two different regions and manages the exchange of matter, energy and information between the regions in a very specific way.

The word membrane comes from Latin word “membrana” that means a skin (Jones, 1987). Today’s word ‘membrane’ has been extended to describe a thin flexible sheet or film, acting as a selective barrier which enables the transport or the retention of compounds between two medium. Different types of driving forces can be at the origin of the transport across the membranes. They are associated with different types of membrane processes. For dialysis of solutes, it is a difference of compound concentration. In the case of electro dialysis and related electromembrane processes, an electric field between electrodes located on the two sides of the membrane enables the selective separation of ionic species in solution. The history of synthetic membrane began in 1748 when Abble Nollet demonstrated semi-permeability for the first time that animal bladder was more semi-permeable to water than to wine. One century later, Fick published his phenomenological law of diffusion, which we still use today as a first-order description of diffusion through membranes. These membranes were made from an ether-alcohol solution of cellulose called “collodion”. After that a lot of research was carried out in this area which gave the pathway to advanced technologies and innovations such as dialysis, different permeability of gases at rubber, osmotic pressure, and Donan’s ion equilibrium phenomena.

Synthetic membranes have occupied an important place in the chemical technology. They are widely used in many technically and commercially important separation processes including desalination, gas separations and to clean food and organic products. They are also key components in systems for the conversion of energy as well as energy storage. Membranes have very important function in artificial organs and drug delivery devices.

Although membranes are widely used scientific and technical instruments in modern industrial society, general ideas about the functioning of the membranes are very limited. Many people constitutes the membrane as a filter, allowing to separate solid particles from liquid. The membranes are much more complex, both in its structure and functions. Membranes may be solid or liquid, homogeneous or heterogeneous, isotropic or anisotropic. The thickness of the

membrane can be a fraction of a micrometer or a few millimeters. The electrical resistance may vary from million ohm/cm to fraction ohm/cm.

With the development of new membranes having better chemical, thermal, and mechanical properties, the selectivity and energy efficient transport facilities of membranes have increased, and is likely to extend far beyond its present level. Presently, there exists many different kinds of membranes which can be divided according to their application, structure or their chemical composition.

The greatest use of membranes is in separation processes. Membrane separation processes operate without heating and therefore use less energy than conventional thermal separation processes such as distillation, sublimation or crystallization. The separation process is purely physical and both fractions (permeate and retentate) can be used. The widely used membrane processes include microfiltration, ultrafiltration, nanofiltration, reverse osmosis, electrolysis, dialysis, electrodialysis, gas separation, vapor permeation, pervaporation, membrane distillation, and membrane contactors. All processes except for pervaporation involve no phase change. All processes except (electro)dialysis are pressure driven. Microfiltration and ultrafiltration is widely used in food and beverage processing (beer microfiltration, apple juice ultrafiltration), biotechnological applications and pharmaceutical industry (antibiotic production, protein purification), water purification and wastewater treatment, the microelectronics industry, and others. Nanofiltration and reverse osmosis membranes are mainly used for water purification purposes. Dense membranes are utilized for gas separations (removal of CO₂ from natural gas, separating N₂ from air, organic vapor removal from air or a nitrogen stream) and sometimes in membrane distillation. The later process helps in the separation of azeotropic compositions reducing the costs of distillation processes.

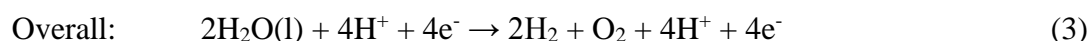
Table 1. Classification of semipermeable membranes

Pore size	Molecular mass	Process	Filtration	Removal of
> 10		“classic” filter		
> 0.1 μm	> 5000 kDa	microfiltration	< 2 bar	larger bacteria, yeast, particles
100-2 nm	5-5000 kDa	ultrafiltration	1-10 bar	bacteria, macromolecules, proteins
2-1 nm	0,1-5 kDa	nanofiltration	3-20 bar	viruses, 2-valent ions
< 1 nm	< 100 Da	reverse osmosis	10-80 bar	salts, small organic molecules

Membranes can also be used in some special devices like electrolyzers, ozone production units, vanadium batteries and fuel cells.

Polymer electrolyte membrane (PEM) electrolysis is the electrolysis of water in a cell equipped with a solid polymer electrolyte (SPE) that is responsible for the conduction of protons, separation of product gases, and electrical insulation of the electrodes. The PEM electrolyzer was introduced to overcome the issues of partial load, low current density, and low pressure operation currently plaguing the alkaline electrolyzer.

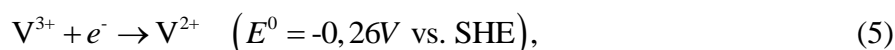
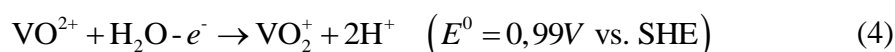
The electrolyte is a thin, solid ion-conducting membrane which is used instead of the aqueous solution used in the alkaline electrolyzers that can be built with materials as simple as two pencils. The reactions are as follows:



In order to convert electrical energy into chemical energy, catalysts are needed to split the water into hydrogen and oxygen.

Another type of device that uses a polymeric membrane is a vanadium battery. This type of battery uses a liquid electrolyte containing vanadium that occurs in four oxidation states [1]. The entire device works by changing the oxidation states of vanadium and the electrolyte thus forms a mixture of different states of the same substance separated by a polymeric membrane.

There are transitions between each oxidation states that release or require protons, electrons, respectively. We can write these processes as:

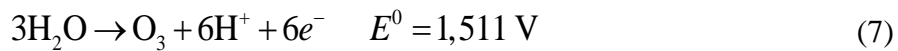
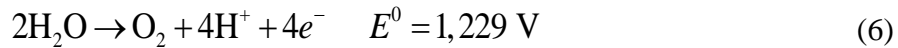


where E^0 indicates the standard electrode potential and the SHE standard hydrogen electrode. The reactions are controlled by the necessary transition of protons through the polymer membrane and electron movement in the outer circuit.

Ozone is usually produced by a silent discharge around which air or pure oxygen flows. In the case of oxygen, the concentration of the ozone is about 15 wt% in the produced gas. If air is used, the concentration is reduced to about 2 wt%. The industrial production of ozone and its subsequent distribution is practically excluded, because ozone is highly explosive at high concentrations, and transport would be very dangerous. Ozone is produced directly in places where it will be used for cleaning purposes. Ozone production using polymeric membranes and

suitable electrodes has more favorable parameters than production by silent discharge or UV absorption.

The principle of electrochemical production of ozone is not very different from electrolysis. The production of oxygen and hydrogen from the water takes place under lower anodic potentials (equation (6)), the reaction (7) predominates with an increasing electrode potential,



Basic information on hydrogen fuel cells has been published, for example, in the great Larminie [2] book. The polymeric membrane forms the central component of these devices, where it separates the reducing part from the oxidative part. It is obvious that the membrane is exposed to a chemically aggressive environment. Resistance to these influences is an essential parameter that a polymeric membrane must meet. But essential are its electrical properties. For electrons it must form an impermeable barrier, positively charged particles (in this case the protons) must pass from the anodic part to the cathodic part.

The fuel cell works on principle of decomposition of hydrogen molecules on the anode where electrons and hydrogen protons are separated. The electrons are conducted to the outer circuit and can do work. At the cathodic part oxygen molecules are decomposed (due to electrons from the outer circuit), and in the presence of the introduced hydrogen protons combine into electrically neutral molecules of water. The emerging water is an important part of the water management of the fuel cell. The un-moistened membrane is not proton-conductive. However, too much water may clog the fuel inlets and the cell does not provide the required power.

The research and development for membranes depends on many parameters such as solute type, separation technique, commercial viability, market demand and so on. By determining the quantitative relationship between membrane structures and its casting properties such as formulation and casting condition, a fine polymer structure can be engineered to satisfy social requirements. By governing the membrane fabrication method and its casting properties, membrane with specific characteristics and desired performances can be produced. Currently, intensive research work is underway in to improve and develop new types of membranes to meet the stringent industrial requirements covering a diverse range of applications especially for water purification and biological applications.

The designing of a particular membrane plays a very significant role in *shaping-up* the properties (such as physical, chemical, thermal and mechanical) and performance of the membrane. The successful use of membrane processes depends on a proper selection of membrane material. Extensive research has been conducted to develop new membrane materials (Wiesner and Chellam 1999). Inorganic membranes, although having very high chemical and temperature resistance, are now still of little commercial use due to brittleness and expense. The main inorganic materials used for membranes are oxide ceramic [3-5], porous glasses [6-8], carbon-like solids [9], porous metals (like sintered stainless steel) or dense metals (like Pd or Pd-based alloys for H₂ separation). Organic polymers remain the most widely used commercial membrane materials. They are usually constructed by coating a thin active polymeric layer onto a microporous support to provide desirable mechanic strength while having higher water permeability and chemical resistance. The polymers typically used for the active layer include cellulose acetates [10, 11], polyethersulfone [12, 13], polyvinylidene fluoride [14, 15], polyacrylonitrile [16], polyamides [17, 18], polypropylene [19, 20], and polysulfones [21, 22].

Different types of materials are used for different types of membranes. Cellulose acetate is used for the separation of ethanol and water [23], or water-oils separation [24], polysulfone is used for reverse osmosis for desalination and brackish waters [25, 26], poly(vinylidene fluoride) is used for filtration of blood or separation algal from water [27, 28], polyaluminium chloride is used for bio-waste filtration [29], aromatic polyimides and polyamides are used for nanofiltration or gas separation [30-33].

Membranes based on poly(ether sulfone) or poly(vinyl alcohol) have been synthesized, tested and reported for fuel cells [34, 35]. However, commercially available Nafion (prepared by polytetrafluoroethylene) is extensively used for low temperature PEM fuel cell applications.

Research centers around the world are trying to develop new membranes to improve the existing membrane processes or to develop membranes for use in new applications.

1.2. Historical development of membranes

The first documented study of membrane phenomena and the discovery of the concept of osmosis can be found at Nollet (1748) [36]. He found that when the pig bladder placed on the one side into contact with the mixture of water and ethanol on the other side with pure water, the water will pass through the membrane preferentially. Nollet was probably the first to recognize the relationship between a semipermeable membrane, osmotic pressure and volume

flow. More systematic studies on the material transport in a semipermeable membrane were made by Graham (1833) [37]. He studied diffusion of gases through various media and discovered that rubber has a different permeability for different gases.

Most of the early studies of membrane permeability were carried out with natural materials like animal intestines, bladder or rubber elastic elements. Traube in 1867 [38] was the first to introduce artificially prepared semipermeable membrane precipitating cupric ferrocyanide in a thin layer of porous porcelain. This type of membrane has been used Pfeffer in his fundamental studies of osmosis. These findings were used van't Hoff in 1887 [39] and this work led directly to the van't Hoff equation. Maxwell took these findings and others for the development of the kinetic theory of gases.

Later, the preferred collodion (nitrocellulose) membranes, because of possible reproducibility. In 1907 Bechhold proposed technique for the preparation of nitrocellulose membranes graded pore size, as determined by assay of bubbles [40]. Other workers, especially Elford [41], Zsigmondy and Bachmann [42] and Ferry [43] Bechholdovu improved the technique and in early 1930 have been microporous membranes commercially available collodion.

Membranes have found their first major use in filtering drinking water at the end of the Second World War. Source of drinking water serving a community in Germany and elsewhere in Europe broke down, and filters for water safety were urgently needed. Research efforts to develop these filters were supported by the US military, were evaluated by Millipore Corporation, the first and still the largest US manufacturer of microfiltration membranes. In 1960, it became part of the development of membranes of modern science but developed membranes were used in only a few laboratories and rarely for specialized industrial applications.

Use of membrane separation process prevented the four basic problems: they were too unreliable, too slow, too expensive and too non-selective. Solving each of these issues have developed over the last 30 years and membrane separation processes are now commonplace.

The key discovery which transforms membrane separation from the laboratory to the industrial process, the development of anisotropic reverse osmosis membrane with a high flux, at the beginning of 1960 in the Loeb-Sourirajan [44]. These membranes are composed of ultra-thin selective surface film applied to the much stronger, but more microporous material that provides mechanical strength. Flow in a first Loeb-Sourirajan reverse osmosis membrane was 10 times higher than any available membranes. Reverse osmosis has been practically used for seawater desalination.

In parallel with the development of membranes for industrial applications ran independent development of membranes for medical separation processes, particularly the development of artificial kidney. W. J. Kolf [45] demonstrated the first successful artificial kidney in the Netherlands in 1945. It took nearly 20 years to improve the technology for use on a large scale, this development was complete in 1960. Since then, the use of membranes in artificial organs become the main life-saving procedure. Another important medical use of the membranes are controlled drug delivery systems. The key figure in this area was Alex Zaffaroni, who founded Alza, a company dedicated to the development of these products in 1966. Membrane technology developed by Alza and its competitors are widely used in the pharmaceutical industry to improve the efficiency and safety of medications.

The period from 1960 to 1980 produced a significant change in membrane technology. Following the initial Loeb-Sourirajan technology have been developed other processes for the manufacture of high performance membranes, including the interfacial polymerization and the laminated casting or coating. Using these processes, membranes with selective thin layers of about 0.1 microns or less, are currently manufactured by a variety of companies.

The main development in 1980 was the emergence of industrial gas membrane separation processes. The first main impulse was the development of membranes for hydrogen separation, with which came in 1980 Monsanto Prism [46]. Within a few years, Dow manufactures systems for separating nitrogen from the air, and Cynara Separex and manufactures systems for separating carbon dioxide from natural gas. Gas separation technology evolves and expands. The ultimate development in 1980 was at GFT, the first commercial evaporative systems for dehydration of alcohol.

Although there are always membranes in nature, systematic study of synthetic membranes began about 100 years ago, and the first practical use of membranes does not take more than 50 years. History of membrane science and technology is therefore relatively short.

1.3. Proton Exchange membranes PEM

Polymer electrolyte membrane fuel cells (PEMFC) are considered as a promising source of clean forms of energy that possess the remarkable properties (such as self-starting at low temperatures, high power density etc.), to replace the prevailing batteries used in electronic products. An integral part of PEMFC unit is the “polymer electrolyte membrane” which lies between anode and cathode, to provide proton conductivity and to prevent internal electronic current between the two electrodes [47]. PEM needs to have specific properties that enable it to

work well in FCs: (1) high proton conductivity to support high currents with minimal resistive losses and zero electronic conductivity; (2) adequate mechanical strength and stability; (3) chemical and electrochemical stability under operating conditions; (4) extremely low fuel or oxidant by-pass to maximize columbic efficiency; (5) low water transport through diffusion, and (6) electro-osmosis and capability for fabrication into membrane electrode assemblies [48].

Over the last century, substantial research has been conducted in developing new proton exchange membranes. For example Hickner describes new membranes based on poly(arylen ether) [49], Kerres made membranes on polysulfone basic [50], Rikukawa prepared hydrocarbon polymer membranes [51], Mikhailenko made membranes base on sulfonated polyether ether keton [52], Li and Lobato worked on polybenzenimidazol membranes [53, 54], Bae made membranes base on polystyrene [55].

1.3.1. Nafion

Nafion®, which has long been considered the state-of-the-art material for proton exchange membranes, is commercially produced by DuPont and has a polyperfluoroacid structure as shown in Figure 1. It is the first of a class of synthetic polymers with ionic properties which are called ionomers. Nafion's unique ionic properties are a result of incorporating perfluorovinyl ether groups terminated with sulfonate groups onto a tetrafluoroethylene (Teflon) backbone.

Nafion is synthesized by free radical polymerization and is extruded in the sulfonyl fluoride form. It is then hydrolyzed and acidified to convert it to the membrane form. Typically, about 13 mol% of the vinyl ether monomer containing the pendent sulfonyl group is employed to achieve an optimized *equivalent weight* of 1100 (*meq of sulfonic acid/g of the dry polymer*). Commercially, Nafion is available by their trade names Nafion 117, 115 and 112. In the case of Nafion 117, the first two numbers represent 1100 equivalent weight, while the 7 represents the thickness in *mils* (1 mil = 0,0254 mm).

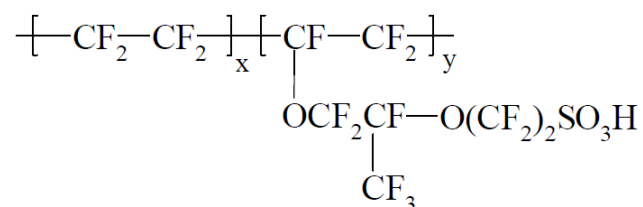


Figure 1. Structure of Nafion.

Nafion soon became a standard for PEMFC and remains so till today. The DuPont Nafion materials, both sulfonate and carboxylate varieties, are not entirely unique, as similar perfluorinated ionomers have been developed by others such as the Asahi Chemical Company

(commercial name: Aciplex) and the Asahi Glass Company (commercial name: Flemion). The comonomer chemical structures of and further information on these materials are given in the recent review article by Doyle and Rajendran [56]. Now commercially unavailable, but once considered a viable alternative, the Dow Chemical Company developed a somewhat similar perfluorinated ionomer that resembled the sulfonate form of Nafion except that the side chain of the former is shorter and contains one ether oxygen, rather than two ether oxygens, that is, $-\text{OCF}_2\text{-CF}_2\text{-SO}_3\text{H}$ [57, 58].

The greatest interest in Nafion in recent years derives from its consideration as a proton conducting membrane in fuel cells. It is clear that the tuning of these materials for optimum performance requires a detailed knowledge of chemical microstructure and nanoscale morphology. In particular, proton conductivity, water management, relative affinity of methanol and water in direct methanol fuel cells, hydration stability at high temperatures, electro-osmotic drag, and mechanical, thermal, and oxidative stability are important properties that must be controlled in the rational design of these membranes. This is a challenge for Nafion materials in which the possible chemical variations are rather limited. And, of course, all of these objectives must be achieved while maintaining low cost for this perfluorinated ionomer in the vast consumer market as well as in military applications. While a number of alternate polymer membranes, including nonfluorinated types, have been developed, Nafion is still considered the benchmark material against which most results are compared.

A number of systems used Nafion membranes are simply proposed rather than in actual commercial applications. For example membranes in fuel cells, electrochemical energy storage systems, chlor-alkali cells, water electrolyzers, Donnan dialysis cells, electrochromic devices, and sensors, including ion selective electrodes, and the use of these membranes as a strong acid catalyst.

The development of new PEMs for PEMFC systems is one of the most active areas of fuel cell research. To overcome the drawbacks of the Nafion membrane, many types of novel PEMs have been developed, and some have shown the potential to substitute Nafion, especially under high operational temperature.

1.3.2. Poly(vinyl alcohol) (PVA) membranes

PVA is a hydrophilic semi-crystalline polymer produced by polymerization of vinyl acetate to poly(vinyl acetate) (PVAc), and subsequent hydrolysis of PVAc to PVA. This reaction is incomplete resulting in polymer with different degree of hydrolysis [59]. Commercial PVA is

available in highly hydrolyzed grades (degree of hydrolysis above 98.5%) and partially hydrolyzed ones (degree of hydrolysis from 80 to 98.5%) [60]. The degree of hydrolysis or the content of acetate groups in PVA affects its chemical properties, solubility and crystallizability.

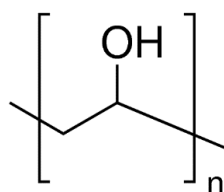


Figure 2. Structure of PVA.

PVA is one of the widely used synthetic polymers owing to its excellent physical properties such as high tensile strength and flexibility, superior barrier to oxygen and aroma, and ease of formation in films. It is also biodegradable under suitable conditions. In addition, PVA is biocompatible and nontoxic. Because of these excellent properties, PVA films have been developed for biomedical applications.

PVA appears to be very attractive material for preparing proton exchange membranes (PEM) because this polymer can function as an excellent methanol barrier. PVA also has both very good mechanical properties and chemical stability, which are adequate for preparing PEMs. Although PVA itself does not have fixed charges, several organic groups like hydroxyl, amine, carboxylate, sulfonate, and quaternary ammonium can be incorporated to impart hydrophilicity and/or ionic group.

Hydrophilic PVA membranes are used in many applications, most notably in organic/inorganic separations, pervaporation, biomedical applications, catalysis, controlled drug release, etc. [61–64]. These membranes have a highly hydrophilic nature, which is considered as an advantage for some applications, but in most cases it becomes a hindrance due to the high swelling capacity of the membranes in water. To enhance the stability and performance of PVA-based membranes, a variety of chemical modifications have been employed, e.g., cross-linking [65–67], electrospinning [68–70], blending [71], sol–gel process [72, 73], and grafting [74, 75].

Cross-linking is considered as a suitable way to alter the physical and chemical properties of membranes. The polyhydroxy structure of PVA enables easy cross-linking with various multifunctional compounds capable of reacting with –OH groups to obtain three-dimensional networks. A majority of the commercially available asymmetric PVA membranes are cross-linked by the phase-inversion technique [76, 77]. Recently, M'barki et al. [78] proposed a unique greener method to prepare porous polymer membranes by combining thermally induced

phase separation and cross-linking of PVA in water. Their results showed that cross-linking control was the key step to obtain a porous membrane morphology. A different approach was followed by Casimiro et al. [79], who prepared PVA-supported catalytic membranes for biodiesel production by the mutual γ -irradiation method. They used adipic acid (AA) and succinic acid (SA) as crosslinkers and a commercial ion-exchange resin as the catalyst. The results showed that a slight increase in the γ -radiation dose leads to an increase of the membrane catalytic activity.

1.4. Objectives

Though Nafion membranes are commercially successful, certain limitations [80-87] prevent the use of the membranes above 80°C. Hence, they are regarded as inappropriate membranes for PEM fuel cells and therefore, intense research efforts are currently focused towards modifying these membranes to improve the thermal stability and proton conductivity.

Several research activities have been implemented to modify Nafion using zirconium phosphate [88], organic-inorganic hybrid materials [89], tetraethylorthosilicate (TEOS) [90], sulfonated graphene oxide [91], Pd nanophases [92] and ionic liquids [93], for better temperature stabilization and proton conductivity.

In the present work Nafion 115 was modified by polyfurfuryl alcohol (PFA) using the same procedure as mentioned in [94]. However the impregnation time of membranes in PFA solution was gradually increased from 24 h to 120 h, to investigate the influence of PFA loading on the performance of the membranes. It was anticipated that highly cross-linked, chemically stable PFA domains with a low swelling rate increased ion conductivity and mechanical and thermal stability of the composite membrane. The results have been published in Journal of Macromolecular Science [95].

Hydrophilic PVA membranes are used in many applications, but lately they have been widely utilized as polymer electrolyte membrane (PEM) for fuel cells. In order to design a good membrane many parameters are involved, such as the properties of casting solution, preparation conditions (temperature, relative humidity and time), reactants etc. Membrane should have good water resistance, mechanical, thermal stability and ion conductivity.

In this work the PVA membranes was modified by TEOS for better water resistance, mechanical and thermal properties, and sulfosuccinic acid (SSA) to increase ion conductivity. The results have been published in Journal of Materials Science and Journal of Physics [96, 97].

1.5. Literature

1. Perry, M. L., Weber, A. Z. (2016), *Journal of The Electrochemical Society* 163(1): A5064-A5067
2. Larminie, J., Dicks, A., McDonald, M. S. (). *Fuel cell systems explained*. J. Wiley, 2003. 400 s. ISBN 0-470-84857-X
3. Mallada, R., Menéndez, M.: *Inorganic Membranes: Synthesis, Characterization and Applications*. Elsevier, 2008. 480 s. ISBN 0080558003
4. Gitis, V., Rothenberg, G.: *Ceramic Membranes: New Opportunities and Practical Applications*. John Wiley & Sons, 2016. 300 s. ISBN 3527696571
5. Li, K.: *Ceramic Membranes for Separation and Reaction*. John Wiley & Sons, 2007. 316 s. ISBN 0470319461
6. Hsieh, H. P. (1996). *Inorganic membranes for separation and reaction (Vol. 3)*. Elsevier.
7. Rodríguez-Reinoso, F., McEnaney, B., Rouquerol, J., & Unger, K. K. (2002). *Characterization of Porous Solids VI: Proceedings of the 6th International Symposium on the Characterization of Porous Solids (COPS-VI)*, Allicante, Spain, May 8-11 2002 (Vol. 144). Elsevier.
8. Bose, A. C. (Ed.). (2008). *Inorganic membranes for energy and environmental applications*. Springer Science & Business Media.
9. Ismail, A. F., Rana, D., Matsuura, T., & Foley, H. C. (2011). *Carbon-based membranes for separation processes*. Springer Science & Business Media.
10. Butterfield, D.A.: *Biofunctional Membranes*. Springer Science & Business Media, 2013. 294 s. ISBN 1475725213
11. Baker, R.W.: *Membrane Technology and Applications*. John Wiley & Sons, 2012. 592 s. ISBN 1118359690
12. Ladewig, B., Al-Ahaeli, M.N.Z.: *Fundamentals of Membrane Bioreactors: Materials, Systems and Membrane Fouling*. Springer, 2016. 150 s. ISBN 9811020140
13. Saito, A., Kawanishi, H., Yamashita, A.C.: *High-Performance Membrane Dialyzers*. Karger Medical and Scientific Publishers, 2011. 200 s. ISBN 3805598122
14. Yan, L., Li, Y. S., & Xiang, C. B. (2005). Preparation of poly (vinylidene fluoride)(pvdf) ultrafiltration membrane modified by nano-sized alumina (Al₂O₃) and its antifouling research. *Polymer*, 46(18), 7701-7706.
15. Yu, L. Y., Xu, Z. L., Shen, H. M., & Yang, H. (2009). Preparation and characterization of PVDF–SiO₂ composite hollow fiber UF membrane by sol–gel method. *Journal of Membrane Science*, 337(1), 257-265.
16. Boerlage, S.F.: *Scaling and Particulate Fouling in Membrane Filtration Systems*. CRC Press, 2001. 258 s. ISBN 9058092429
17. Wang, L.K., Chen, J.P., Hung, Y.T., Shammass, N.K.: *Membrane and Desalination Technologies*. Springer Science & Business Media, 2010. 716 s. ISBN 1597452785
18. Ohya, H., Kudryavsev, V.V., Semenova, S.I.: *Polyimide Membranes: Applications, Fabrications and Properties*. CRC Press, 1997. 328 s. ISBN 9056990241
19. Howe, K.J., Clark, M.M.: *Coagulation Pretreatment for Membrane Filtration*. American Water Works Association, 2002. 264 s. ISBN 1583212655
20. Gryta, M. (2007). Influence of polypropylene membrane surface porosity on the performance of membrane distillation process. *Journal of Membrane Science*, 287(1), 67-78.
21. Cheryan, M.: *Ultrafiltration and Microfiltration Handbook*. CRC Press, 1998. 552 s. ISBN 1566765986
22. Visakh P.M., Nazarenko, O.: *Nanostructured Polymer Membranes*. John Wiley & Sons, 2016. 560 s. ISBN 1118831802

23. Dubey, V., Pandey, L. K., & Saxena, C. (2005). Pervaporative separation of ethanol/water azeotrope using a novel chitosan-impregnated bacterial cellulose membrane and chitosan–poly (vinyl alcohol) blends. *Journal of Membrane Science*, 251(1), 131-136.
24. Li, H. J., Cao, Y. M., Qin, J. J., Jie, X. M., Wang, T. H., Liu, J. H., & Yuan, Q. (2006). Development and characterization of anti-fouling cellulose hollow fiber UF membranes for oil–water separation. *Journal of Membrane science*, 279(1), 328-335.
25. Ghosh, A. K., & Hoek, E. M. (2009). Impacts of support membrane structure and chemistry on polyamide–polysulfone interfacial composite membranes. *Journal of Membrane Science*, 336(1), 140-148.
26. Jeong, B. H., Hoek, E. M., Yan, Y., Subramani, A., Huang, X., Hurwitz, G. & Jawor, A. (2007). Interfacial polymerization of thin film nanocomposites: a new concept for reverse osmosis membranes. *Journal of Membrane Science*, 294(1), 1-7.
27. Chang, Y., Shih, Y. J., Ruan, R. C., Higuchi, A., Chen, W. Y., & Lai, J. Y. (2008). Preparation of poly (vinylidene fluoride) microfiltration membrane with uniform surface-copolymerized poly (ethylene glycol) methacrylate and improvement of blood compatibility. *Journal of Membrane Science*, 309(1), 165-174.
28. Babel, S., & Takizawa, S. (2010). Microfiltration membrane fouling and cake behavior during algal filtration. *Desalination*, 261(1), 46-51.
29. Wang, J., et al. "Characterization of floc size and structure under different monomer and polymer coagulants on microfiltration membrane fouling." *Journal of Membrane Science* 321.2 (2008): 132-138.
30. Sun, S. P., Wang, K. Y., Peng, N., Hatton, T. A., & Chung, T. S. (2010). Novel polyamide-imide/cellulose acetate dual-layer hollow fiber membranes for nanofiltration. *Journal of Membrane Science*, 363(1), 232-242.
31. Kosuri, M. R., & Koros, W. J. (2008). Defect-free asymmetric hollow fiber membranes from Torlon®, a polyamide–imide polymer, for high-pressure CO₂ separations. *Journal of Membrane Science*, 320(1), 65-72.
32. Vaughn, J. T., Koros, W. J., Johnson, J. R., & Karvan, O. (2012). Effect of thermal annealing on a novel polyamide–imide polymer membrane for aggressive acid gas separations. *Journal of membrane science*, 401, 163-174.
33. Setiawan, L., Wang, R., Li, K., & Fane, A. G. (2011). Fabrication of novel poly (amide–imide) forward osmosis hollow fiber membranes with a positively charged nanofiltration-like selective layer. *Journal of Membrane Science*, 369(1), 196-205.
34. Krishnan, N. N., Henkensmeier, D., Jang, J. H., Kim, H. J., Rebbin, V., Oh, I. H. & Lim, T. H. (2011). Sulfonated poly (ether sulfone)-based silica nanocomposite membranes for high temperature polymer electrolyte fuel cell applications. *International Journal of Hydrogen Energy*, 36(12), 7152-7161.
35. Wang, F., Hickner, M., Kim, Y. S., Zawodzinski, T. A., & McGrath, J. E. (2002). Direct polymerization of sulfonated poly (arylene ether sulfone) random (statistical) copolymers: candidates for new proton exchange membranes. *Journal of Membrane Science*, 197(1), 231-242.
36. Nollet, J. A.: *Recherches Sur Les Causes Particulieres Des Phenomenes Electriques*. University of Michigan, 1754
37. Graham, T. (1833). XXVII. On the law of the diffusion of gases. *Philosophical Magazine Series* 3, 2(9), 175-190.
38. Traube, L. (1867). *Die Symptome der Krankheiten des Respirations-und Circulations-Apparats: Vorlesungen gehalten an der Friedrich-Wilhelms-Universität zu Berlin*. August Hirschwald.

39. van't Hoff, J. H. (1887). Die Rolle des osmotischen Druckes in der Analogie zwischen Lösungen und Gasen. *Zeitschrift für physikalische Chemie*, 1(1), 481-508.
40. Bechhold, H.: *Colloids in Biology and Medicine*. Hardpress Limited, 2013. 530 s. ISBN 1313852600
41. Elford, W. J. (1937). Principles governing the preparation of membranes having graded porosities. The properties of "gradocol" membranes as ultrafilters. *Transactions of the Faraday Society*, 33, 1094-1104.
42. Zsigmondy, R.: *The Chemistry of Colloids*. BiblioBazaar, 2008. 300 s. ISBN 0559856172
43. Ferry, J. D. (1936). Ultrafilter Membranes and Ultrafiltration. *Chemical Reviews*, 18(3), 373-455.
44. Loeb, S., Sourirajan, S. (1963) American Chemical Society, 117–132
45. Kolff, W. J., Berk, H. T. H. J., Welle, N. M., Ley, A. J. W., Dijk, E. C., & Noordwijk, J. (1944). The artificial kidney: a dialyser with a great area. *Journal of Internal Medicine*, 117(2), 121-134.
46. Henis, J. M., & Tripodi, M. K. (1980). A novel approach to gas separations using composite hollow fiber membranes. *Separation Science and Technology*, 15(4), 1059-1068.
47. Zaidi, J., Matsuura, T.: *Polymer Membranes for Fuel Cells*. Springer Science & Business Media, 2010. 550 s. ISBN 0387735321
48. Hickner, M. A., Ghassemi, H., Kim, Y. S., Einsla, B. R., & McGrath, J. E. (2004). Alternative polymer systems for proton exchange membranes (PEMs). *Chemical reviews*, 104(10), 4587-4612.
49. Hickner, M. A., Ghassemi, H., Kim, Y. S., Einsla, B. R., & McGrath, J. E. (2004). Alternative polymer systems for proton exchange membranes (PEMs). *Chemical reviews*, 104(10), 4587-4612.
50. Kerres, J., Ullrich, A., & Hein, M. (2001). Preparation and characterization of novel basic polysulfone polymers. *Journal of Polymer Science Part A: Polymer Chemistry*, 39(17), 2874-2888.
51. Rikukawa, M., & Sanui, K. (2000). Proton-conducting polymer electrolyte membranes based on hydrocarbon polymers. *Progress in Polymer Science*, 25(10), 1463-1502.
52. Mikhailenko, S. D., Zaidi, S. M. J., & Kaliaguine, S. (2001). Sulfonated polyether ether ketone based composite polymer electrolyte membranes. *Catalysis Today*, 67(1), 225-236.
53. Li, Q., He, R., Berg, R. W., Hjuler, H. A., & Bjerrum, N. J. (2004). Water uptake and acid doping of polybenzimidazoles as electrolyte membranes for fuel cells. *Solid State Ionics*, 168(1), 177-185.
54. Lobato, J., Canizares, P., Rodrigo, M. A., & Linares, J. J. (2007). PBI-based polymer electrolyte membranes fuel cells: temperature effects on cell performance and catalyst stability. *Electrochimica acta*, 52(12), 3910-3920.
55. Bae, B., & Kim, D. (2003). Sulfonated polystyrene grafted polypropylene composite electrolyte membranes for direct methanol fuel cells. *Journal of Membrane Science*, 220(1), 75-87.
56. Doyle, M., & Rajendran, G. (2003). Perfluorinated membranes. *Handbook of fuel cells*.
57. Utracki, L. A., & Weiss, R. A. (Eds.). (1989). *Multiphase polymers: blends and ionomers*. American Chemical Society.
58. Xu, G. (1993). X-ray scattering study of new perfluorinated ionomers. *Polymer journal*, 25(4), 397-400.

59. Hassan, C., & Peppas, N. (2000). Structure and applications of poly (vinyl alcohol) hydrogels produced by conventional crosslinking or by freezing/thawing methods. *Biopolymers· PVA Hydrogels, Anionic Polymerisation Nanocomposites*, 37-65.
60. Wang, T., Turhan, M., & Gunasekaran, S. (2004). Selected properties of pH- sensitive, biodegradable chitosan–poly (vinyl alcohol) hydrogel. *Polymer International*, 53(7), 911-918.
61. Lin, W., Zhu, T., Li, Q., Yi, S., & Li, Y. (2012). Study of pervaporation for dehydration of caprolactam through PVA/nano silica composite membranes. *Desalination*, 285, 39-45.
62. Ceia, T. F., Silva, A. G., Ribeiro, C. S., Pinto, J. V., Casimiro, M. H., Ramos, A. M., & Vital, J. (2014). PVA composite catalytic membranes for hyacinth flavour synthesis in a pervaporation membrane reactor. *Catalysis Today*, 236, 98-107.
63. Yang, D., Li, Y., & Nie, J. (2007). Preparation of gelatin/PVA nanofibers and their potential application in controlled release of drugs. *Carbohydrate Polymers*, 69(3), 538-543.
64. Yadav, R., & Kandasubramanian, B. (2013). Egg albumin PVA hybrid membranes for antibacterial application. *Materials Letters*, 110, 130-133.
65. Wu, Y., Wu, C., Li, Y., Xu, T., & Fu, Y. (2010). PVA–silica anion-exchange hybrid membranes prepared through a copolymer crosslinking agent. *Journal of Membrane Science*, 350(1), 322-332.
66. Chen, H., Yuan, D., Li, Y., Dong, M., Chai, Z., Kong, J., & Fu, G. (2013). Silica nanoparticle supported molecularly imprinted polymer layers with varied degrees of crosslinking for lysozyme recognition. *Analytica chimica acta*, 779, 82-89.
67. Liu, Z., Dong, Y., Men, H., Jiang, M., Tong, J., & Zhou, J. (2012). Post-crosslinking modification of thermoplastic starch/PVA blend films by using sodium hexametaphosphate. *Carbohydrate polymers*, 89(2), 473-477.
68. Santos, C., Silva, C. J., Büttel, Z., Guimarães, R., Pereira, S. B., Tamagnini, P., & Zille, A. (2014). Preparation and characterization of polysaccharides/PVA blend nanofibrous membranes by electrospinning method. *Carbohydrate polymers*, 99, 584-592.
69. Li, G., Zhao, Y., Lv, M., Shi, Y., & Cao, D. (2013). Super hydrophilic poly (ethylene terephthalate)(PET)/poly (vinyl alcohol)(PVA) composite fibrous mats with improved mechanical properties prepared via electrospinning process. *Colloids and Surfaces A: Physicochemical and Engineering Aspects*, 436, 417-424.
70. Na, H., Chen, P., Wong, S. C., Hague, S., & Li, Q. (2012). Fabrication of PVDF/PVA microtubules by coaxial electrospinning. *Polymer*, 53(13), 2736-2743.
71. Zhu, M., Qian, J., Zhao, Q., An, Q., & Li, J. (2010). Preparation method and pervaporation performance of polyelectrolyte complex/PVA blend membranes for dehydration of isopropanol. *Journal of Membrane Science*, 361(1), 182-190.
72. Irani, M., Keshkar, A. R., & Moosavian, M. A. (2012). Removal of cadmium from aqueous solution using mesoporous PVA/TEOS/APTES composite nanofiber prepared by sol–gel/electrospinning. *Chemical engineering journal*, 200, 192-201.
73. Zeng, C., He, Y., Li, C., & Xu, Y. (2013). Synthesis of nanocrystalline LaMn 0.5 Fe 0.5 O 3 powders via a PVA sol–gel route. *Ceramics International*, 39(5), 5765-5769.
74. Holloway, J. L., Lowman, A. M., VanLandingham, M. R., & Palmese, G. R. (2013). Chemical grafting for improved interfacial shear strength in UHMWPE/PVA-hydrogel fiber-based composites used as soft fibrous tissue replacements. *Composites Science and Technology*, 85, 118-125.
75. Ajji, Z., & Ali, A. M. (2010). Separation of copper ions from iron ions using PVA-g-(acrylic acid/N-vinyl imidazole) membranes prepared by radiation-induced grafting. *Journal of hazardous materials*, 173(1), 71-74.

76. Morgado, P. I., Lisboa, P. F., Ribeiro, M. P., Miguel, S. P., Simões, P. C., Correia, I. J., & Aguiar-Ricardo, A. (2014). Poly (vinyl alcohol)/chitosan asymmetrical membranes: Highly controlled morphology toward the ideal wound dressing. *Journal of Membrane Science*, 469, 262-271.
77. Li, N., Xiao, C., An, S., & Hu, X. (2010). Preparation and properties of PVDF/PVA hollow fiber membranes. *Desalination*, 250(2), 530-537.
78. M'barki, O., Hanafia, A., Bouyer, D., Faur, C., Sescousse, R., Delabre, U. & Pochat-Bohatier, C. (2014). Greener method to prepare porous polymer membranes by combining thermally induced phase separation and crosslinking of poly (vinyl alcohol) in water. *Journal of Membrane Science*, 458, 225-235.
79. Casimiro, M. H., Silva, A. G., Alvarez, R., Ferreira, L. M., Ramos, A. M., & Vital, J. (2014). PVA supported catalytic membranes obtained by γ -irradiation for biodiesel production. *Radiation Physics and Chemistry*, 94, 171-175.
80. Le Canut, J. M., Latham, R., Mérida, W., & Harrington, D. A. (2009). Impedance study of membrane dehydration and compression in proton exchange membrane fuel cells. *Journal of Power Sources*, 192(2), 457-466.
81. Freire, T. J., & Gonzalez, E. R. (2001). Effect of membrane characteristics and humidification conditions on the impedance response of polymer electrolyte fuel cells. *Journal of Electroanalytical Chemistry*, 503(1), 57-68.
82. Andreaus, B., McEvoy, A. J., & Scherer, G. G. (2002). Analysis of performance losses in polymer electrolyte fuel cells at high current densities by impedance spectroscopy. *Electrochimica acta*, 47(13), 2223-2229.
83. Mérida, W., Harrington, D. A., Le Canut, J. M., & McLean, G. (2006). Characterisation of proton exchange membrane fuel cell (PEMFC) failures via electrochemical impedance spectroscopy. *Journal of power sources*, 161(1), 264-274.
84. Paganin, V. A., Oliveira, C. L. F., Ticianelli, E. A., Springer, T. E., & Gonzalez, E. R. (1998). Modelistic interpretation of the impedance response of a polymer electrolyte fuel cell. *Electrochimica Acta*, 43(24), 3761-3766.
85. Collette, F. M., Lorentz, C., Gebel, G., & Thominet, F. (2009). Hygrothermal aging of Nafion®. *Journal of Membrane Science*, 330(1), 21-29.
86. Matos, B. R., Isidoro, R. A., Santiago, E. I., Tavares, A. C., Ferlauto, A. S., Muccillo, R., & Fonseca, F. C. (2015). Nafion–titanate nanotubes composites prepared by in situ crystallization and casting for direct ethanol fuel cells. *international journal of hydrogen energy*, 40(4), 1859-1867.
87. Jung, C. Y., & Yi, S. C. (2013). Influence of the water uptake in the catalyst layer for the proton exchange membrane fuel cells. *Electrochemistry Communications*, 35, 34-37.
88. Costamagna, P., Yang, C., Bocarsly, A. B., & Srinivasan, S. (2002). Nafion® 115/zirconium phosphate composite membranes for operation of PEMFCs above 100 C. *Electrochimica acta*, 47(7), 1023-1033.
89. Lin, C. W., Fan, K. C., & Thangamuthu, R. (2006). Preparation and characterization of high selectivity organic–inorganic hybrid-laminated Nafion 115 membranes for DMFC. *Journal of membrane science*, 278(1), 437-446.
90. Jung, D. H., Cho, S. Y., Peck, D. H., Shin, D. R., & Kim, J. S. (2002). Performance evaluation of a Nafion/silicon oxide hybrid membrane for direct methanol fuel cell. *Journal of power sources*, 106(1), 173-177.
91. Chien, H. C., Tsai, L. D., Huang, C. P., Kang, C. Y., Lin, J. N., & Chang, F. C. (2013). Sulfonated graphene oxide/Nafion composite membranes for high-performance direct methanol fuel cells. *international journal of hydrogen energy*, 38(31), 13792-13801.

92. Kim, Y. M., Park, K. W., Choi, J. H., Park, I. S., & Sung, Y. E. (2003). A Pd-impregnated nanocomposite Nafion membrane for use in high-concentration methanol fuel in DMFC. *Electrochemistry Communications*, 5(7), 571-574.
93. Schmidt, C., Glück, T., & Schmidt-Naake, G. (2008). Modification of Nafion membranes by impregnation with ionic liquids. *Chemical engineering & technology*, 31(1), 13-22.
94. Liu, J., Wang, H., Cheng, S., & Chan, K. Y. (2005). Nafion–polyfurfuryl alcohol nanocomposite membranes for direct methanol fuel cells. *Journal of Membrane Science*, 246(1), 95-101.
95. Remiš, T., Dodda, J. M., Tomáš, M., Novotný, P., & Bělský, P. (2016). Influence of polyfurfuryl alcohol (PFA) loading on the properties of Nafion composite membranes. *Journal of Macromolecular Science, Part A*, 53(12), 757-767.
96. Dodda, J. M., Bělský, P., Chmelař, J., Remiš, T., Smolná, K., Tomáš, M. & Kadlec, J. (2015). Comparative study of PVA/SiO₂ and PVA/SiO₂/glutaraldehyde (GA) nanocomposite membranes prepared by single-step solution casting method. *Journal of materials science*, 50(19), 6477-6490.
97. Remiš, T. (2017, January). Rheological properties of poly (vinyl alcohol)(PVA) derived composite membranes for fuel cells. In *Journal of Physics: Conference Series* (Vol. 790, No. 1, p. 012027). IOP Publishing.

2. Pedagogy

2.1. Didactic

Didactics is the pedagogical discipline that deals with education and teaching. Didactics can be defined as a theory of education and teaching. It is therefore a tool of teachers use to try to do streamline their teaching more effectively.

J. A. Comenius (1592-1670) as a creator of didactic systematic in his work *Methodology large* (1657) sees didactics as a "universal art to teach everything to everyone". This concept involves a Comenius didactics educational theory, the system not only teaching students of different age levels, but also issues of education, especially moral education. This study defines the outline didactics (general didactics) as a theory of learning and teaching. General Methodology deals with the content and also the process in which the students learn the content i.e., teaching and learning. In addressing educational issues, topics are closely associated with pedagogical disciplines such as general education, history of education, philosophy of education, sociology of education and training, educational psychology, special education. Basically, didactics uses knowledge as well as a number of other disciplines, such as biology, sociology, ethics, etc.

Very interesting is concept of didactic from the leading Czech expert, Jarmila Skalková: We define the didactics as the theory of education and teaching. It deals with the issue of educational content, which, as a result of the socio-historical experience of humanity, becomes in the process of teaching the individual ownership of the students. It also deals with a process that characterizes the activities of a teacher and students, in which students acquire this content [1].

2.1.1. Motivation

Any human activity would hardly do without motivation. If we want to identify the cause of any human behaviour, you have to look for the cause that motivated him. In psychology, the concept of motivation usually seen as the driving force influencing behaviour [2]. It is derived from Latin word *moveo*, which means to move. Motivation activates human activity, giving it a specific direction and goal. It is the basic condition of purposeful activity of individuals in each area. We differentiate between several kinds of motivation and it is clear that this is an important element of the human psyche. Each person wishes to meet their needs and behaves in a manner that leads to the fulfilment of these needs. Individual needs have diverse origins.

Some are directly associated with physiological processes, others are based on the need for self-fulfilment. In general, “needs” can be divided into two categories: (a) Primary needs (biological) - these needs have their origin in physiological processes in the human body such as hunger, thirst, rest or sleep. (b) Secondary needs (psychological) - these needs are based on a person's personality. Here we can include the need for social recognition, for security and for self-realization. If you are filled with various biological and psychological needs, then the organism is in a state called Homeostasis (balance). For example, sleep deficit organism leaves this state and is motivated to restoring homeostasis (in this case sleep). The teaching practice is important to meet the psychological needs, however, biological needs also play an important role. It is witnessed that students are not too motivated just before lunch or late evening. These are the factors that must be considered when planning for major tests and discussing more challenging curriculum.

Interestingly, the primary needs can be subdivided into more specific categories. For example, the need for hunger or thirst. At different time intervals of the day we observe the need for a particular kind of food or drink, for example, coffee or tea. The need for "specific hunger" can identify the physical needs that require balancing deficits of specific substances like fats, carbohydrates, proteins, vitamins, etc. The aforementioned example of the need for drinking tea/coffee is more commonly practiced [3].

Motivation can be further divided into internal motivation (intrinsic motivation) and external motivation (extrinsic motivation). Intrinsic motivation is based on inner motivation of man. This is his own interests and own needs. External motivation is determined by the environment, when this environment directs the man and put him on claims that are trying to accomplish. In education, we meet with both kinds of motivation. Intrinsic motivation is a natural part of children's learning. They observe spontaneous interest in learning, which is often very intense. Supporting this interest is a fundamental objective of the teaching process. Extrinsic motivation is often associated with prestige. Pupils try their surroundings (parents, teachers, classmates, etc.) to convince their success. Their reward could be a success in the evaluation. Since this is the motivation associated with the performance, we talk often about power motivation. This kind of motivation is closely associated with reward or praise. After a good performance must be followed by appropriate praise, which further motivates pupils and show an increased interest in other studies. This is supported by creativity, which is among the most important skills of scholars. As already indicated, it provides the need of external motivation and a kind of prestige among fellow classmates. Different kinds of competition within the classroom support this kind of motivation and can lead to increased performance in

the class. The highly competitive environment of the class, however, can result in too intensely experienced failure. An appropriate degree of motivation thus leads to increased student performance. Extrinsic motivation is closely connected with the social environment that surrounds the pupil outside school.

Motivation is divided according to many aspects. Individual breakdown may vary significantly and is often criticized for their sloppiness or lack thereof. One of the interesting breakdown of the model is designed by A. H. Maslow. This model is its hierarchical arrangement, progressing from basic physiological needs to higher intellectual. The model is depicted as a pyramid, with the first individual meets the needs at the base of the pyramid and subsequently needed at higher levels.

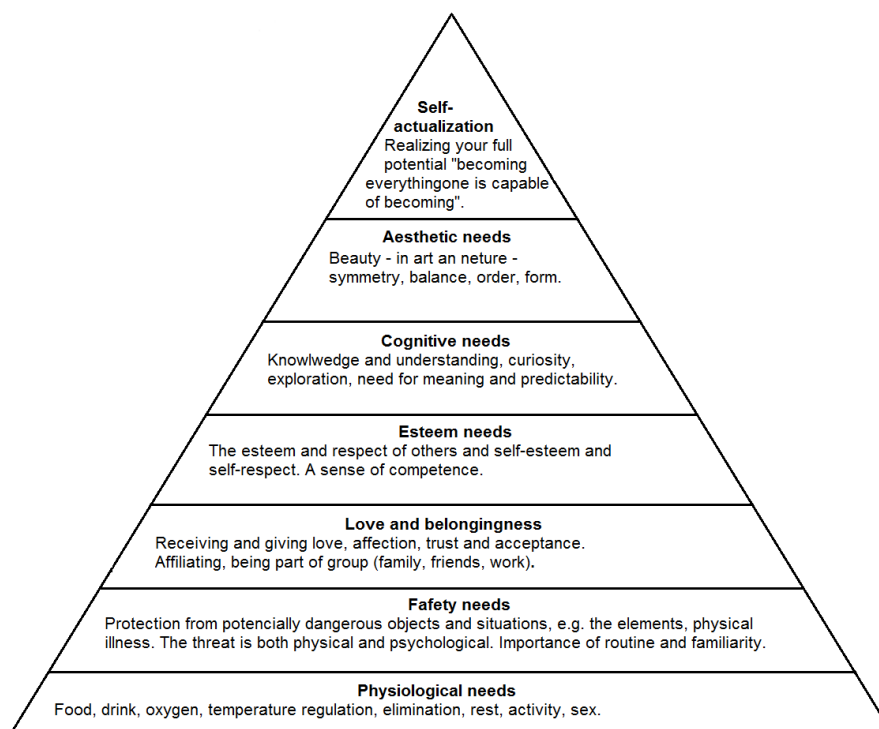


Figure 3. Maslow's Hierarchy of Needs.

One of the general division of motivation is based on the components of conscious and unconscious. Already the name suggests that these two components is related to the awareness of the various motifs. Conscious motivation is when an individual is fully aware of the motives of his/her behaviour. Conversely, unconscious motivation is the driving force of an individual without the awareness of the motives of their behaviour.

Many people today are increasingly aware of the need to start taking care of the earth. The pollution from traditional energy sources, which every day enters the air, water and soil is alarming. But the effort to start using renewable energy sources, which behave much more

friendly to nature is very improbable. Czech Republic is currently one of the countries with the cleanest air in the world, but if we do not make use of renewable energy sources and take better care of our nature, after few years, we can't go outside without a mask in our mouth. The inclusion of laboratory tasks performed on top equipment in research centres is designed to motivate students for future work and to do much advanced research in one of the domestic or international research centres.

Ecological thinking is a need to instil in children from an early age and extend this awareness while in school. The doctrine of renewable energy sources should appear in the high school curriculum to the extent that the students had a chance to decide whether to go to university to study a discipline that focuses on renewable energy sources and to prepare students for future work in this sector. The inclusion of several laboratory exercises in the course of Physics Lab can motivate students to study science for future work in the research centre. The prospective physics teachers can motivate the spread of the knowledge about renewable energy during their teaching activities.

The aim of the study, is to find a way to motivate students to study technical subjects on pedagogical faculty or on other technical faculties and subsequently teach students, work in research centres or in industry sector.

Currently, the study on technologies related to renewable energy source is a burning issue in the scientific community worldwide. Among the renewable energy sources we can also include fuel cells. A fuel cell is an electrochemical cell that converts the chemical energy from a fuel into electricity through an electrochemical reaction of hydrogen-containing fuel with oxygen or another oxidizing agent. Fuel cells can be a promising source of clean electricity in the future. Cells with less power could be used for vehicles, cells with high power could be situated in houses as one of the electricity sources. In conjunction with solar panels and/or vanadium batteries, the house may be completely energy independent.

Unfortunately the knowledge of university students about renewable energy sources, especially about fuel cells is insufficient. This fact is confirmed by the questionnaire survey.

2.2. Questionnaire survey of knowledge about renewable energy among college students

The issue of renewable energy sources, especially fuel cells, isn't sufficiently represented in teaching at primary and secondary schools. Renewable sources are neglected, even though their use is becoming increasingly important for the company and its importance is increasingly debated. Every school discuss the issue differently, so it is not clear what level of knowledge have university students. The aim of this investigation is to determine to what extent we can dominate college students to the basic terms and concepts of teaching about renewable energy. Usability survey results lies in the possibility of accurate drafting of teaching the subject in the basic university course. Processed results are also valuable feedback for secondary school and university teachers.

The questionnaire survey was conducted among 344 students of University of West Bohemia in Pilsen. Respondents were selected from students of Astronomy for everyone Astronomical knowledge on the first grade of primary school, Basic of chemistry for natural science, Organic chemistry, General and physical chemistry and Chemistry. These subjects were opened by the Department of Mathematics, Physics and Technical Education and the Department of Chemistry, Faculty of Education, and had a high attendance at the seminars. Respondents had therefore a positive approach to physics and chemistry. Investigations were carried out in the winter semester of the academic year 2016/2017.

Each question in the questionnaire has been created to monitor very basic knowledge about fuel cells. In addition to these basic questions, other questions following the fundamental concepts of the whole science of energy sources were created. In the final part of the questionnaire, students in the form of open questions should cite the fuel that is used in fuel cells.

Before completing the questionnaire, the students were informed about the anonymous questionnaire and purpose of its processing. Students were also reminded to fill in all the questions. Highlighted was the question no. 8, which assumes for a successful resolution the selection of improper claims. To complete the questionnaire there was not specified timeout, all respondents completed the questionnaire within 15 minutes of the deal. When evaluating the questionnaire, the success of solving the questionnaire depended on the age of respondents. Next we processed to draw the correlation between the successes of solving the questionnaire given to the field of study and the age of respondents.

In the first part of the questionnaire respondents filled personal information by which we can determine the age structure, the field of study, faculty or year of study. These data were

graphically presented. All dates in the each graphs are given in percentages. The questionnaires in Czech and in English language are connected (Appendix 1, 2).

From the Figure 4 is clear that a significant majority of respondents achieved the age between 20 and 22 years.

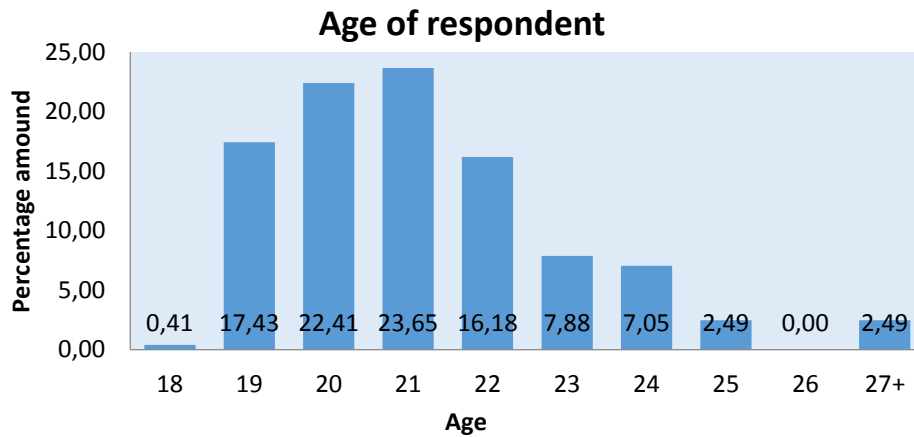


Figure 4. Age of respondent.

Each of the respondents in the questionnaire survey stated subject studied and faculty. From the data obtained, it is clear (Figure 5) that the vast majority of respondents studied on the Faculty of Education.

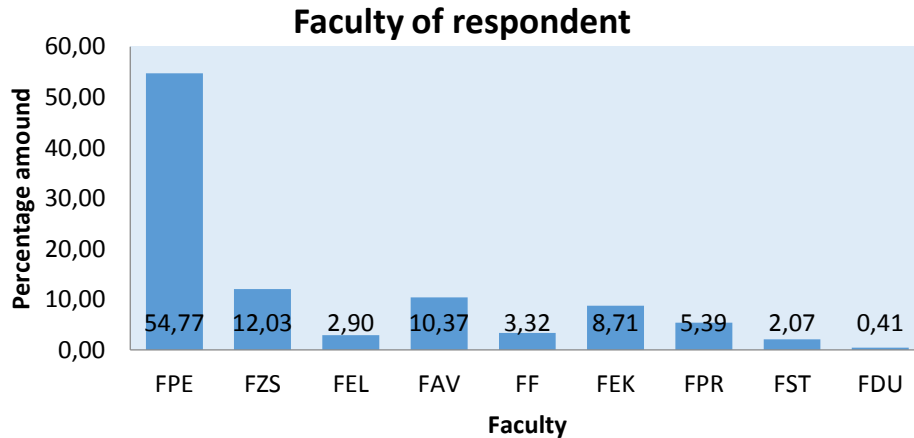


Figure 5. Faculty of respondent.

Abbreviations used of each faculties: FPE - Faculty of Education, FEL - Faculty of Electrical Engineering, FAV - Faculty of Applied Sciences, FF - Faculty of Philosophy, FEK - Faculty of Economics, FST - Faculty of Engineering, FPR - Faculty of Law and FZS - Faculty of Health Studies.

Individual items of the questionnaire were evaluated separately. For each question is given the exact wording and graph that shows the percentage distribution of responses. Questions 1-

13 were formulated as closed with a single correct answer. The respondent had a choice of four possible answers.

Question 1

Text: As fuel for the diesel engine is used:

- a) coal
- b) gasoline
- c) diesel
- d) methanol

This question follows the basic knowledge of the difference between diesel and gasoline engines, which are currently the two most used types of engines, especially for automobiles. Fuel for diesel engines is the only diesel, while gas is used in gasoline engines, methanol can be used as fuel for fuel cells and coal is not used as a fuel for engines.

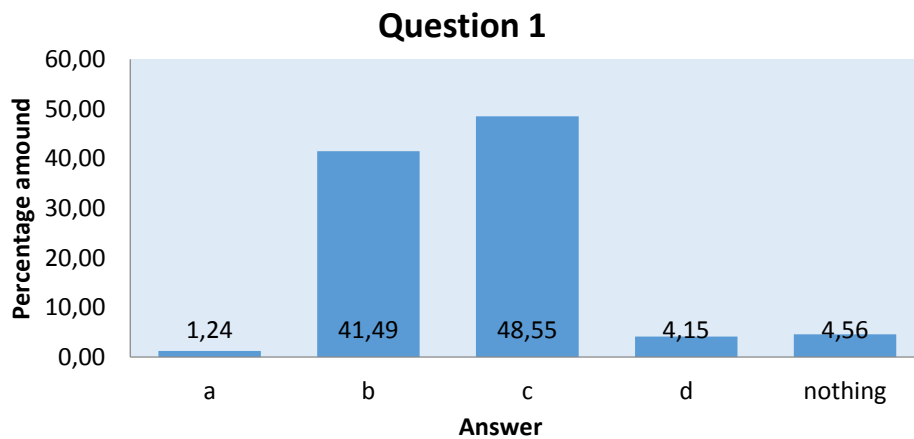


Figure 6. Question 1.

Although respondents were reminded to fill all issues and options for marking only one correct answer, they appeared questionnaires without marked answer or with labelled more answers. Because it was a very small number of such questionnaires they hadn't been excluded from the evaluation. The graphs show that most students know that we use gasoline or diesel engines. Less than half the students could not correct assign the diesel for the diesel engine.

Question 2

Text: Fuel cell:

- a) converts electrical energy to chemical
- b) use solid fuels
- c) converts chemical energy to electrical
- d) is a kind of perpetuum mobile

The second question is focused on the knowledge of the basic principle of a fuel cell which is able to convert chemical energy into electrical energy. To convert electrical energy into chemical energy don't use fuel cells, but e.g. galvanic cells or batteries. Solid fuels aren't used

in the fuel cells. Perpetuum mobile is not in accordance with the laws of thermodynamics to assemble.

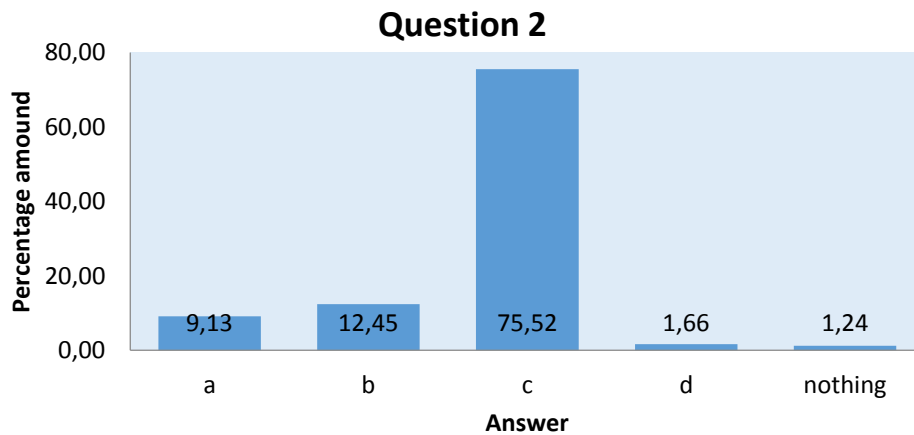


Figure 7. Question 2.

Evaluation of this item is quite unique compared to the first question. The graph shows that most students are able to identify the basic principle of the fuel cell.

Question 3

Text: PEMFC stands for:

- a) fuel cells with alkaline electrolyte
- b) fuel cells with phosphoric acid
- c) fuel cells with polymeric membrane
- d) fuel cells with solid oxide

The third question is quite difficult. All types of fuel cells exist and to determine the exact label you need to have some experience with the issue. Students can also find the correct answers from the English name for the fuel cell with a polymer membrane - polymer electrolyte membrane fuel cell (PEMFC).

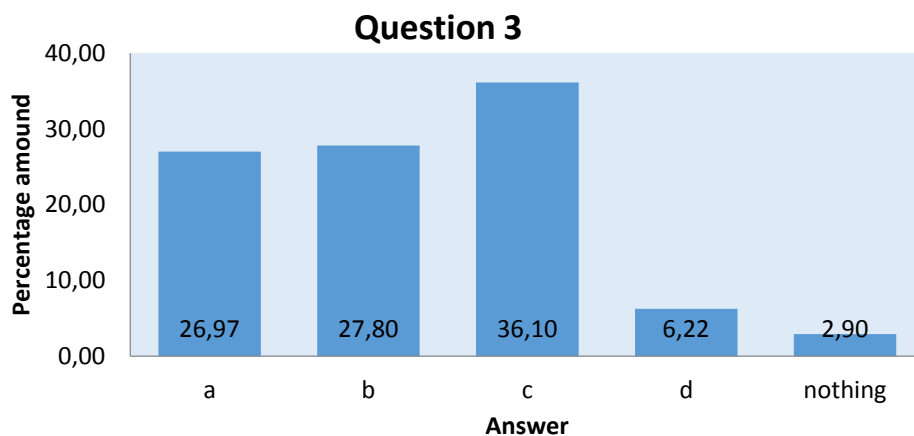


Figure 8. Question 3.

Distribution of responses shows, that the students don't have a basic overview of the types of fuel cells. Though most students have marked the correct answer c) the wrong answers have much greater advantage.

Question 4

Text: Provide the fuel that is used in fuel cells:

This question follows the material, which the respondents thought that it is used as fuel in fuel cells. There are several types of fuel cells, which are divided by the type of electrolyte. Usually pure hydrogen is used, but it is possible to use other types of fuels such as methane, methanol, propane, carbon monoxide, ammonia, hydrazine, zinc, sodium, or carbon. As an oxidizer is exclusively used pure oxygen.

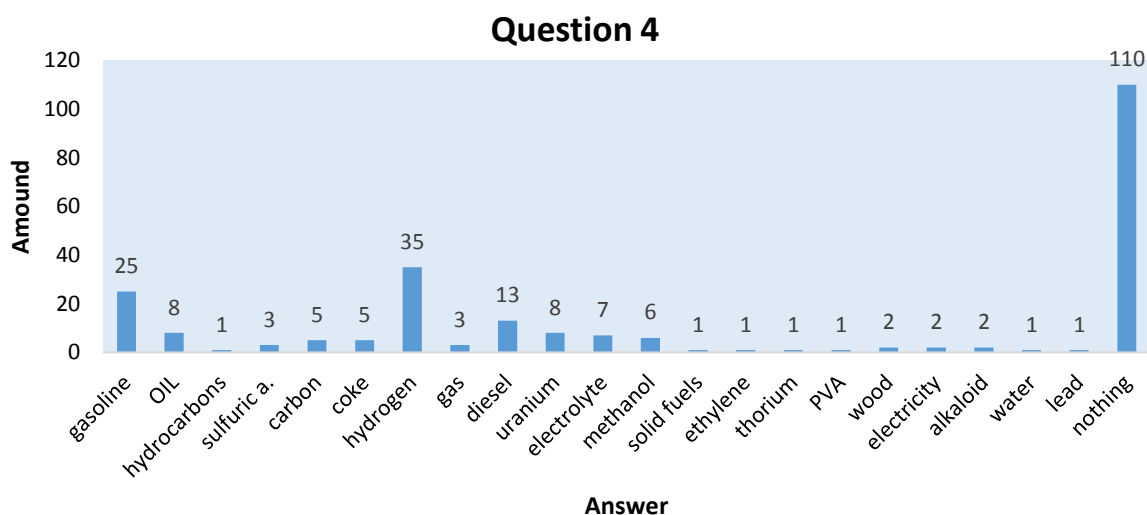
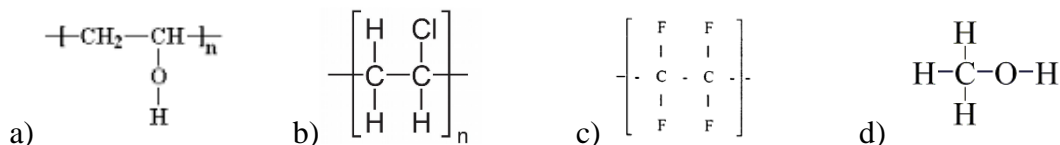


Figure 9. Question 4.

Distribution of responses shows Figure 9, where we can see that the students include the entire spectrum of fuels. 46 respondents marked one of the correct answers.

Question 5

Text: Polyvinylalcohol has the structural formula:



This issue is already focused on the knowledge of basic concepts of organic chemistry. Mentioned chemical macromolecular material has clearly defined structural formula.

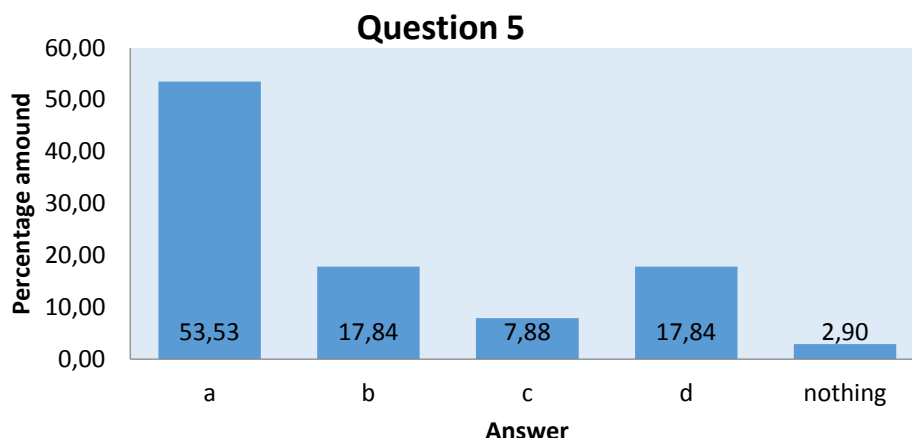


Figure 10. Question 5.

The graph shows that most students are able to correctly identify the structural formula for polyvinylalcohol. The same number of responses for b) and d) shows that students chose answer b) for polymeric character formula and the answer d) due to alcohol groups occurring in the formula.

Question 6

Text: Nafion is membrane produced on the basis of:

- a) polyvinylalcohol
- b) polysulfone
- c) hydrochloric acid
- d) polytetrafluoroethylene

Question six is very specific and examines deeper knowledge of students in the field of polymeric membranes. Nafion is one of the most commercially available polymeric membranes on the world market. The basic structure of the membrane consists sulphonated polytetrafluoroethylene. Polyvinylalcohol and polysulfone are used to produce different types of membranes. HCl itself isn't used for membranes production.

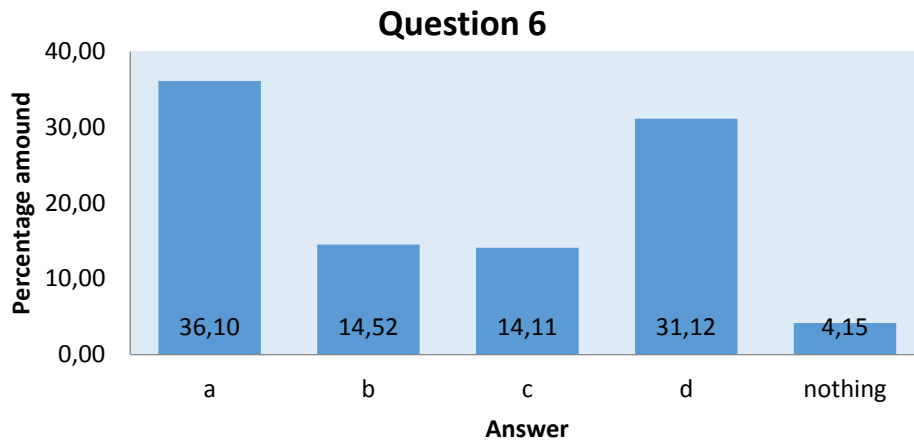


Figure 11. Question 6.

Nevertheless, the true answer d) is one of two most common answers, it is not clear that students have basic knowledge in polymer membranes.

Question 7

Text: Polymerization is a chemical reaction in which:

- a) from polymers are formed monomers
- b) from small molecules formed high molecular substances
- c) from alcohol is formed acid
- d) is formed ester and water

This question is focused on the basic knowledge of the principle of polymerization, where small molecules are formed to high-molecular structures. Answer a) is the opposite of the polymerization, c) is oxidation, d) is esterification. Polymerization is the basis chemical reaction in formation of polymeric membranes.

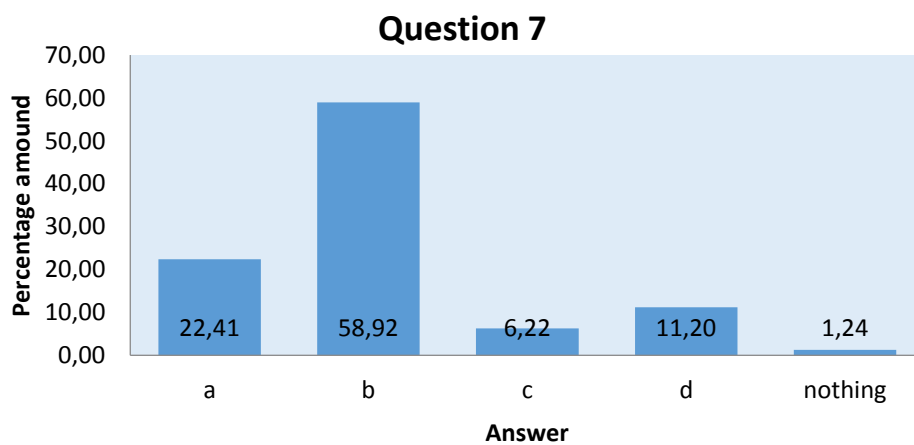


Figure 12. Question 7.

The graph shows that the vast majority of students can correctly identify the principle of polymerization.

Question 8

Text: The fuel cell **is not** formed:

- a) anode
- b) cathode
- c) membrane or electrolyte
- d) spark plug

Students were specifically warned about this question, it contains a negative response. It is focused on the composition of the fuel cell. The basic elements occurring in the fuel cell includes an anode, cathode and membrane or electrolyte.

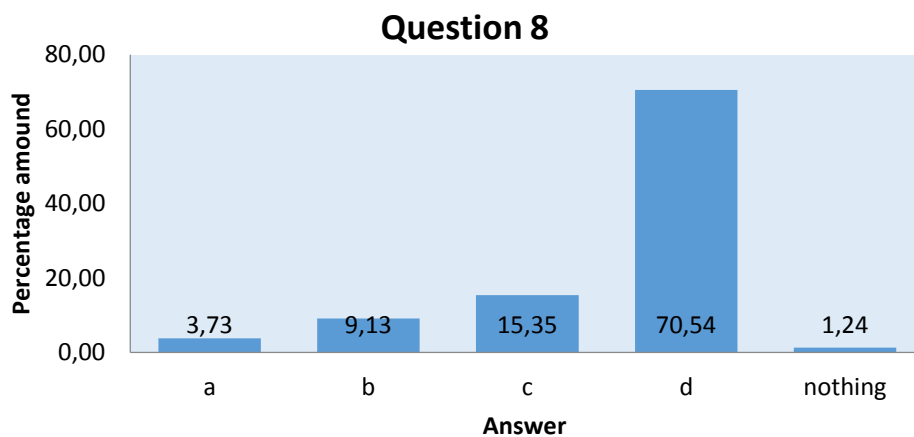


Figure 13. Question 8.

Most of the students by this question correct determined that the answer d) spark plug does not occur in the fuel cell.

Question 9

Text: Functions of the membrane in a hydrogen fuel cell is:

- a) transmit protons
- b) transmit electrons
- c) transmit gas
- d) not transmit protons

Question 9 deals with the basic functions of the membrane in a hydrogen fuel cell. Its function is to allow the hydrogen protons H^+ , electrons simultaneously go to the electric circuit.

Answer d) is the opposite of the correct answers. When through the membrane passes the gas H_2 , it is an undesirable property of the membrane.

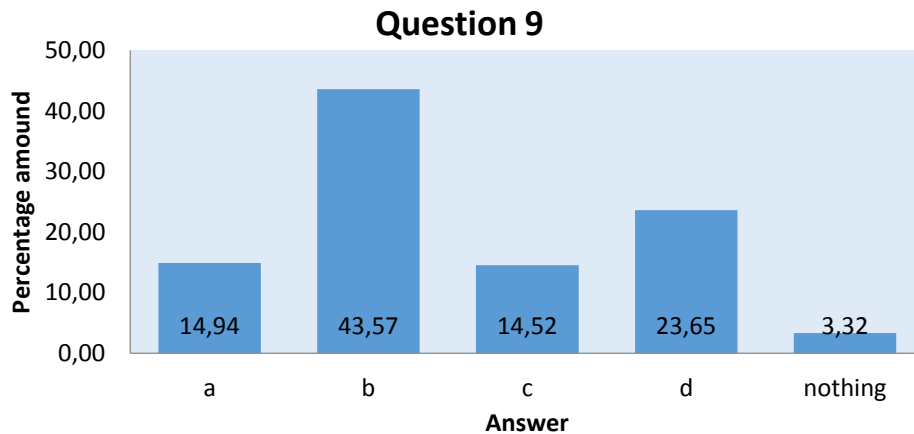


Figure 14. Question 9.

The results for this question suggest that students know the basic principle of operation of the fuel cell.

Question 10

Text: Teflon is stands for:

- a) polyvinylalcohol
- b) polytetrafluoroethylene
- c) polyethylenterephthalate
- d) polyethylenglycol

Tenth question ascertains knowledge of one of the most common polymer materials known as Teflon. Teflon is an abbreviation for polytetrafluoroethylene. It is used for many household items such as pans and tableware. Polyvinylalcohol is used for producing foils, polyethylene terephthalate particular for PET bottles, polyethylene glycol is used in the cosmetic and pharmaceutical industries.

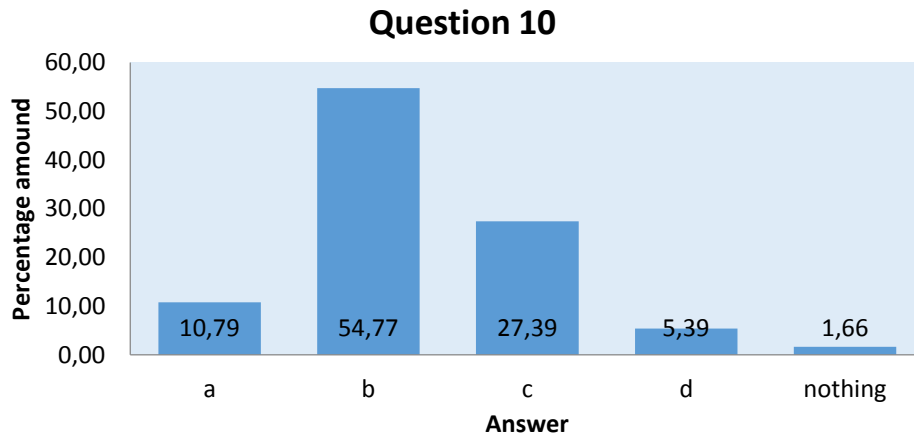


Figure 15. Question 10.

Majority of respondents correctly assigned the shortcut of Teflon to the polymer substance polytetrafluoroethylene.

Question 11

Text: Rheology is the science that deals:

- a) magnetic phenomena
- b) electrical phenomena
- c) the chemical reactivity of substances
- d) investigation and modelling of deformation properties of substances

Question 11 had examined the respondents' knowledge about one of the fundamental material science. Rheology is the science concerned with the exploration and modelling of deformation properties of substances. Magnetic and electric phenomena deals with physics, specifically electricity and magnetism, chemical reactivity of substances (generally deals with chemistry).

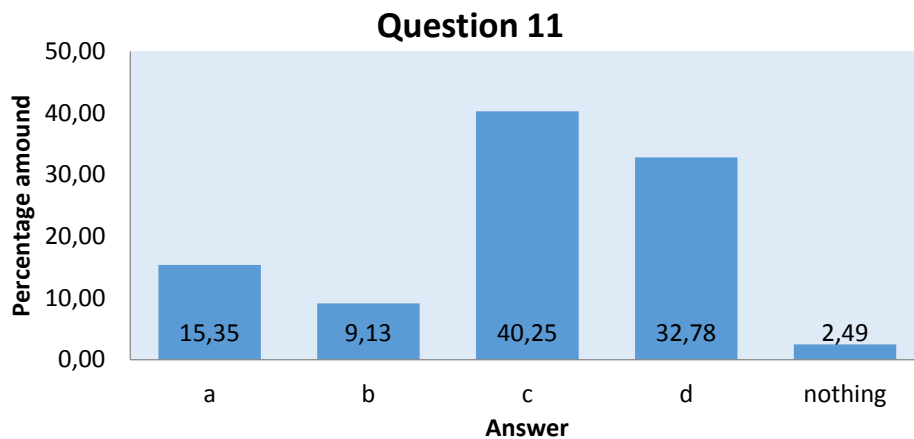


Figure 16. Question 11.

The graph shows that most of students haven't met with the concept of rheology yet.

Question 12

Text: Thermogravimetry:

- a) examine the deformation of the material in dependence on the mechanical stress
- b) examine the weight change according to the thermal changes
- c) examine the water absorption of material
- d) deal with measuring of temperature

This question seeks to investigate whether respondents are able to assign the correct process to construct thermogravimetry (TG), which examines the change in weight, depending on the thermal change. Others processes a), c), d) we can explore using DMA, DVS and thermometry in order.

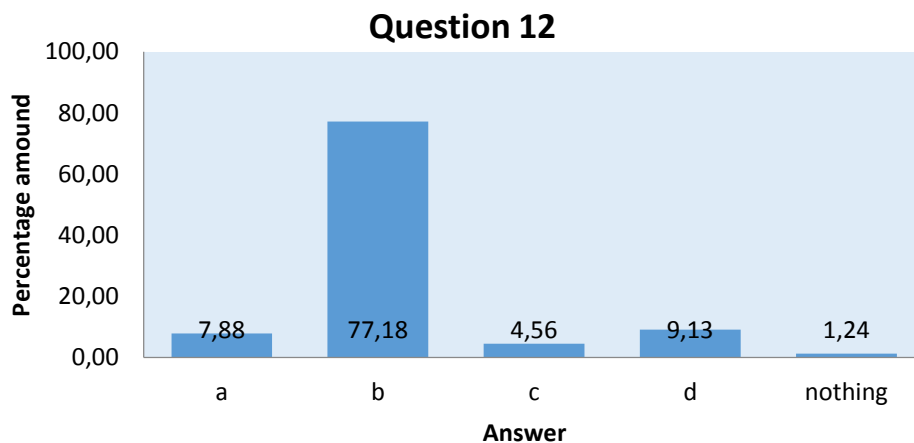


Figure 17. Question 12.

Most respondents correctly identified the thermogravimetry dealing with weight change depending on thermal changes.

Another object of the research was the dependence of the success of respondents on their age. Individual questionnaires were therefore evaluated according to the number of correct responses and subsequently divided by age respondent. In this part of the evaluation the item 4 was not included, because it is an open question, and we are able to determine more than one accurate answer for it. The maximum number of correct answers is therefore 11. This number did not reach any respondent. Only four respondents reached 10 correct answers, whereas, questions 5, 9 and 11 were answered incorrectly. The question 5 can be considered moderately difficult, as it requires a basic knowledge of chemistry. Questions 9 and 11 can be considered

more difficult for the students due to the lack of appropriate knowledge of these phenomena, and the absence of scientific disciplines dealing with these issues in the curriculum of secondary schools and higher education in most technical fields. Only one respondent filled wrong answers to all the questions. In Figure 18 you can see the graphical representation of the results obtained from the students, based on the age group and the average number of correct answer. Due to the small number of students in age 18 years, 25 years and over, these respondents form a single group. The resulting values among respondents in this group cannot be considered as relevant for a small number of students. This age group formed together only 5.35% (Figure 4) of the total number of respondents. So small sample is not representative and therefore we doubt the relevance of these data. Nevertheless the graph (Figure 18) appears to increase success in the age group of 24 years, or 22 and 19 years. The reason for this increase is not entirely clear. It is possible to deduce the relationship between this result and the course of study at a university. At the age of 22 years, is starting transition of students from the bachelor's degree program to the Master's degree program. At the age of 24 years, students are almost completing their studies, so full of masters and engineers.

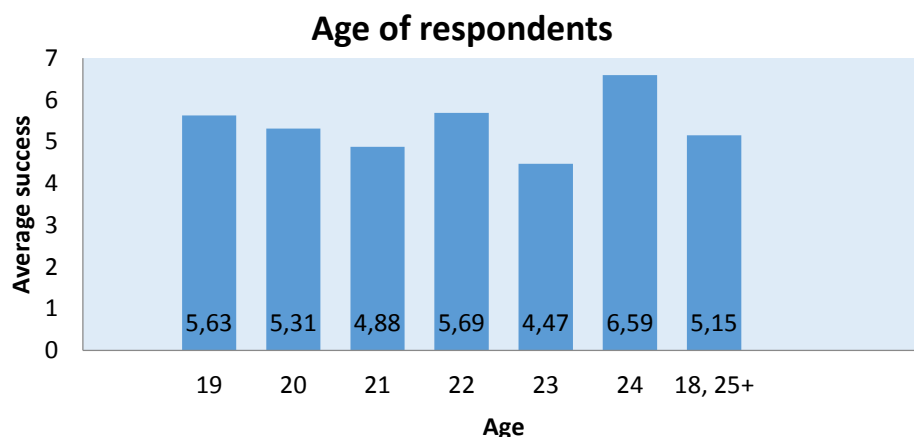


Figure 18. Age of respondent.

It was also examined the success of students depending on their field of study. From Figure 19 it is evident that most successful respondents were students of Mechanical Engineering, Faculty of Engineering, who achieved an average number the correct answers 7.2. For a successful researcher, with a gain of more than half number of points we can be considered students of Bi, Ch, ČJ, TEK, PR, IS and ZL. Table 2 gives an overview of the success of individual fields of study. Yellow color indicates the fields in which only two or less students participated in the survey. These results can be considered as relevant, and therefore were not included in the final evaluation (Figure 19).

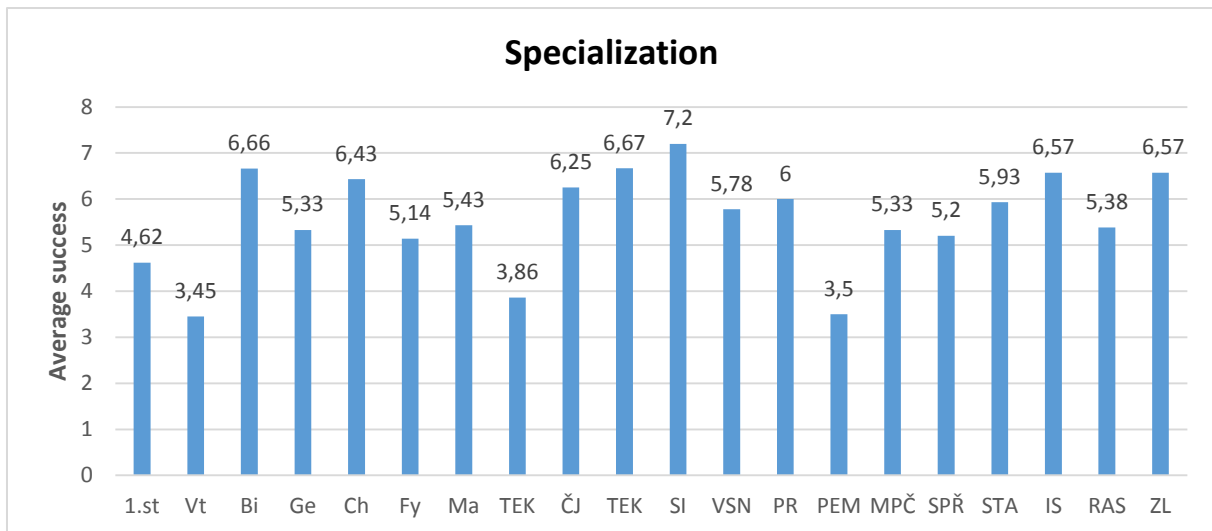


Figure 19. Age of respondents.

From the ratio of correct answers for each items we can suggest on high level of knowledge regarding the basic concepts of the science of renewable energy sources. General terms such as "fuel cell" or "thermogravimetrics" didn't create major problem to students. Also, mutual resolution Teflon and PVA can be regarded as generally successful. Conversely, surprising result were obtained for more specific questions relation to fields of polymer membranes, Nafion and function of the membranes in the fuel cell. For questions 6 students were able to connect answer a) with the previous question number 5. The results also show that the majority of students have never met with the concept of Rheology. A small number of students correctly reported at least one example in question 4, which is an obvious lack of knowledge of materials, which are used as fuel in fuel cells. Overall, I evaluated the questionnaire as a demanding and therefore relatively high proportion of correct answers is positive. The doctrine of renewable energy sources should be an integral part of teaching physics.

Questionnaire was created to monitor the knowledge of renewable energy sources, particularly fuel cells, their components and their analysis. From obtained results, it is clear that students approached individual questions separately, so that they didn't recognize continuity issues. This is fairly typical for the evaluation surveys. Students approach the issues, without realizing the possible link between these issues. In evaluation of the survey wasn't a direct link between the items, but information from one item could significantly help to solve other items. An example might be a question 3, which may be in response to questions 6 and 9 to select the answer, which contained the term "membrane". In the results, we can still observe that this answer didn't mark a predominant number of respondents.

Table 2. Fields of study			
FPE	1st grade Teacher	1.st	4,62
	Computer Science	Vt	3,45
	Biology	Bi	6,66
	Geography	Ge	5,33
	Chemistry	Ch	6,43
	Physic	Fy	5,14
	Mathematics	Ma	5,43
	Technical Education	TEK	3,86
	Music	Hv	4,5
	Applied chemistry	ACH	7
	Kindergarten Teacher	MŠK	4
	Russian language	RJ	6
	Visual culture	VV	3
	History	D	3
	English language	AJ	8
	Czech language	ČJ	6,25
Art Education	Vv	3	
FEL	Environmental Engineering	TEK	6,67
	Energetics	EN	4
FDU	Product design	DD	4
FST	Mechanical engineering	SI	7,2
FPR	Public administration	VSN	5,78
	Law and Legal Science	PR	6
FF	Sociology	So	3
	Archeology	ARCH	5
	International relationships	MV	4
	Political Science	POL	0
	General history	OD	5
	Middle Eastern Studies	BVS	4
FEK	Economic and Regional Geography	ERG	5,5
	Business Management	PEM	3,5
	Management of business	MPČ	5,33
	Project Management Systems	SPŘ	5,2
FAV	Applied and Engineering Technology	AIF	9
	Cybernetics	K5T	7
	architecture	STA	5,93
	Information Systems	IS	6,57
FZS	Radiology Asistent	RAS	5,38
	Laboratory Assistant	ZL	6,57

2.3. Tasks for Physical Laboratory practise

In the context of this work, we designed a laboratory task for Physical Laboratory 1. The students have completed this exercise in thermal laboratory New Technologies - Research Centre (NTC), Department of Engineering special materials (ISM). Total measurement is attended by four students of Faculty of Education, Natural Science Studies - Physics. Before the measurement the students were introduced to the safety methods and followed by the detail experimental procedures of the instrument. Apart from experiments, the students were also

explained regarding the interpretation of the results obtained by the thermal instruments. They were asked to measure the rheological properties of 5% PVA solution with varying concentrations of sulfosuccinic acid. The measurements were performed on a rheometer ARES G2 from TA Instruments.

The aim of this practise is an effort to bring knowledge about fuel cells, especially about polymer electrolyte membranes closer to students. Students can due to the similar measurements try to work with modern measuring instruments.

2.3.1. Manual for measurement

The manual in Czech and in English language is connected (Appendix 3, 4). Manual has 6 parties. The *Introduction* describes PVA membranes, rheology and rheometers. In *Measurement methods* is described setting the task on the rheometer ARES G2. In *Tasks* have students an accurate description of the workflow. In *Discussion* is discussed the importance of the task. The *Creating measurement record* contains tasks for students. In *Literature* are provide the appropriate resources for the task.

In the protocol students had to respond 5 questions:

- 1) Identify what is happening with the viscosity of the sample due to increasing concentrations of substances added to the PVA solution.
 - *From obtained graph (Figure 20) students were able to determine what happened with viscosity. Viscosity decrease with increasing concentrations of SSA. For concentration 0.5, 1 and 2 wt% SSA is viscosity higher then for pure PVA.*
- 2) Use literature [4] and discuss how to change the internal structure of the solution due to the concentration of the additives.
 - *Understanding the literature was worse for students. The couldn't say what happened with structure of solutions after adding SSA.*
- 3) Why is for the measurement of polymer solutions using cone and plane geometries. What other geometry types would be suitable for these solutions?
 - *Students correctly determined the use of the given geometry and designed other suitable types. Cone and plane or parallel plane are used for low viscosity solutions.*
- 4) Discuss and assess possible measurement errors.

- Possible measurement errors were correctly determined by students. For example bubbles in the solution or unequal distribution of the sample between geometries.
- 5) Describe the difference between Newtonian and non-Newtonian fluids and give at least four examples of non-Newtonian fluids.
- Students were able to find in the literature the difference between the mentioned fluids and give examples of non-Newtonian fluids.

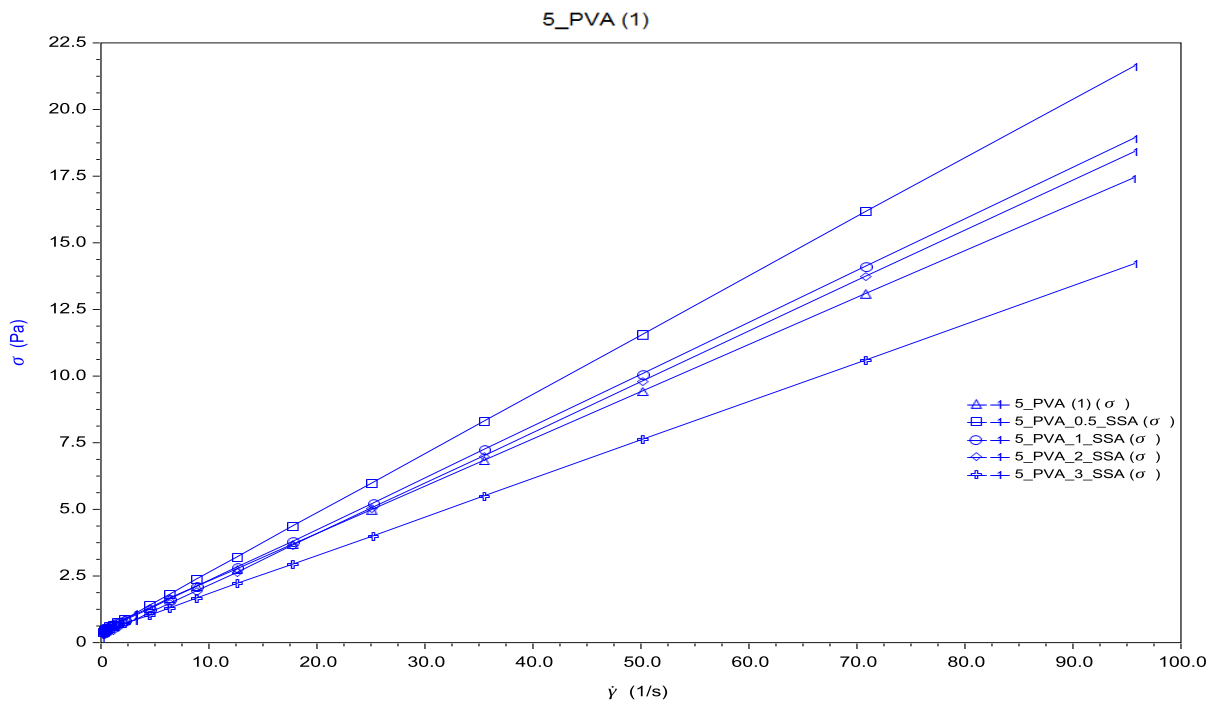


Figure 20. Viscosity of PVA_SSA solutions.

2.4. Literature

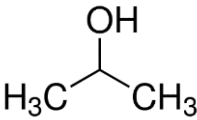
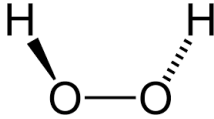
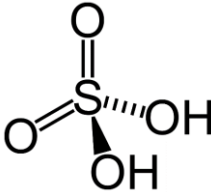
1. Skalková, J.: Obecná didaktika. Grada, 2007. 328 s. ISBN 978-80-247-1821-7
2. Pavlovský, P.: Soudní psychiatrie a psychologie. Grada Publishing, 2001. 184 s. ISBN 80-247-0181-2
3. Hošková, M., Šteflová, J.: Základní pojmy z psychologie II. díl – Pedagogická a sociální psychologie. Pedagogická fakulta v Plzni, 1980, 116 s.
4. Chien, H. C., Tsai, L. D., Huang, C. P., Kang, C. Y., Lin, J. N., & Chang, F. C. (2013). Sulfonated graphene oxide/Nafion composite membranes for high-performance direct methanol fuel cells. international journal of hydrogen energy, 38(31), 13792-13801.

3. Experimental

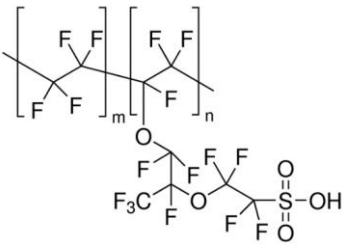
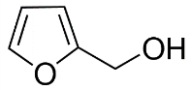
3.1. Material

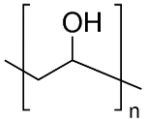
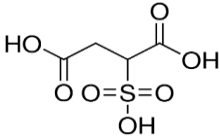
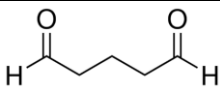
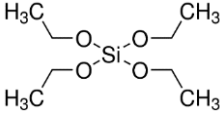
All the chemicals were of analytical grade and used as received. Deionized water was utilized for all the membrane preparation experiments.

3.1.1. Solvents

Table 3. Used solvents.			
Materials/Chemicals	Code	Chemical Structure	Company
Isopropanol	$(\text{CH}_3)_2\text{CHOH}$		Sigma Aldrich
Hydrogen peroxide	H_2O_2		Lach-Ner
Sulphuric acid	H_2SO_4		Lach-Ner
Sodium hydroxide	NaOH	$\text{Na}-\text{O}-\text{H}$	Lach-Ner
Hydrochloric acid	HCl	$\text{H}-\text{Cl}$	Merck Chemicals

3.1.2. Monomers

Table 4. Used monomers.			
Materials/Chemicals	Code	Chemical Structure	Company
Nafion 115	N115		Sigma Aldrich
Furfuryl alcohol	FA		Sigma Aldrich

Poly(vinyl alcohol)	PVA		Sigma Aldrich
Sulfosuccinic acid	SSA		Sigma Aldrich
Glutaraldehyde	GA		Sigma Aldrich
Tetraethyl orthosilicate	TEOS		Merck Chemicals

3.1.3. Tools

Magnetic stirrer with heating, magnetic stirring bars, Petri dishes, glass beakers, pipettes and pipette pumps, micropipettes and plastics tips, glass flasks, tweezers, spoon, scalpel, graduated cylinder, plexiglass plates, electric oven, automatic film applicator.

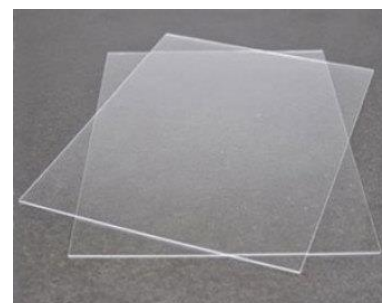


Figure 21. a) electric oven, b) automatic film applicator, c) plexiglass plates.

3.2. Membrane preparation

3.2.1. Modification of Nafion

The chemical modification of Nafion 115 membranes by poly(furfuryl alcohol) (PFA) is shown in Scheme 1. Commercial N115 membrane sheet was cut in the size 50x50 mm and boiled in 2% hydrogen peroxide (12,6 ml 30% H₂O₂ + 200 ml H₂O) at the temperature 90°C for 1 hour. The obtained membranes were then rinsed with deionized water and boiled in 0.5

M sulphuric acid (5.3 ml H₂SO₄ + 194.7 ml H₂O) following the same conditions as H₂O₂, in order to remove the impurities present in the membranes. The acid treated membranes were thoroughly washed with distilled water. They were then immersed in 0.5 M NaOH and heated at 90°C for 1 h, to convert the membrane into Na⁺ form. This helps to improve the mechanical properties of the membrane and to withstand the following process. Subsequently, they were rinsed in water and dried in the oven at 80°C for 30 min. The purified Na⁺ membranes were immersed in solution mixture consisting of 13.9 ml furfuryl alcohol (FA), 46 ml isopropanol and 36 ml deionized water for 24 h, 48 h and for 120 h, respectively (represented as NF24, NF48 and NF120). Further, the impregnated membranes were transferred into a 1.0 M sulfuric acid solution (10.7 ml H₂SO₄ + 189.3 ml H₂O) at room temperature for 2 min, and placed in an oven at 80°C for 2 days to initiate polymerization of the FA inside the Nafion. Membranes were prepared based on the work [1]. The assimilation of PFA into Nafion matrix is shown in Figure 22.

To test the repeated loading of these membranes, modified NF24 membrane was activated and was immersing in the FA solution mixture for the next 24 h (NF24×2), and again for next 24 h (NF24×3).

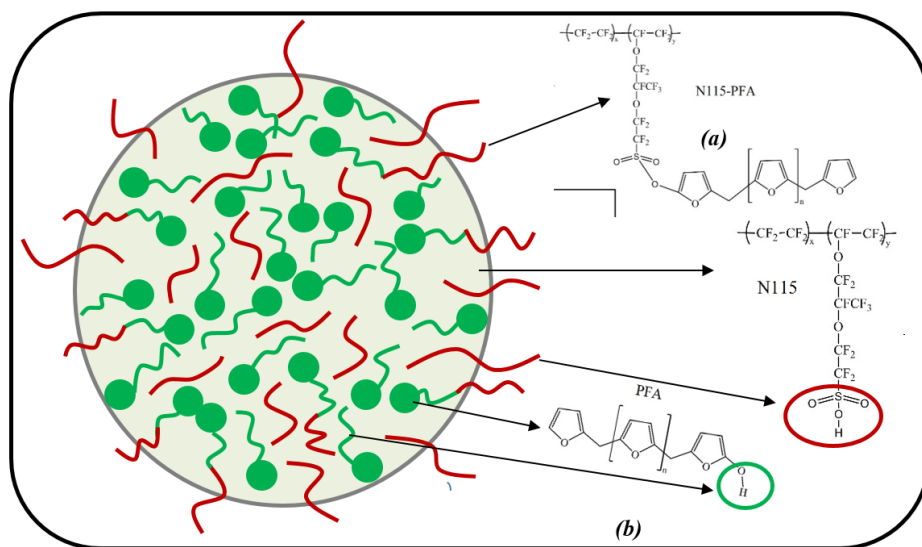
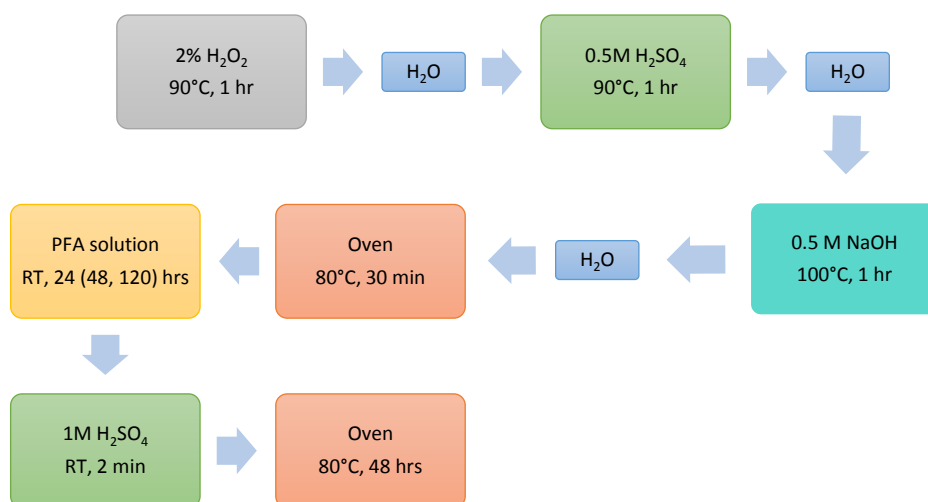


Figure 22. Incorporation of PFA into Nafion domains via *in-situ* polymerization.

Table 5. - Immersion of Nafion 115 in PFA	
Immersion in PFA solution	Sample code
24 hours	NF24
48 hours	NF48
120 hours	NF120
2x24 hours	NF24x2
3x24 hours	NF24x3



Scheme 1. Chemical modification of N 115 membrane.

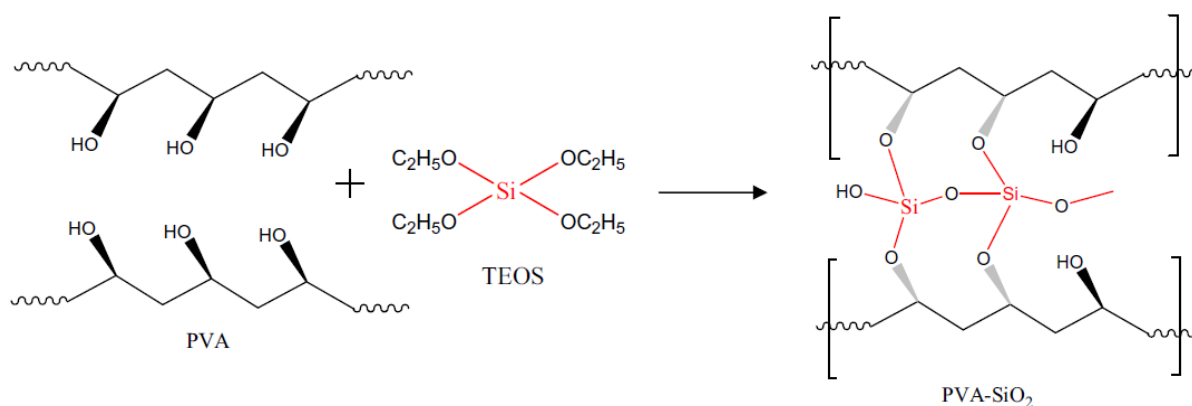
3.2.2. Preparation of PVA membranes

a) PVA/SiO₂/GA composite membranes

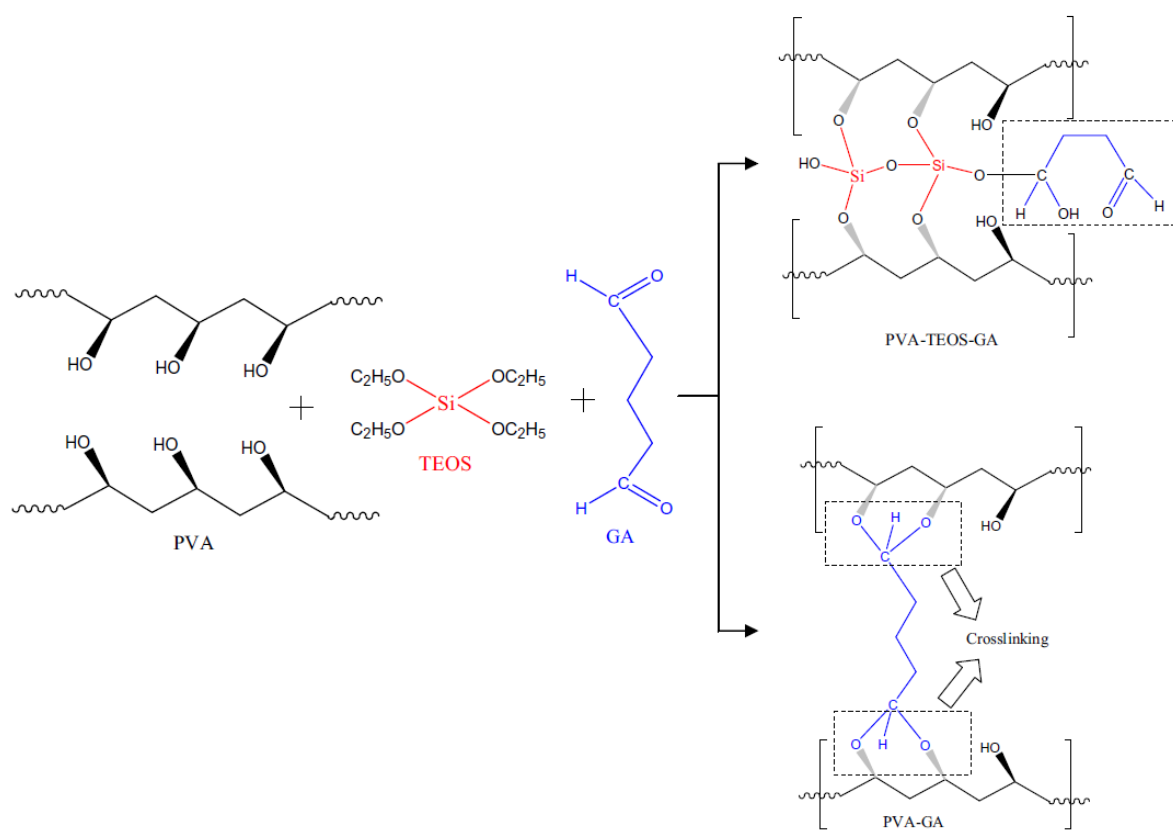
Composite PVA/SiO₂/GA membranes were developed by the solution casting method. Firstly, PVA (5 wt% in water) solution was prepared by continuous stirring at 90°C until the complete dissolution was achieved. Subsequently, TEOS mixtures and GA were directly added to the PVA solution at room temperature and the stirring was continued for 4 h. The composition of each solution is specified in Table 6. The prepared solution was poured into the film applicator equipped with a glass plate and was fabricated into membranes with uniform thickness. The expected reactions and membrane structures are shown in Schemes 2 and 3.

Table 6. - Composition of polymer solutions, PVA, TEOS, GA

Sample	Solution mixture	Composition
5PVA	5% PVA	25ml H ₂ O, 1.25g PVA
5PVA_1TEOS	5% PVA, 1%TEOS	25ml H ₂ O, 1.25g PVA, 0.25ml TEOS (0.00625ml HCl, 0,0625ml H ₂ O)
5PVA_2TEOS	5% PVA, 2%TEOS	25ml H ₂ O, 1.25g PVA, 0.5ml TEOS (0.0125ml HCl, 0,125ml H ₂ O)
5PVA_3TEOS	5% PVA, 3%TEOS	25ml H ₂ O, 1.25g PVA, 0.75ml TEOS (0.01875ml HCl, 0,1875ml H ₂ O)
5PVA_4TEOS	5% PVA, 4%TEOS	25ml H ₂ O, 1.25g PVA, 1ml TEOS (0.025ml HCl, 0,25ml H ₂ O)
5PVA_1GA	5% PVA, 1%GA	25ml H ₂ O, 1.25g PVA, 0.25ml GA
5PVA_2GA	5% PVA, 2%GA	25ml H ₂ O, 1.25g PVA, 0.5ml GA
5PVA_3GA	5% PVA, 3%GA	25ml H ₂ O, 1.25g PVA, 0.75ml GA
5PVA_4GA	5% PVA, 4%GA	25ml H ₂ O, 1.25g PVA, 1ml GA
5PVA_1TEOS_1GA	5% PVA, 1%TEOS_1%GA	25ml H ₂ O, 1.25g PVA, 0.25ml TEOS (0.00625ml HCl, 0,0625ml H ₂ O), 0.25ml GA
5PVA_1TEOS_2GA	5% PVA, 1%TEOS_2%GA	25ml H ₂ O, 1.25g PVA, 0.25ml TEOS (0.00625ml HCl, 0,0625ml H ₂ O), 0.5ml GA
5PVA_1TEOS_3GA	5% PVA, 1%TEOS_3%GA	25ml H ₂ O, 1.25g PVA, 0.25ml TEOS (0.00625ml HCl, 0,0625ml H ₂ O), 0.75ml GA
5PVA_1TEOS_4GA	5% PVA, 1%TEOS_4%GA	25ml H ₂ O, 1.25g PVA, 0.25ml TEOS (0.00625ml HCl, 0,0625ml H ₂ O), 1ml GA



Scheme 2. Expected chemical reactions during the formation of the PVA/SiO₂ membranes.

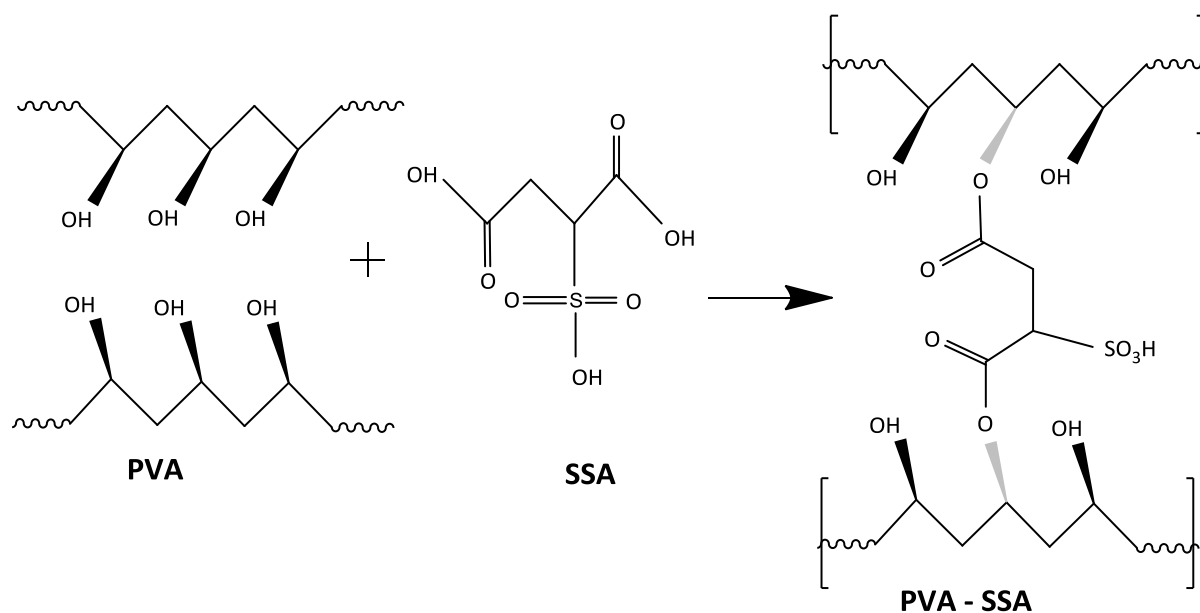


Scheme 3. Expected chemical reactions during the formation of the PVA/SiO₂/GA membranes.

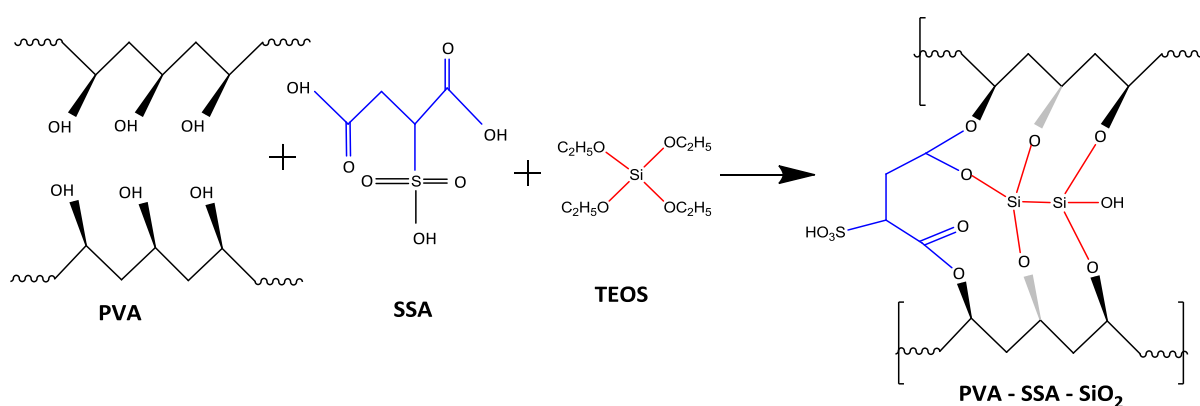
b) PVA/SSA/TEOS membranes

PVA/SSA membranes were fabricated by solution casting method. At first, a 5 wt% solution of PVA (1.25 g PVA + 25 ml H₂O) in water was prepared by continuous stirring at 90°C until the complete dissolution was achieved (2 – 3 hours). The PVA solution was mixed

with SSA for 24 h at room temperature. Further, TEOS mixture was prepared by mixing H₂O, HCl and TEOS in the molar ratio of 4:0.1:1, which was stirred at room temperature for 2 h [2] and added to the PVA-SSA solution. The composition of each solution is specified in Table 7. The prepared solution was poured into the automatic film applicator (TQC, Germany) equipped with a plexiglass plate and was fabricated into membranes with uniform thickness and dried at 40°C.



Scheme 4. Expected chemical reactions during the formation of the PVA/SSA membranes.



Scheme 5. Expected chemical reactions during the formation of the PVA/SSA membranes.

Table 7. - Composition of polymer solutions, PVA, SSA, TEOS		
Sample	Solution mixture	Composition
5PVA	5% PVA	25ml H ₂ O, 1.25g PVA
5PVA_0.5SSA	5% PVA, 0.5%SSA	25ml H ₂ O, 1.25g PVA, 0.125ml SSA
5PVA_1SSA	5% PVA, 1%SSA	25ml H ₂ O, 1.25g PVA, 0.25ml SSA
5PVA_2SSA	5% PVA, 2%SSA	25ml H ₂ O, 1.25g PVA, 0.5ml SSA
5PVA_5SSA	5% PVA, 5%SSA	25ml H ₂ O, 1.25g PVA, 1.25ml SSA
5PVA_10SSA	5% PVA, 10%SSA	25ml H ₂ O, 1.25g PVA, 2.5ml SSA
5PVA_1TEOS	5% PVA, 1%TEOS	25ml H ₂ O, 1.25g PVA, 0.25ml TEOS (0.00625ml HCl, 0,0625ml H ₂ O)
5PVA_2TEOS	5% PVA, 2%TEOS	25ml H ₂ O, 1.25g PVA, 0.5ml TEOS (0.0125ml HCl, 0,125ml H ₂ O)
5PVA_5TEOS	5% PVA, 5%TEOS	25ml H ₂ O, 1.25g PVA, 1.25ml TEOS (0.032ml HCl, 0,32ml H ₂ O)
5PVA_10TEOS	5% PVA, 10%TEOS	25ml H ₂ O, 1.25g PVA, 2.5ml TEOS (0.064ml HCl, 0,64ml H ₂ O)
5PVA_0.5SSA_1TEOS	5% PVA, 0.5%SSA, 1%TEOS	25ml H ₂ O, 1.25g PVA, 0.125ml SSA, 0.25ml TEOS (0.0064ml HCl, 0,064ml H ₂ O)
5PVA_0.5SSA_2.5TEOS	5% PVA, 0.5%SSA, 2.5%TEOS	25ml H ₂ O, 1.25g PVA, 0.125ml SSA, 0.625ml TEOS (0.016ml HCl, 0,16ml H ₂ O)
5PVA_3SSA_5TEOS	5% PVA, 3%SSA, 5%TEOS	25ml H ₂ O, 1.25g PVA, 0.75ml SSA, 1.25ml TEOS (0.032ml HCl, 0,32ml H ₂ O)
5PVA_5SSA_5TEOS	5% PVA, 5%SSA, 5%TEOS	25ml H ₂ O, 1.25g PVA, 1.25ml SSA, 1.25ml TEOS (0.032ml HCl, 0,32ml H ₂ O)
5PVA_10SSA_5TEOS	5% PVA, 10%SSA, 5%TEOS	25ml H ₂ O, 1.25g PVA, 2.5ml SSA, 1.25ml TEOS (0.032ml HCl, 0,32ml H ₂ O)

3.3. Experimental technique

Prepared and modified membranes were investigated by following methods:

3.3.1. Water uptake measurements

The water uptake studies were carried out:

- a) at temperatures from 30 to 90°C with a 20°C step. The membranes were placed in deionized water, heated to 30°C and kept at this temperature for 1h at ambient pressure. The wet membranes were then wiped with a filter paper and weighted. Temperature was then increased by 20°C and the whole process was repeated until the data were acquired at all desired temperatures.
- b) at 24, 48 and 120 h at room temperature. The membranes were placed in deionized water for specified time. The wet membranes were then wiped with a filter paper and weighted.

The water uptake (W_u) was calculated using the following equation:

$$W_u = \frac{W_s - W_d}{W_d}, \quad (8)$$

where W_s and W_d are the weights of swollen and dry membranes, respectively.

3.3.2. Thermogravimetric Analysis (TGA)

Dynamic TG analyses were performed to assess the relative thermal stabilities of the polymer membranes. TGA Q500 thermogravimetric analyser (TA Instruments, USA) was used to evaluate the relative thermal stability of the pure N115 and N115-PFA membranes. Samples of about 5 mg were heated at a rate of 10°C/min in N₂ atmosphere. The weight of the samples was measured as a function of temperature/time.

3.3.3. Dynamic Mechanical Analysis (DMA)

Dynamic mechanical measurements of polymeric membranes were performed using a TA Instruments DMA Q800 (USA) to determine the storage modulus, loss modulus and $\tan \delta$. Samples of sizes 17x5 mm and thickness 0.1 mm were used for the measurements. Experiments were performed at frequencies of 1, 10 and 20 Hz, from room temperature to 450°C (at a heating rate of 5°C/min). The phase angle shift between stress and strain is represented by δ .

$$\frac{E''}{E'} = \tan(\delta), \quad (9)$$

where E' is storage modulus (elastic component) and E'' is loss modulus (viscous component) of the material. The glass transition temperature (T_g) of a material is obtained from the peak of $\tan \delta$ vs. temperature data. The temperature dependence of the storage modulus (E') was measured in the range from 30 to 200°C. At higher temperatures (>150°C), where the material enters the rubbery phase, the storage modulus is referred to as rubbery modulus, E_R .

3.3.4. Rheology

The rheological studies of the PVA solutions were measured on a rheometer ARES G2 from TA Instruments. The polymer solutions were inserted between two parallel plate geometries ($d = 25$ mm). For each measurement, the shear rate from 0.1 to 100 s⁻¹, for a duration 30 s was carried out at room temperature. Membranes were cut ($d = 25$ mm) and inserted

between two parallel plate geometries ($d = 25$ mm). For these measurements angular frequency from 1 to 100 $\text{rad}\cdot\text{s}^{-1}$, strain 5%, was used.

3.3.5. Fourier Transform Infrared Spectroscopy (FTIR)

FT-IR studies of membranes were performed using NICOLET 380-FTIR spectrometer in ATR mode with ZnSe crystal and the spectra were corrected on single-bounce ATR environment. Analysis was conducted in the spectral range of 400 – 4000 cm^{-1} , with angle of incidence at 45° and sample refractive index of 1.5.

3.3.6. Dynamic Vapor Sorption (DVS)

The Dynamic Vapor Sorption (DVS-ET) unit provided by Surface Measurement System was utilized to measure the water vapour sorption properties of the individual sample. The sorption tests were conducted at 25°C . The sorption test procedure consisted of two cycles. The first part of the test procedure was represented by drying the sample at 0% relative humidity (RH) and at the desired temperature for 18 h by dry nitrogen with volumetric flow 150 ml/min. The second part of the test procedure was represented by humidifying the sample at $RH = 95\%$ with accuracy $\pm 0.7\%$ and desired temperature for 48 h by wet nitrogen with volumetric flow 150 ml/min. The desired RH was set by the DVS-ET unit by mixing of the dry and wet nitrogen. Figure 22 shows typical cycle of the test procedure. During the test procedure mass changes of the individual samples were measured with ultra-balance with sensitivity 0.1 μg . The obtained data were used for determination of the water vapour uptake of the individual sample. An influence of the sample modification on the individual sample is studied in the selected times of the second part of the test procedure, i.e. in times 0, 0.5, 1, 6, 12, 24 and 48 h.

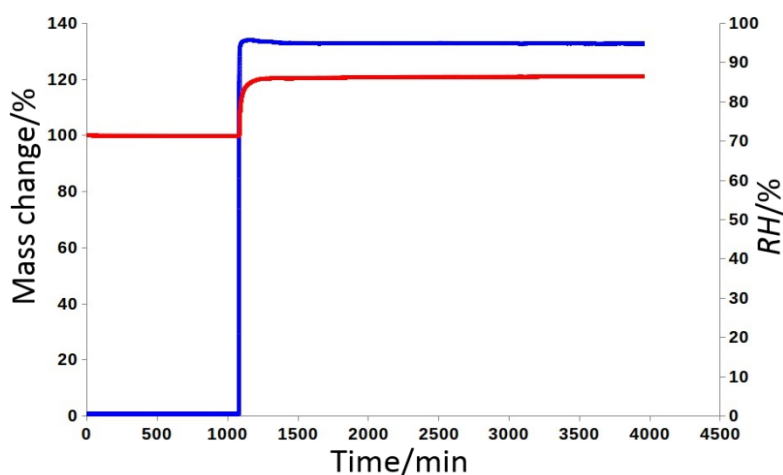


Figure 22. Cycles of the test procedure.

3.3.7. SAXS/WAXS

The SAXS/WAXS experiments were performed on a SAXSess mc² instrument (Anton Paar, Austria). The instrument uses a GeniX Microfocus X-ray point source with a Cu anode (50 kV and 1 mA), single-bounce focusing X-ray optics, and an advanced collimation block. This configuration enables to measure in point collimation geometry only. The experiments were performed in the standard transmission setup, and imaging plates together with the CyclonePlus[®] Reader (PerkinElmer, Inc.) were used for detection. The sample exposure time was 30 min and four pieces of the membranes were stacked for each measurement. The range of the scattering vector magnitude for the used experimental setup starts at about 0.2 nm⁻¹ and goes up to 28 nm⁻¹. It therefore covers both the SAXS and the WAXS range. The scattering vector magnitude q is defined as $q = (4\pi/\lambda) \sin\theta$, where λ is the X-ray wavelength (0.15418 nm for Cu K α) and θ is the half-scattering angle (Bragg angle). The 1D radial intensity profiles were created from the measured 2D patterns by azimuthal averaging using the SAXSquant software (Anton Paar, Austria), which could be performed thanks to the azimuthal symmetry of these patterns (indicating the isotropic nature of the investigated samples).

3.3.8. Electrical impedance

The ionic conductivity was obtained by measuring the impedance of the membranes at room temperature. To ensure the proper contact, each membrane was inserted between two liquid mercury electrodes with a diameter of 4 mm (Figure 23). The spectra were obtained on a Solartron 1287A/1260 impedance spectra analyser in the frequency range of 10⁻¹ to 10⁶ Hz at amplitude value of the AC signal 10 mV. Ionic conductivity was calculated using the following equation:

$$\sigma = \frac{l}{S \cdot R}, \quad (10)$$

where σ is the ionic conductivity of the membrane [S/cm], S is the membrane area [cm²], l is the membrane thickness [cm], R and represents the impedance of the membrane [Ω] at zero loss angle. Equivalent circuit simulating measurements were compiled using ZPlot[®] software and a subsequent fit for each spectrum was performed using ZView[®] software.

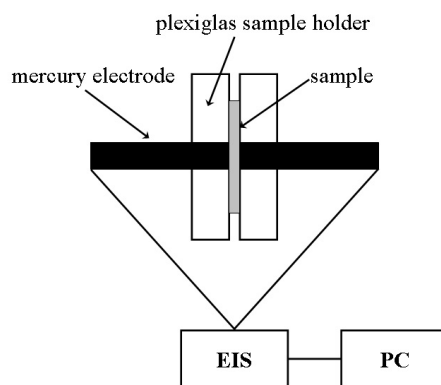


Figure 23. Model of used equipment for the impedance measurement.

3.3.9. Raman spectroscopy

The Raman measurements were carried out on a DXR Raman microscope (Thermo Scientific, USA). Three excitation lasers (532, 633, and 780 nm) and four apertures (slit and pinhole, 25 and 50 μm) were tested. The best results were obtained using the 532 nm laser with the 50- μm pinhole aperture. This configuration was thus used for all measurements. The laser power was set to 10 mW and 1000 scans with a 1-s exposure time were recorded for each spectrum. To check sample homogeneity and eliminate any possible artifacts, at least four spectra at different points were collected for each sample. Since the bands relevant to this study are in the range from approximately 800–1700 cm^{-1} , we used the high-resolution grating for all experiments. This grating provides the spectral resolution of 2 cm^{-1} in the range from 70 to 1870 cm^{-1} . The band at 855 cm^{-1} was not influenced by adding TEOS or GA [3] and was therefore used for the intensity normalization of the Raman spectra, when required for evaluation purposes.

3.3.10. Atomic force microscopy

The morphological measurements were conducted on the atomic force microscope Ntegra (NT–MDT, Russia) in the semi-contact mode. Several semi-contact probes were tested and the probe HA–NC (also NT–MDT) with a force constant of 3.5 N/m was chosen as the most suitable for the morphological mapping of prepared PVA membranes. The typical scanning frequency was 0.6 Hz and the free oscillating amplitude (FOA) was 1.8 V. The set point amplitude (SPA) was individually chosen for each sample to the value of $\text{SPA} = 0.5 \cdot \text{FOA}$. The NT–MDT software allows the scanning of four images during one AFM scan. We scanned two topological images (trace and retrace), one phase image and one magnitude image. The magnitude image was recorded for each measurement and helped in nonambiguous image

interpretations. A comparison of the trace and retrace images allows in excluding artifacts which could be created by wrong SPA.

3.3.11. Differential scanning calorimetry

A DSC Q200 differential scanning calorimeter (TA Instruments, USA) was used to measure the phase transition behaviour of the membranes. Samples of about 5 mg were weighed into a DSC aluminium pan. Dynamic heating scans were carried out from 50 to 300°C at a heating rate of 10°C/min in N₂ atmosphere.

3.4. Literature

1. Liu, J., Wang, H., Cheng, S., & Chan, K. Y. (2005). Nafion–polyfurfuryl alcohol nanocomposite membranes for direct methanol fuel cells. *Journal of Membrane Science*, 246(1), 95-101.
2. Rhim, J. W., Park, H. B., Lee, C. S., Jun, J. H., Kim, D. S., & Lee, Y. M. (2004). Crosslinked poly (vinyl alcohol) membranes containing sulfonic acid group: proton and methanol transport through membranes. *Journal of Membrane Science*, 238(1), 143-151.
3. Martinelli, A., Matic, A., Jacobsson, P., Börjesson, L., Navarra, M. A., Fericola, A. & Scrosati, B. (2006). Structural analysis of PVA-based proton conducting membranes. *Solid State Ionics*, 177(26), 2431-2435.

4. Results and discussion

4.1. Modification of Nafion® 115 by polyfurfuryl alcohol.

In the present work, we synthesized N115-PFA composites using the same procedure as mentioned in [1], however the impregnation time of membranes in PFA solution was gradually increased from 24 h to 120 h, to investigate the influence of PFA loading on the performance of the membranes. The resultant membranes were characterized by ATR-FTIR, SAXS/WAXS, TGA, DMA, Wu, DVS and electrical impedance. Additionally, we also examined the effect of repeating the impregnation process on the properties of the composite membranes.

4.1.1. FT-IR ATR

Figure 24 shows the FT-IR ATR spectra of the N115 and NF24×3 membranes. It was reported that the spectral bands at 1056, 982 and 967 cm^{-1} are ascribed to the characteristic functional groups of Nafion [2]. The intensities of these bands decreased with increasing perturbation of the sulfonate group influence of assimilation of PFA into Nafion matrix. The bands at 1711, 1510 and 890 cm^{-1} are attributed to furan rings [3, 4]. Aliphatic segments give rise to the bands at 2920, 2848 and 1421 cm^{-1} , whereas the signal at 3449 cm^{-1} is assigned to the stretching of the -OH end groups in the PFA [5, 6]. These results clearly confirm that the PFA was successfully incorporated into Nafion membrane.

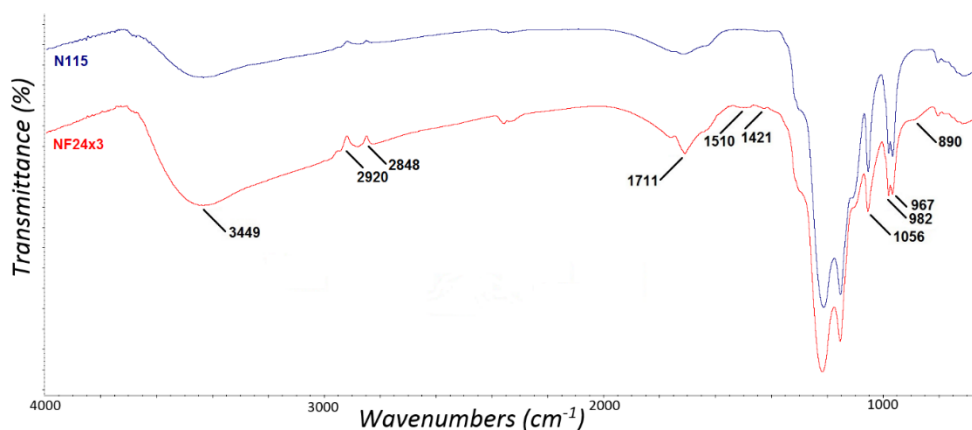


Figure 24. FT-IR ATR spectra of N115 and NF24×3.

4.1.2. SAXS/WAXS

Figure 25 shows SAXS/WAXS profiles of the pure N115 and the composites. The profile of pure N115 shows two pronounced peaks in the SAXS range and two broad diffraction

maxima in the WAXS range. The peak at around 5 \AA^{-1} represents the “matrix peak” and is related to Teflon-like (fluorocarbon) hydrophobic domains [7]. The corresponding d-spacing (spacing of crystalline domains) lies around 11–12 nm. The peak at approximately 0.2 \AA^{-1} is called “ionomer peak” and it corresponds to a characteristic dimension within the ionic (hydrophilic) domains formed from the Nafion side chains terminated by sulfonic groups [7]. The corresponding d-spacing is approximately 3 nm. The broad diffraction peaks in the WAXS range (with the maxima at 5.2 \AA^{-1} and 2.3 \AA^{-1}) can be attributed to the internal structure of the Teflon-like domains [8].

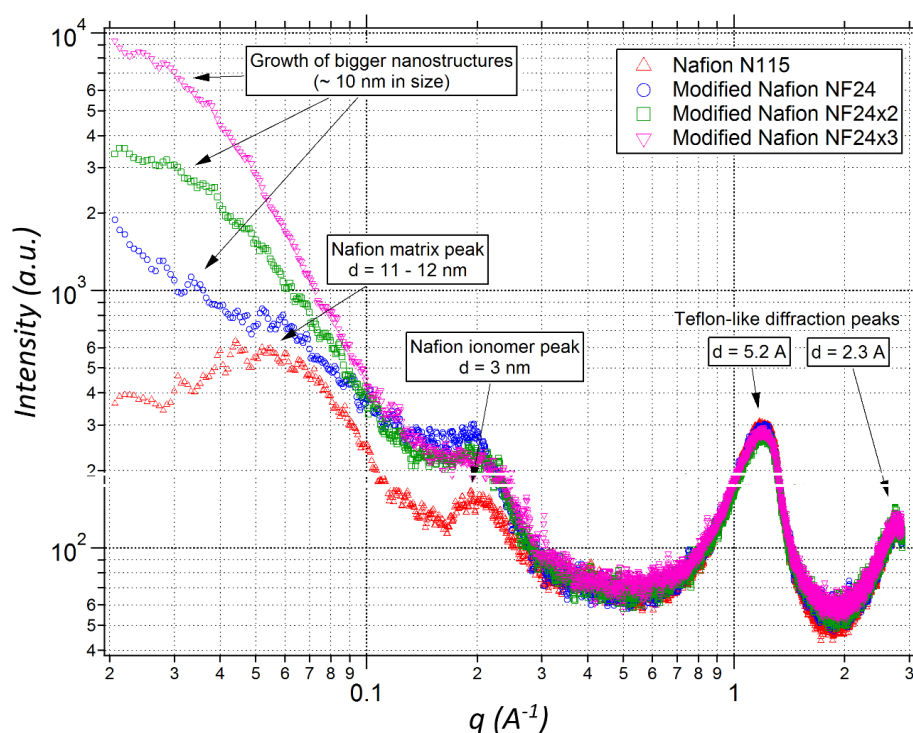


Figure 25. SAXS/WAXs profile of N115, NF24, NF48 and NF120 membranes.

It can be seen that the position of the ionomer peak does not virtually change after the modification. The change of its intensity can be caused by a change in the scattering contrast (related to the difference of the electron density) due to the incorporation of the PFA into the polymer. The structure of NF48 and NF120 samples is similar to N115 graph, whereas in case of NF24, NF24×2 and NF24×3 a shoulder at low q arises indicating the formation of nanostructure or a distribution of nanostructures with a size of approximately 10 nm. Their quantity increases from NF24 to NF24×3. The shoulder is superimposed on the matrix peak, which can be well seen in the profile of NF24. For NF24×2 and NF24×3 no matrix peak is observed any more, which does not necessarily mean that it is not present. The peak can be “covered” by the increasing intensity of the above mentioned shoulder.

4.1.3. Thermal analysis

In the present investigation, TGA was utilized in two ways: (a) to investigate the thermal properties of the membranes, which is important for the constant stability maintenance of membranes when operated under harsh conditions, (b) to confirm the presence of FA loading in the membranes. In general, the stability is strongly affected by the concentration of FA loading and may tend to alter the properties of membranes depending on the amount of loading. Hence, it's quite important to have in-depth thermal study of these membranes. TGA thermograms of N115 and N115-PFA membranes are shown in Figure 26.

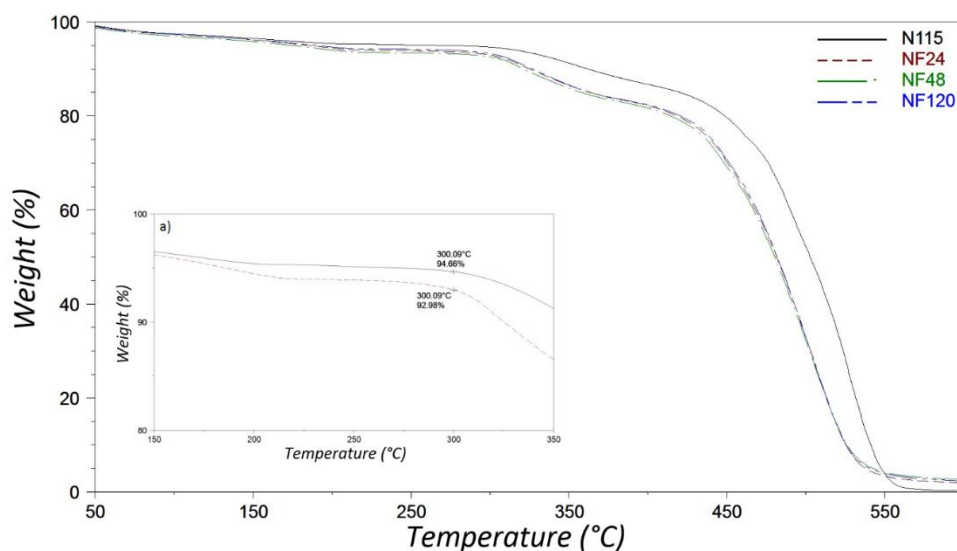


Figure 26. TGA thermograms of N115, NF24, NF48 and NF120.

Thermal degradation of the membranes takes place in three stages, as shown by the derived weight of curve peaks (Figure 27). The initial weight loss of about 5% between 50°C and 300°C is almost the same for pure N115 and the composites (NF24, NF48 and NF120), which can be associated with loss of residual water in the membrane. The slight difference of about 2% between 175°C and 300°C, may be due to a slight decomposition of PFA (FA: boiling point = 170°C) (Figure 26a).

The second stage of the degradation is different for N115 (Figure 27a) and composites (Figure 27b). The weight loss of about 10% was seen in the case of N115, which can be attributed to the decomposition of sulfonic groups with a small influence of the breakdown of side chains. However, a higher amount of loss (about 13%) was witnessed for NF24, demonstrating the existence of greater amount of inbound water molecules in the membranes, which does not evaporate in the first stage. The loading of PFA has substantially enhanced the hydrophilic nature of the Nafion membrane. The second stage weight loss between 300 and

400°C is considered as very crucial, not only because it is a temperature range where the disorder is initiated but also because the membrane loses ion exchange functions that are most important membrane properties [9-13].

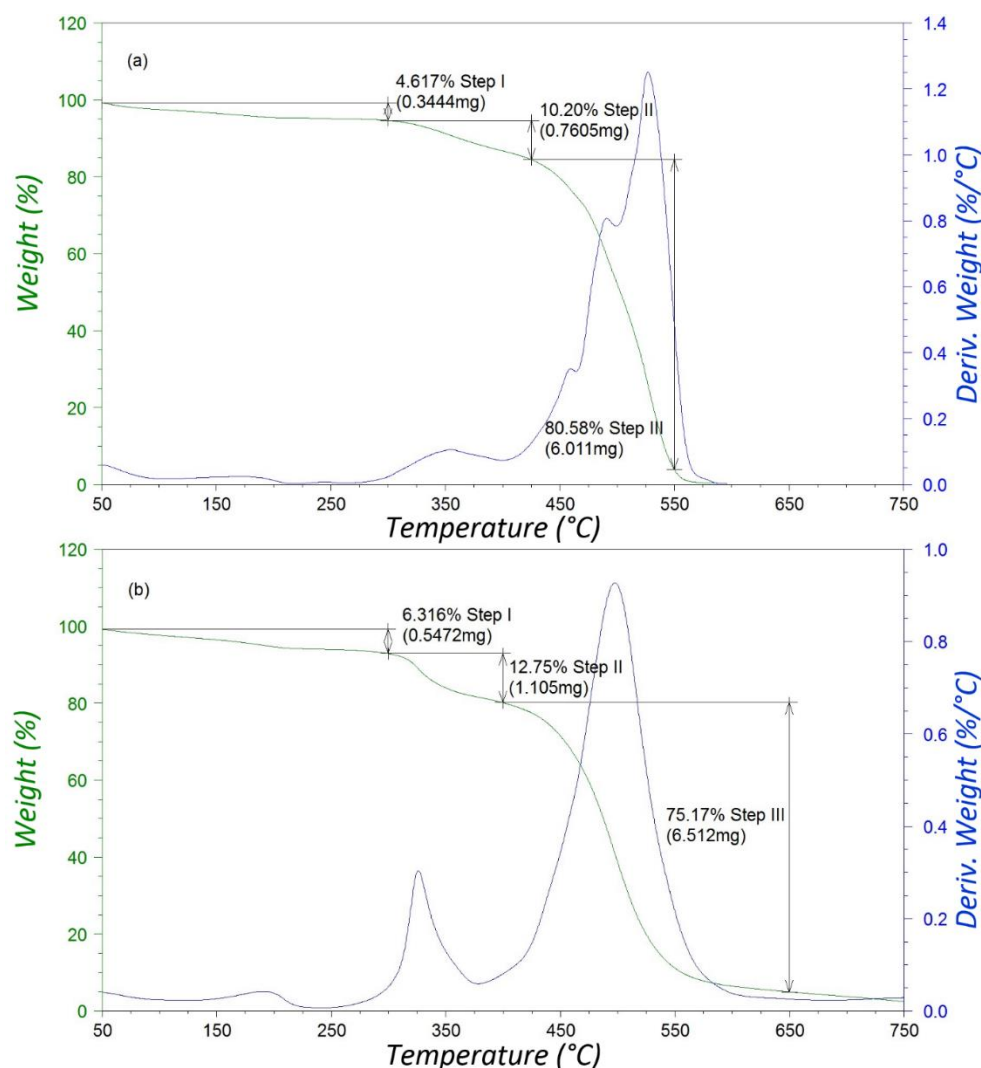


Figure 27. TGA thermograms of *a*) N115 and *b*) NF24.

In the third degradation stage, N115 extends between 425°C and 550°C, with a sharp drop around 460°C. It can be clearly seen that complete degradation of N115 happened <600°C, which can be credited to the complete loss of sulfonic acid groups, side chains, and also degradation of the backbone structure of Nafion to low-molecular weight aliphatic products. For N115-PFA composites, the degradation happens in the same range as for N115, however, the degradation is not completed within 600°C, displaying a better thermal stability compared to N115. Figure 28 shows the residual weight for modified membranes for the temperature at 600°C. In these membranes the degradation is accompanied by the pyrolysis of PFA polymer structure [14].

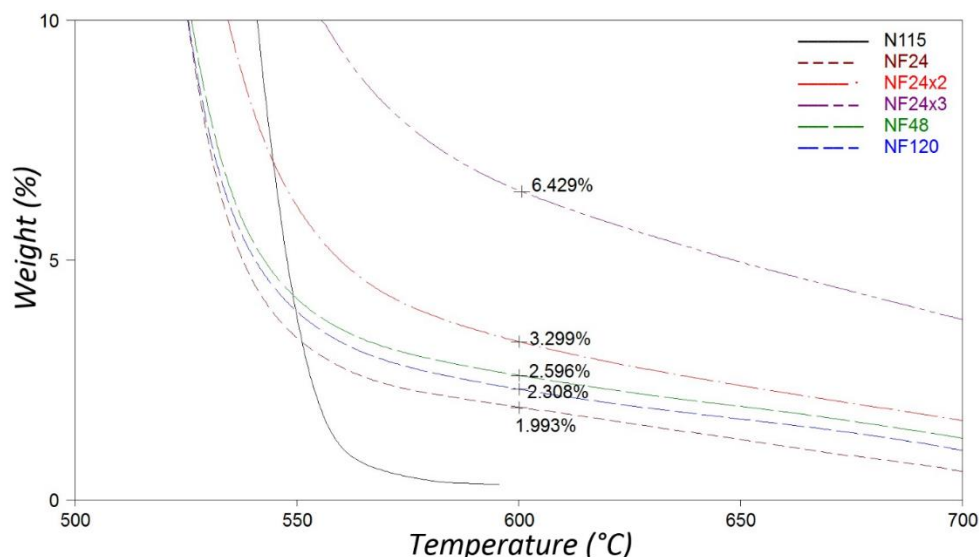


Figure 28. TGA thermogram of N115 and N115-PFA membranes.

The effect of repeating the FA loading process is clearly seen at the end of third phase. The residual weight for NF24 is 1.4%, for NF24×2 is 3.3% and for NF24×3 is 6.4% for 600°C (Figure 28). From the results, it is clearly evident that all composite membranes have shown higher thermal stability compared to N115. The stability increases with loading of PFA. The effect of repeating the PFA loading process has positive effect on the thermal properties and it is clearly witnessed for NF24×3, with a char yield of 6.4%. The above results give a clear indication of the possibility of using these membranes for low temperature PEMFC.

4.1.4. Dynamic mechanical properties

DMA analysis was performed to investigate the thermomechanical properties of the membranes. Figure 29 shows the DMA graph of membranes dynamically heated from 30 to 200°C. At low temperatures (~ 30°C), all the membranes have shown higher E' , which lies between 300 to 400 MPa. However, with the increase in temperature E' starts to drop gradually above 80°C and collapses completely around 150°C.

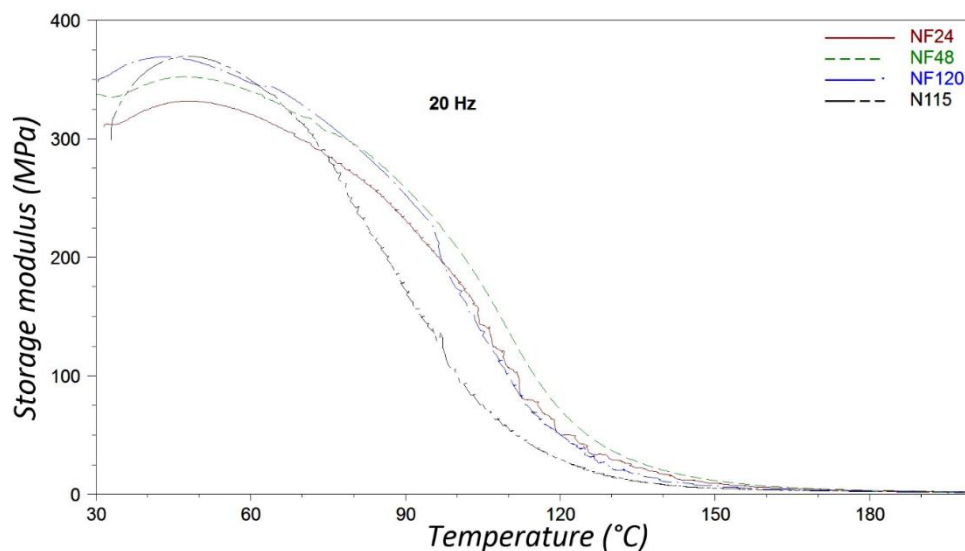


Figure 29. DMA E' curves of N115, NF24, NF48 and NF120.

Table 8 provides the complete DMA data corresponding to E' , T_g and break-point, at different frequencies. It is noticeable from Figure 29, at temperature above 70°C, N115 starts to collapse prior to the composite membranes, exhibiting a lower thermo-mechanical stability. It can be well correlated with thermal stability data in TGA section, where N115 had undergone complete degradation by 560°C, whereas, N115-PFA composites remained thermal stable till 700°C, demonstrating a better thermal stability compared to N115. Figure 30 shows the cracking in membranes for NF24 and NF48 at high temperatures.

Table 8. DMA obtained data for N115 and modified N115-PFA membranes.					
Sample	Frequency (Hz)	E' (Mpa)	T_g^* ($\tan \delta$) (°C)	Break-point (°C)	
N115	1	311	108	234	flexible
N115	10	340	122	241	flexible
N115	20	369	122	231	flexible
NF24	1	296	119	413	brittle
NF24	10	332	132	413	brittle
NF24	20	332	136	413	brittle
NF24x2	1	309	119	418	brittle
NF24x2	10	353	127	275	flexible
NF24x2	20	393	133	236	flexible
NF24x3	1	357	124	340	brittle
NF24x3	10	411	136	275	brittle
NF24x3	20	433	139	276	brittle
NF48	1	434	120	413	flexible
NF48	10	407	129	278	flexible
NF48	20	352	138	263	brittle
NF120	1	363	121	416	flexible
NF120	10	372	131	272	flexible
NF120	20	369	131	241	flexible

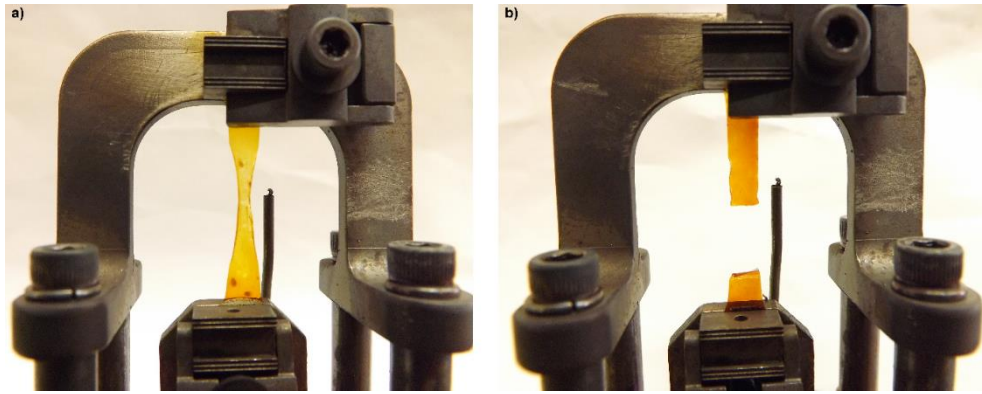


Figure 30. Dynamic Mechanical cracking in membranes: a) NF48 extension and b) NF24 cracking (1 Hz).

Figure 31 (Table 8) shows the DMA plot between $\tan \delta$ vs temperature for N115 and composite membranes. From the graph, only one α -transition peak was noticed, which corresponds to the glass transition temperature (T_g). The T_g for all composites shifts to higher temperatures. The highest T_g was observed for NF24 \times 3, with repeated loading of furfuryl alcohol. At 20 Hz, a difference of about 100°C was witnessed between N115 and other membranes. From the literature, it is known that above 115°C the network of hydrophilic clusters, made up from the sulfonic groups, becomes extremely mobile, before the clustered structure finally collapses [15]. This can be either due to loss of water under dry and hot conditions, or due to additional uptake of solvents if exposed to saturated solvent/water vapor.

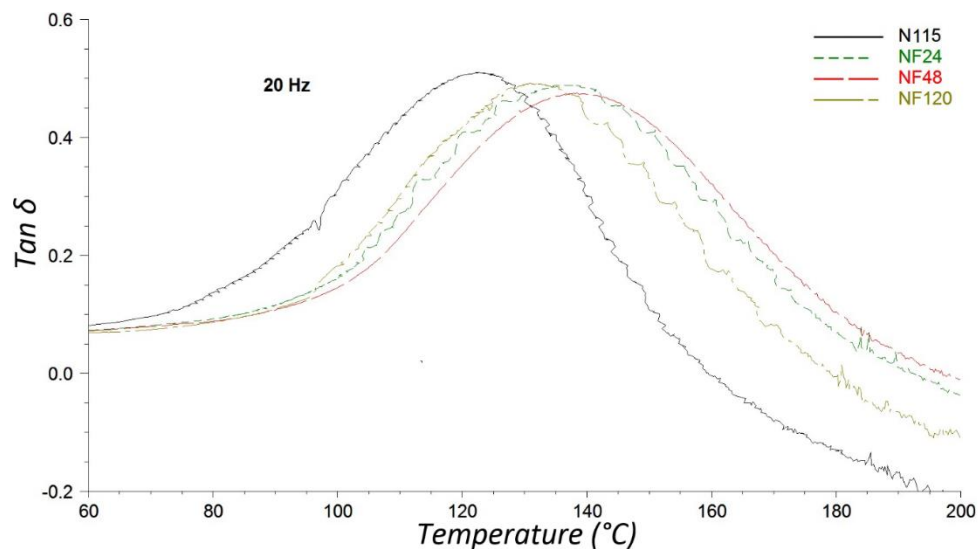


Figure 31. DMA $\tan \delta$ curves for N115 and N115-PFA composites.

As shown in Figure 32 at 20 Hz, the number of repetitions has greater influence to E' than the exposure time. The highest value for E' (433 MPa) was observed for NF24×3 membrane, at 20 Hz (Table 8).

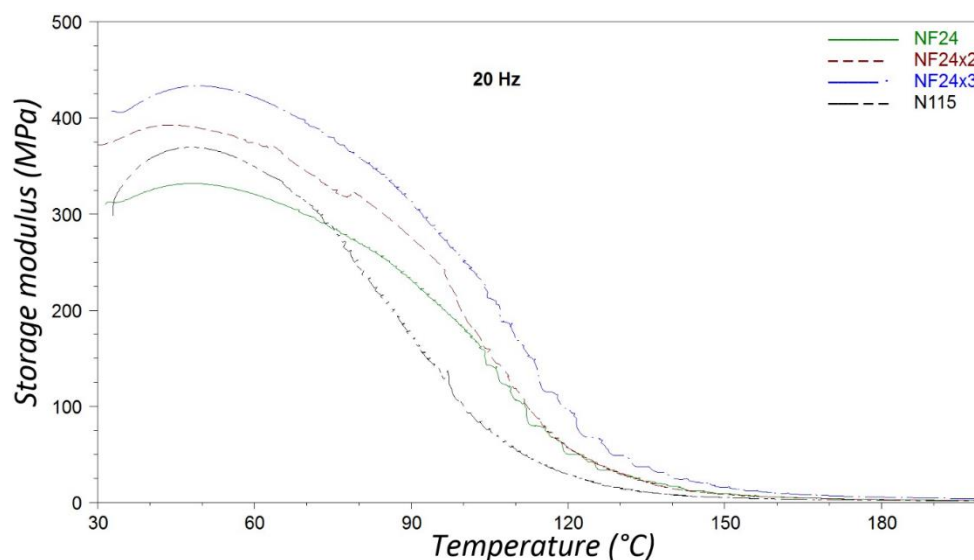


Figure 32. DMA E' curves for NF24, NF24×2 and NF24×3.

It can be concluded that N115-PFA composites exhibit better mechanical properties than N115. E' and T_g increased with PFA loading and with number of repetitions, respectively. The best thermo-mechanical properties were seen for NF24×3. These results correlated well with thermal stability data in TGA section (4.1.3).

4.1.5. Water uptake (W_u)

Previously, many research groups have reported that the water uptake in Nafion increases as a function of both temperature and water activity [16, 17]. Following a similar trend, our membranes displayed a gradual increase in W_u and witnessed the maximum uptake at 95% relative humidity (RH). Figure 33 shows the W_u measurements of the N115 and composite membranes at different RH.

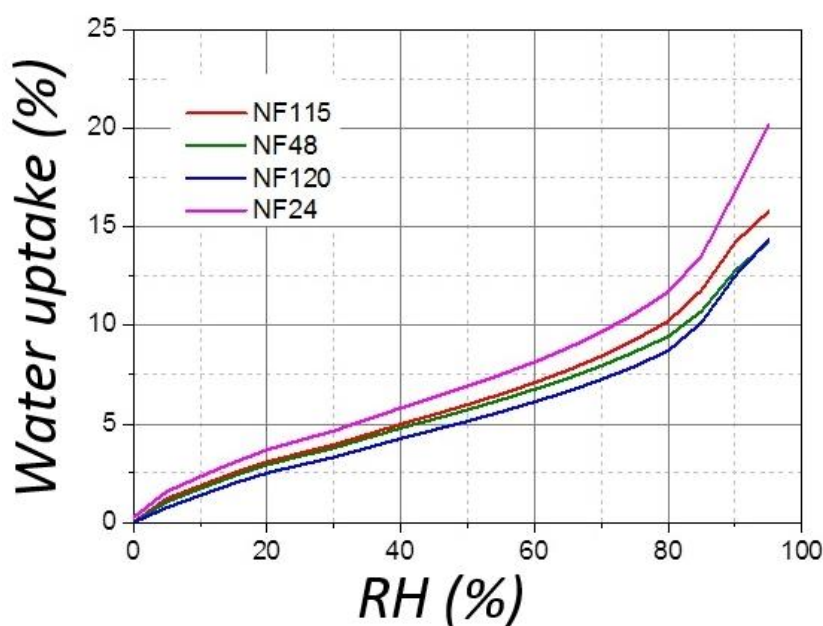


Figure 33. Water Uptake vs RH for composites (NF24, NF48 and NF120) and N115 membranes.

The highest level of uptake was witnessed for NF24 .i.e., ~ 20% at 95% RH, which is slightly higher than N115. Further, it can be found that the W_u of composites decreased with the increase in the loading time of PFA. Composite NF48 and NF120 showed somewhat lower W_u (14%) when compared to NF24. The decrease in W_u indicated that the sulfonated groups of N115 were combined with PFA, and the hydration of ion cluster was decreased due to the hydrophobic property of PFA [18, 19].

In general, water uptake is closely related to the basic properties of the membrane and plays a major role in its performance. The higher/lower absorption of water has a greater impact on the ionic conductivity of the membrane. The water presented in the membrane influences the ionomer microstructure, cluster, channel size and alters the mechanical properties [20]. The ionic conductivity of pure N115 membrane increases about linearly with absorbed water in the membrane [21]. The results obtained for W_u can be attributed to the hydrophilic nature of the PFA within the pores of N115, which increased surface area of nanoparticles, as proved by SAXS (Figure 25). Further, these outcomes of composite membranes correspond to calculated ionic conductivity from the Equation 10. The W_u decreases with the increase of loading time of PFA. Besides, the ionic conductivity also followed a similar trend and displayed a decreased pattern with increased PFA loading time. This phenomenon can be attributed to the greater number of PFA groups attached to the Nafion, which reduces vacant space for water. The higher water uptake of NF24 resulted in greater proton conductivity, which would apparently result in better fuel cell performance under different conditions.

4.1.6. Dynamic vapor sorption

All the composites exhibited increased water vapor uptake (W_{vu}) when compared to virgin N115. As shown in Figure 34, NF24 exhibited the highest W_{vu} (> 30%) at 25°C, whereas, other membranes displayed a lower uptake below 30%. Moreover, with the increase in absorption time from 0.5 to 48 h, the W_{vu} in NF24 also increased gradually from 15% to 32%, illustrating a better uptake properties when compared to N115. From DVS measurements, it can be concluded that NF24 has higher water uptake than N115 and all other membranes. W_{vu} increases with time of water action and decreases with increasing the loading time of PFA. This result can be correlated with W_u data in previous sections, where NF24 exhibited the best water uptake properties from all composite membranes. W_{vu} of composite membranes increased with time of water action and decreased with time of PFA loading.

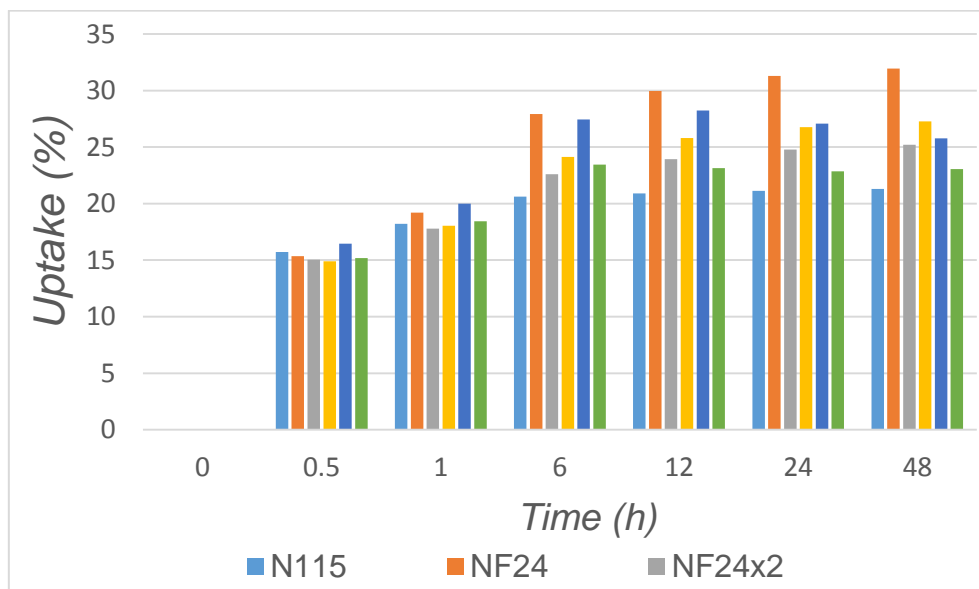


Figure 34. DVS water sorption properties of N115 and N115-PFA composites at 25°C.

4.1.7. Electrical properties

The ionic conductivities of membranes are shown in Figure 35. In case of composites the conductivity significantly decreased with PFA loading. Nevertheless, composite NF24 exhibits higher ionic conductivity compared with pure N115. It can be noticed that the conductivity was increased when a small amount of PFA was incorporated. This is probably due to the hydrophobic PFA molecules supplemented Nafion hydrophilic regions with lower density, and giving rise to densely packed polymer chains with less soluble domains that are effective in the

charge transfer. However, at high loading, large cluster-like domains tend to pack the Nafion loosely, which results in lower ionic conductivity. By using the appropriate amount of PFA, we can still produce N115-PFA composites with reasonably higher ionic conductivity, which is essential for fuel cell application.

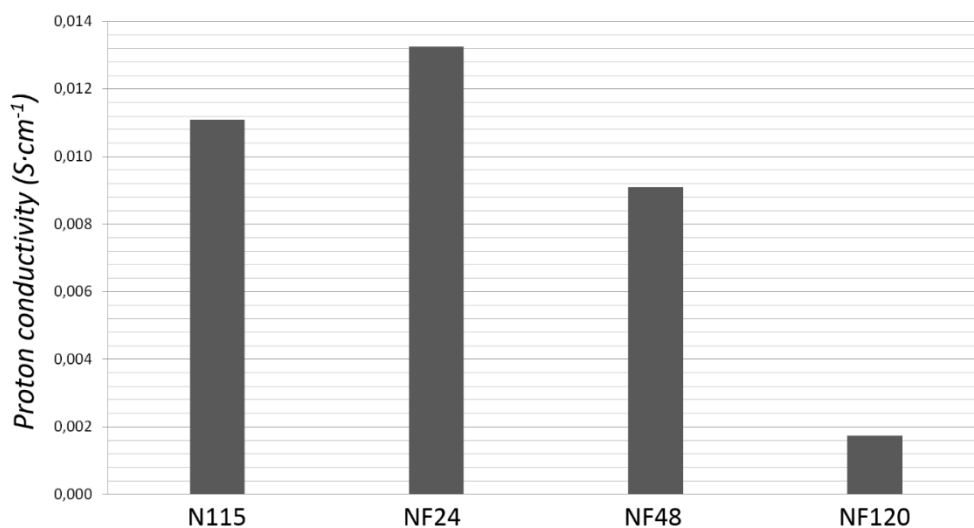


Figure 35. Ionic conductivity of N115, NF24, NF48 and NF120.

Figure 36 shows the impedance spectra of N115 and composites. The angle of slope of the linear portion of the spectrum gradually decreases towards the real axis Z' with the time of PFA loading. The highest value of ionic resistance was seen for NF24. Ionic resistance of composites decreases with time of PFA loading. These results are correlated with R1 data from Table 9.

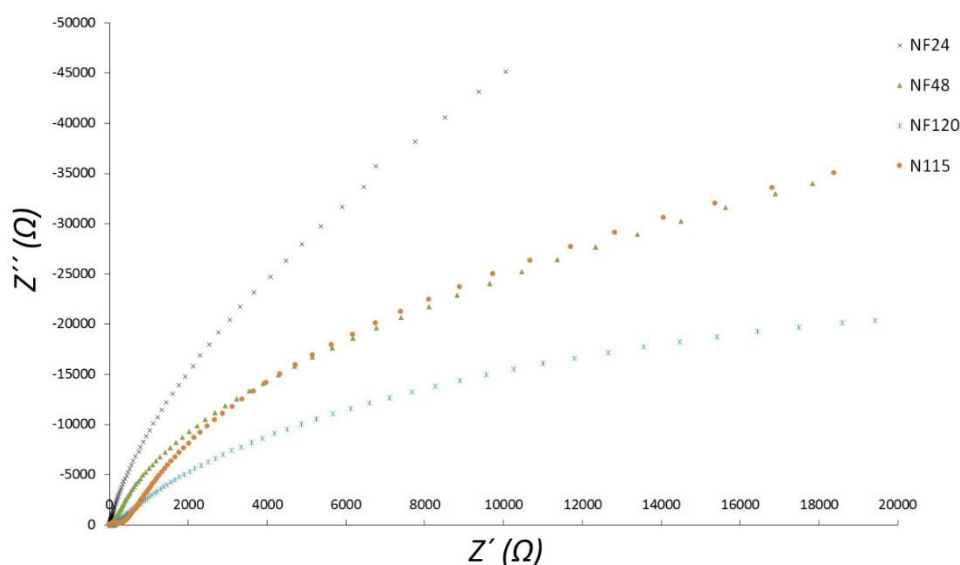


Figure 36. Impedance spectra of N115, NF24, NF48 and NF120.

Table 9. Fit for N115 and composite membranes			
membrane	Element	Value	Error %
N115	R1 (Ω)	9,935	N/A
	C1 (F)	2,8313 e-7	1,5215
	R2 (Ω)	608,1	0,99286
NF24	R1 (Ω)	7,4954	N/A
	C1 (F)	2,7114 e-5	0,62901
	R2 (Ω)	162420	7,1346
NF24×2	R1 (Ω)	8,11	N/A
	C1 (F)	3,725 e-5	0,47074
	R2 (Ω)	115930	5,1415
NF24×x3	R1 (Ω)	8,721	N/A
	C1 (F)	3,8335 e-5	0,5639
	R2 (Ω)	71126	4,0101
NF48	R1 (Ω)	10,935	N/A
	C1 (F)	2,196 e-5	1,5658
	R2 (Ω)	59439	6,2811
NF120	R1 (Ω)	56,369	N/A
	C1 (F)	1,8938 e-5	4,2866
	R2 (Ω)	15171	6,6153

The interpretation and quantification of impedance spectra requires a deep understanding of the involved processes and the selection of a suitable equivalent electric circuit. In practice, it is just as important as the adequate reflection of the real system and the simplicity of the circuit [22]. For this reason, it is necessary to understand the physical processes in the cell and identify the major components that contribute to the overall system impedance in order to create accurate equivalent circuit.

Figure 37 shows a representative equivalent circuit showing proton conducting polymeric membrane sandwiched between two mercury electrodes (Figure 23). Element R1 represents an ionic membrane resistance. Parallel combination of capacity C1 and resistor R2 corresponds to the behaviour of the double layer membrane-mercury electrode. The element C1 is the capacity at the charge transfer between the membrane and the mercury electrode, element R2 represents the electrical resistance at the charge transfer between the membrane and the mercury electrode.

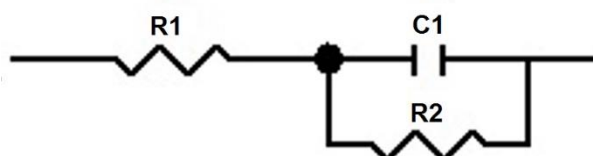


Figure 37. Equivalent circuit for the impedance measurement.

Table 9 shows the values obtained using the corresponding fit for the N115 and composites. For membranes NF24, NF24×2 and NF24×3 ionic resistance R1 is lower than for N115 and significantly increases with loading of PFA. All the composite membranes show orders of

magnitude higher ion-exchange capacity C1 than N115. This is due to the hydrophobic property of PFA [23]. The ideal capacitance behaviour would result the vertical linear line in the Z' vs. Z'' diagram. However, it is generally known that the capacity for solid electrodes deviate from ideal behaviour in the form of the frequency dependence of the phase angle. This capacitance dispersion is a consequence of anomalies on the electrode surface [22].

In Figure 38, we can see comparison of the real measurements for NF24 and graph obtained using the corresponding fit.

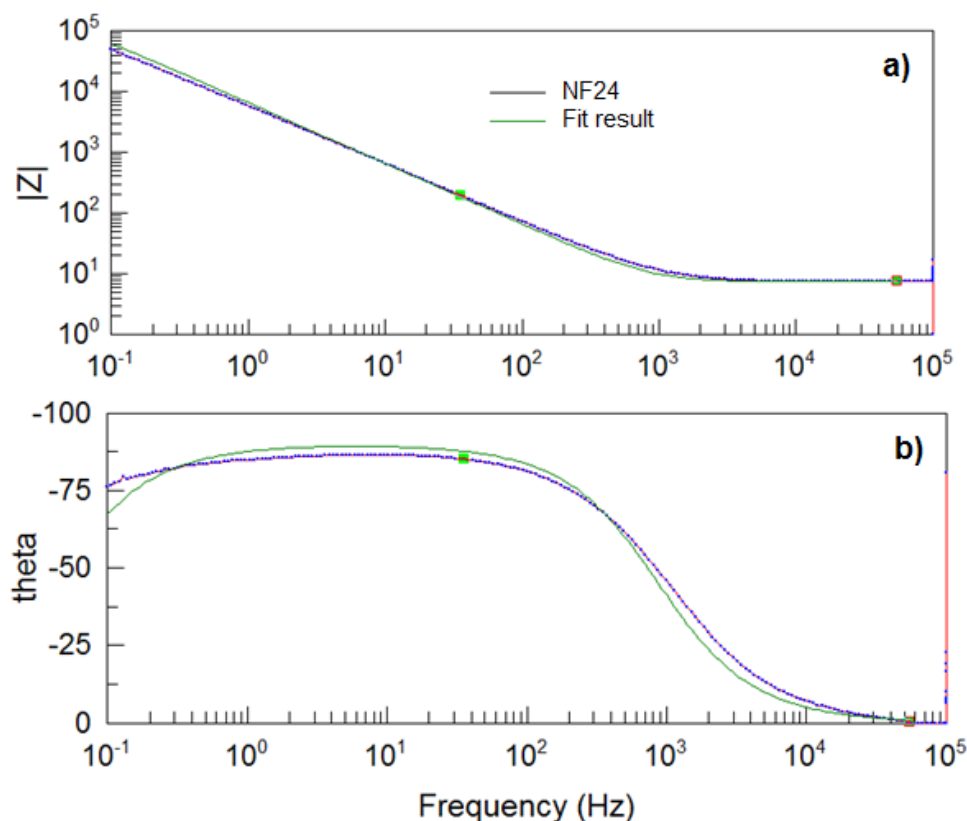


Figure 38. Fit results for NF24, a) impedance, b) loss angle.

Composite NF24 showed the best electrical properties, highest ionic conductivity and lowest ionic resistance from all measured modified membranes. Ion-exchange capacity is orders of magnitude higher than for N115. Therefore, NF24 may be considered as the best composite membrane for PEM fuel cell, though it may need further modification for use at temperatures above 80°C .

4.2. PVA/SiO₂ and PVA/SiO₂/GA membranes

Membranes with different contents of silica and GA were characterized by Raman spectroscopy, small- and wide angle X-ray scattering (SAXS/WAXS), atomic force microscopy (AFM), thermogravimetric analysis (TGA), differential scanning calorimetry (DSC), dynamic mechanical analysis (DMA), and water uptake experiments. The effect of silica and GA incorporation on the properties and morphology of the nanocomposite membranes was systematically investigated.

4.2.1. Raman spectroscopy

The Raman spectra of the pure PVA, PVA/SiO₂, and PVA/SiO₂/GA membranes were measured and the assignment of the major Raman bands is summarized in Table 10. In the pure PVA membrane spectrum (Figure 39), strong characteristic bands were observed at 856, 919, 1147, and 1442 cm⁻¹. The bands at 856 and 919 cm⁻¹ are due to the C–C stretching of the PVA polymer backbone. The band at 919 cm⁻¹ corresponds to the amorphous phase (non-crystalline conformation of the PVA carbon backbone), while the band at 856 cm⁻¹ is independent of the crystallinity [24] and was therefore used for intensity normalization, as mentioned in the experimental section. The bands at 1365 and 1442 cm⁻¹ result from the C–H and O–H bending vibrations and the bands at 1147 and 1124 cm⁻¹ correspond to the C–C and C–O stretching in the crystalline and the amorphous phase of the PVA matrix, respectively.

Table 10. Assignment of Raman bands for PVA, PVA/SiO ₂ , and PVA/SiO ₂ /GA membranes	
Frequency (cm ⁻¹)	Assignment
856	C–C stretching [25, 27, 28]
919	C–C stretching [24, 25, 27, 28]; increase in the intensity can be related to the decrease of the crystallinity, i.e., represents non-crystalline conformation of the PVA carbon backbone
980	Si–OH stretch [26, 26]
1071	C–O stretching, O–H bending [24, 25]
1093	C–O stretching, O–H bending [24, 25, 27]
1124	very weak in this spectrum; C–O and C–C stretching [25]; C–O–C stretching in the cross-linked network [24]; indicative of the amorphous phase [24, 25]
1147	C–O and C–C stretching [24, 25, 27]; indicative of the crystalline phase [24, 25, 28]
1365	C–H and O–H bending [24, 25, 28]
1442	C–H and O–H bending [24, 25, 27, 28]

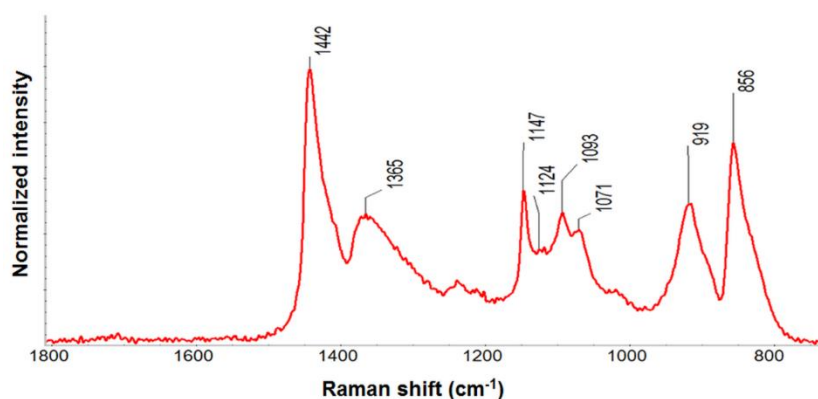


Figure 39. Raman spectrum of pure PVA.

The spectra of the pure PVA, 5PVA_2TEOS, and 5PVA_4TEOS membranes are compared in Figure 40. It is clearly visible that the incorporation of silica reduced the crystallinity of the membranes. The “crystalline” band at 1147 cm^{-1} decreased and the “amorphous” band at 1118 cm^{-1} increased with the increasing silica loading. The intensity ratio of the bands at 916 and 856 cm^{-1} increased with the increasing SiO_2 content, also indicating a decrease of the crystallinity. A new feature in the spectrum is the weak scattering band at 980 cm^{-1} corresponding to Si–OH vibrations [25, 26]. A significant shoulder appears around 1337 cm^{-1} for 5PVA_2TEOS and then forms a second maximum for 5PVA_4TEOS. The same trend was observed by Martinelli et al. [24] for PVA membranes with various contents of GA and silica. The band at 1094 cm^{-1} completely disappeared upon the addition of TEOS. Since this band is related to O–H vibrations, this could be evidence that the OH groups in PVA reacted with TEOS. The small band that would represent unreacted OH groups is probably overlapped by the neighbouring strong and broad band at 1118 cm^{-1} .

The spectra of samples 5PVA_1TEOS_1GA, 5PVA_1TEOS_2GA, and 5PVA_1TEOS_4GA are compared with that of pure PVA in Figure 41. The intensity of the band at 1147 cm^{-1} decreased with the increasing GA content and, simultaneously, a slight increase in the 1118 cm^{-1} band intensity was observed, clearly indicating a decrease of the membrane crystallinity. However, the decrease of the crystallinity was gradual in the case of PVA/ SiO_2 /GA membranes, in contrast with the PVA/ SiO_2 samples.

The addition of GA resulted in the emergence of several new bands, especially at the highest GA content (sample 5PVA_1TEOS_4GA). These bands were at 1710 , 1676 , 1638 , 1256 , 1201 , and 804 cm^{-1} , respectively, and can be attributed to various vibrations in pure GA [24]. Martinelli et al. [24] measured the Raman spectra of PVA crosslinked by various amounts of GA and suggested that only a limited amount of GA was incorporated into the PVA network. We would therefore suggest that the observed bands originate from GA molecules that did not

fully incorporate into the cross-linked network. This is supported by the fact that the intensity of these bands increased with the increasing GA content, in agreement with [24]. Furthermore, several of these bands (1710, 1256, 1201, and 804 cm^{-1}) were not observed at the lowest GA content (5PVA_1TEOS_1GA), supporting the assumption that a small amount of GA incorporates into the membrane. The band at 1369 cm^{-1} broadens to lower wavenumbers, although this effect is less notable for PVA/SiO₂/GA than for the corresponding PVA/SiO₂ membranes, probably indicating a lower incorporation of silica into the membrane structure when GA is present. This assumption was confirmed by SAXS.

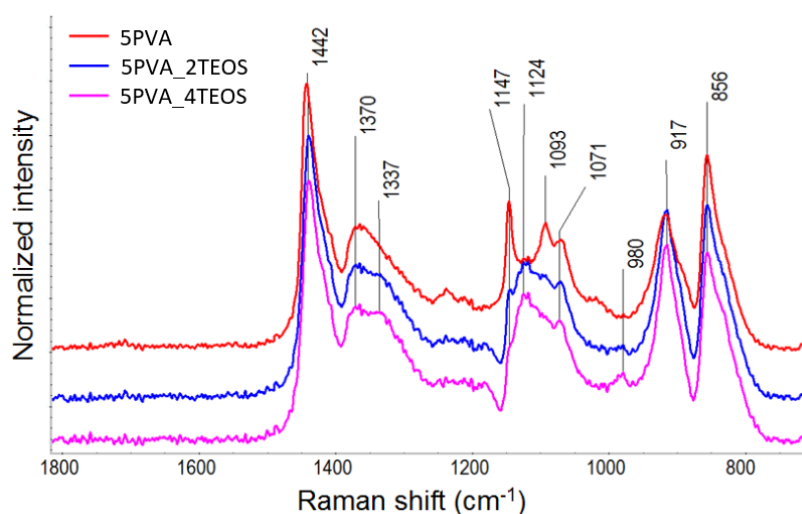


Figure 40. Comparison of Raman spectra of PVA and PVA/SiO₂.

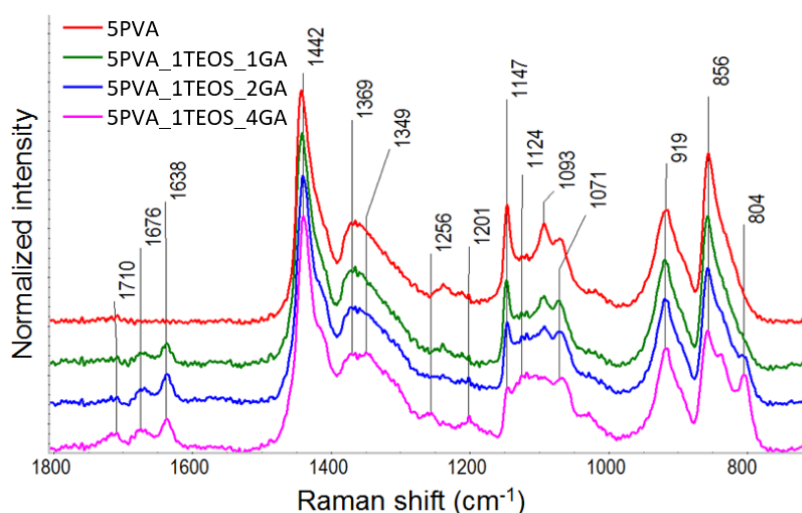


Figure 41. Comparison of Raman spectra of PVA and PVA/SiO₂/GA membranes.

4.2.2. Small- and wide-angle X-ray scattering

Figures 42-44 show the SAXS profiles of the PVA/SiO₂, PVA/SiO₂/GA, and PVA/GA samples, respectively. The profile of pure PVA is shown in all cases for comparison. The

profiles are expressed as dependencies of the scattering intensity on the scattering vector magnitude q on a log–log scale. The corresponding WAXS profiles are shown in Figures 45-47 and expressed as dependencies of the scattering/diffraction intensity on the 2θ angle.

The WAXS profile of the pure PVA membrane shows several crystalline peaks that could be well assigned to crystallographic planes of the monoclinic PVA system [29, 30]. The crystalline peaks are superimposed on a broad amorphous halo corresponding to the amorphous phase. Thus, the WAXS profile verified the semi-crystalline nature of the pure PVA membrane.

The nanometer-scale structure can be estimated from the SAXS profile. The peak in the SAXS profile of the pure PVA membrane at q of approximately 0.6 nm^{-1} is an evidence for the nanophase separation of the material, i.e., mixed crystalline and amorphous regions with dimensions in the range of nanometers, in accordance with the literature [31]. The corresponding approximate d -spacing calculated from the position of the peak maximum is: $d = 2\pi / q_{\text{max}} = 2\pi / 0.7 = 9 \text{ nm}$. The pronounced peak shows that the structure is well ordered with a relatively narrow distribution of both the size of the crystallites and their spacing. If we assume small crystallites randomly distributed in an amorphous polymer matrix [31], their size and average distance can be estimated from the SAXS profile. For this purpose, we utilized the Irena software package for small-angle scattering analysis [32]. If the crystallites are assumed to be spherical, the SAXS profile fitting provides an average diameter of about 6 nm with an average d -spacing of about 8 nm.

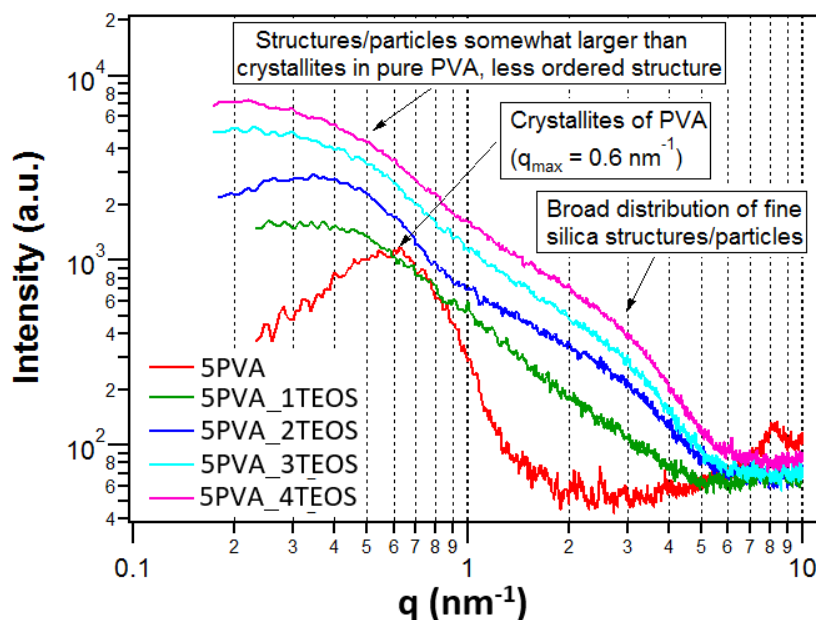


Figure 42. SAXS profiles of PVA/SiO₂ membranes.

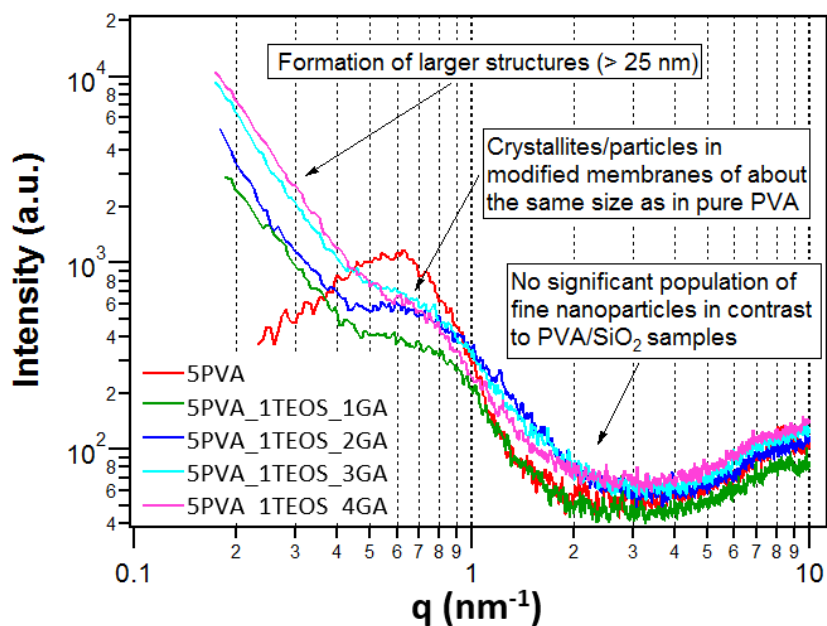


Figure 43. SAXS profiles of PVA/SiO₂/GA membranes.

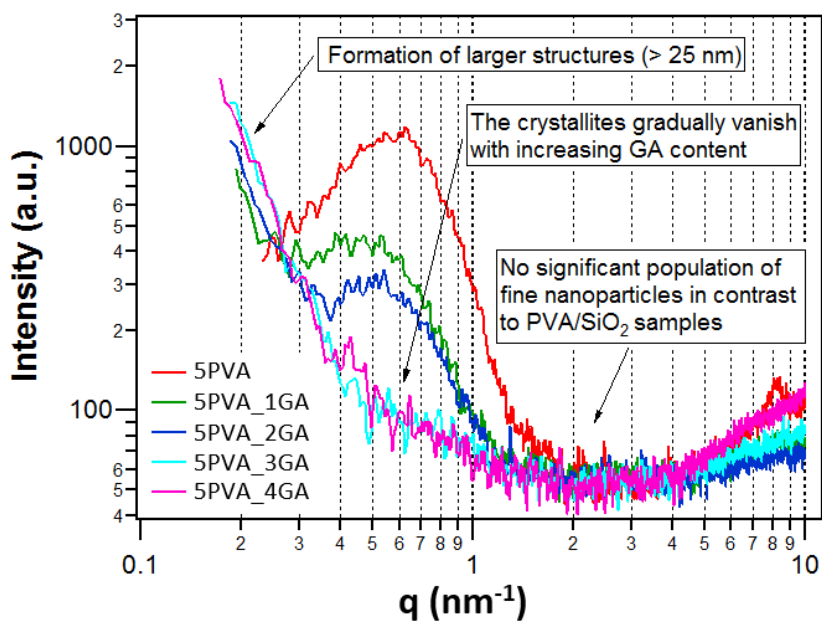


Figure 44. SAXS profiles of PVA/GA membranes.

With the increasing silica (TEOS) loading, the crystalline peaks decrease in intensity or vanish (Figure 45), indicating a decrease in the crystallinity of the membranes. For 5PVA_3TEOS and 5PVA_4TEOS, all peaks corresponding to crystalline PVA virtually vanished. This observation correlates very well with the results of Raman spectroscopy. The SAXS profiles of the PVA/SiO₂ samples provide further information. First, the fact that the peak of PVA did not vanish indicates that there still exists phase separation on the nanometer scale with similar dimensions as in the pure PVA structure. However, we can hardly talk about

semi-crystalline structure because, as discussed above, the crystallinity of the PVA/SiO₂ membranes decreased or virtually vanished with the increasing silica loading. With the increasing SiO₂ loading, the peak of PVA becomes broader and shifts to lower values of q , which indicates that the structure is less ordered than that of the pure PVA membrane, presumably with a wider distribution of the particle sizes. The shift of the peak position to lower values of q does not necessarily mean that the average d -spacing grows, but it can also be caused just by the less sharp structure factor profile due to the less ordered structure. The new broad shoulder at higher scattering vectors, which is not present in pure PVA, indicates the presence of fine nanoparticles/nanostructures (with dimensions down to about 1 nm), which must be silica or silica-containing particles/structures distributed in the polymer matrix. The above observations are clear evidence that silica is extensively incorporated into the PVA structure. Furthermore, a successful formation of organic–inorganic composites of PVA and silica was already reported and studied by SAXS and FTIR in [33], where the same reaction of PVA with TEOS was used for the composite preparation.

Figure 46 shows the WAXS profiles of the PVA/SiO₂/GA samples. It can be seen that when TEOS and GA are added, the intensity of the crystalline peaks decreases, as in the previous case. However, the influence of increasing the GA concentration on the crystallinity is not that strong as in the case of TEOS, in a good agreement with the results of Raman spectroscopy. Figure 43 shows the SAXS profiles of the PVA/SiO₂/GA membranes. In this case, the situation is completely different compared to the PVA/SiO₂ membranes. The peak corresponding to the PVA crystallites does not shift, which means that their size is preserved. No significant shoulder at higher scattering vector q is present, which means that silica does not incorporate into the polymer in the form of fine nanoparticles. The steep rise of the scattering intensity towards low q originates from the presence of bigger particles (at least 25 nm). Such particles did not form in the PVA/SiO₂ membranes. Thus, in the case of PVA/SiO₂/GA membranes, silica prefers to form bigger particles, presumably together with GA. This correlates very well with the TGA results, which showed that the PVA/SiO₂/GA membranes are less stable than the PVA/SiO₂ membranes and that their thermal stability did not even increase in comparison with the pure PVA membranes. These findings correspond very well with the AFM results, which showed the presence of such big particles in the PVA/SiO₂/GA samples, whereas the morphology of PVA/SiO₂ was similar to that of pure PVA.

Figures 44 and 47 show the SAXS and WAXS profiles of the PVA/GA samples, which were additionally prepared for selected supplementary analyses. It can be observed from the SAXS profiles that the addition of GA leads to a gradual decrease of the peak corresponding to

the nanocrystallites. In the case of 5PVA_3GA and 5PVA_4GA, the peak totally vanished. The WAXS profiles of the PVA/GA samples (Figure 47) confirm the decrease in crystallinity with the increasing GA content. It can therefore be concluded that a sufficiently high concentration of GA prevents the formation of the fine semi-crystalline structure. This indicates that GA effectively reacts with the hydroxyl groups of PVA and cross-links the PVA chains when the GA concentration is sufficiently high. The GA side chains and cross-links then prevent the formation of the nanocrystallites, which form in pure PVA. This is a different situation compared with the PVA/SiO₂/GA samples, where the SAXS peak did not vanish even at the highest GA concentration (only its intensity was reduced). Simultaneously, the crystallinity determined by WAXS did not decrease that intensely as in the case of the corresponding PVA/GA samples. These observations further support the conclusion that GA preferably reacts with TEOS (silica) and not with PVA. Therefore, it can be concluded that GA is not a suitable cross-linking agent of PVA in the presence of TEOS and that the cross-linking is significantly more effective when TEOS is not present.

The steep rise of the SAXS profiles (Figure 44) towards low q values indicates the formation of bigger domains (at least 25 nm) in the PVA/GA membranes (same as in the case of the PVA/SiO₂/GA samples). These domains are formed either by unreacted free GA or some ordered structures on larger scale due to the effective GA crosslinking.

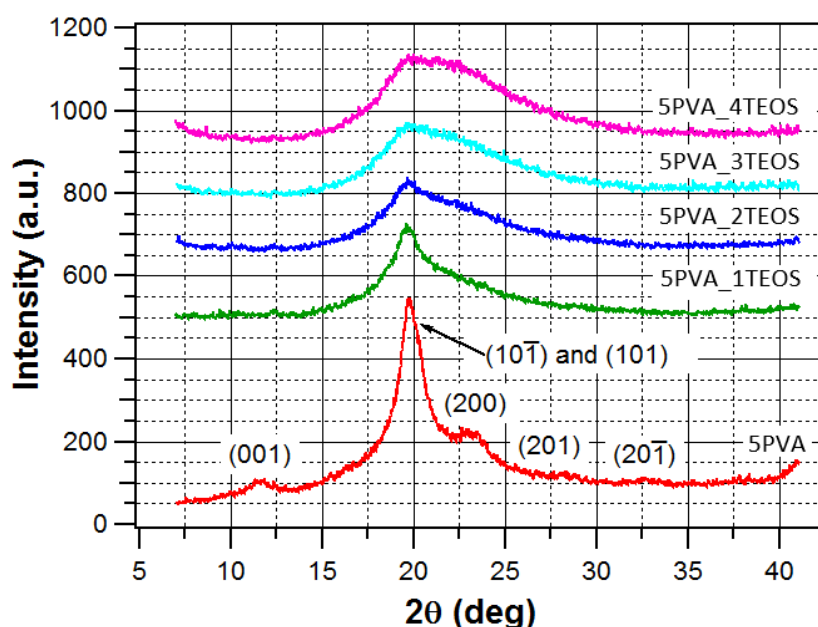


Figure 45. WAXS profiles of PVA/SiO₂ membranes.

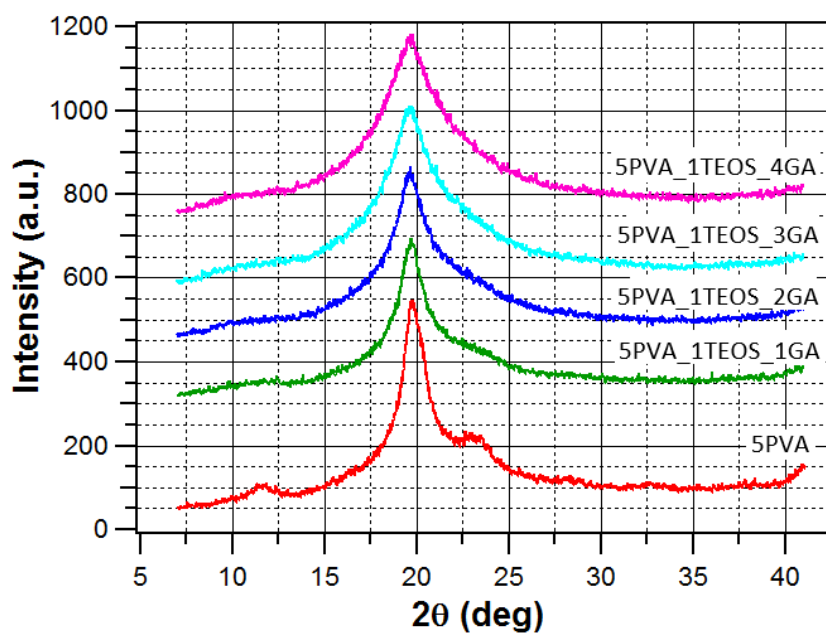


Figure 46. WAXS profiles of PVA/SiO₂/GA membranes.

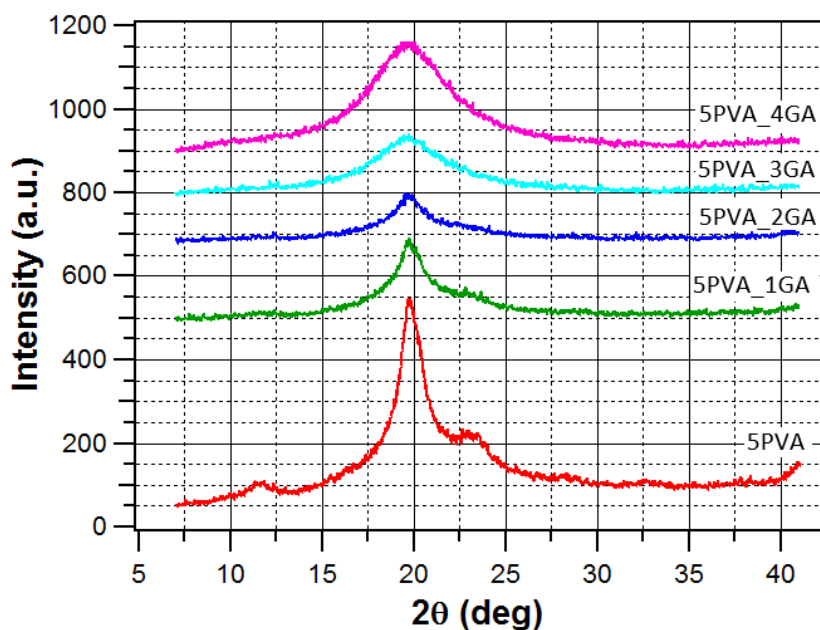


Figure 47. WAXS profiles of PVA/GA membranes.

4.2.3. Atomic force microscopy

The morphology of the pure PVA membrane and the composite 5PVA_4TEOS and 5PVA_1TEOS_3GA membranes was studied by AFM and is presented in Figures 48, 49 and 50. The surface of pure PVA on the microscale is finely homogeneous, as seen in Figure 48a. The closely packed semicrystalline PVA structure is shown in Figure 48b on a finer scale, although the fine nanometer structure is beyond the resolution capabilities of the instrument due to the size of the AFM tip which is at least 10 nm.

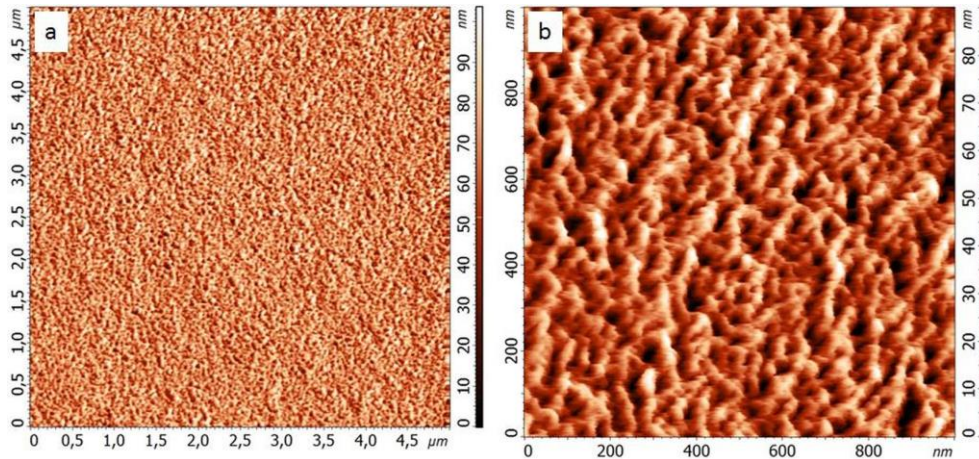


Figure 48. AFM topological images of 5PVA membrane on **a)** micron and **b)** submicron scale.

At the microscale, the 5PVA_4TEOS membrane showed a homogeneous morphology (Figure 49a), which is very similar to that of the pure PVA membrane (Figure 48a). At the finer scale, the morphology of the composite membrane (Figure 49b) showed to be smoother than that of the pure PVA membrane (Figure 48b). This can also be clearly observed by comparing the z-axis of the AFM images in Figures 48 and 49. The given conclusions are in a very good agreement with the SAXS analysis, which showed the presence of fine nanometric particles in the PVA/SiO₂ composite membranes and no formation of bigger particles.

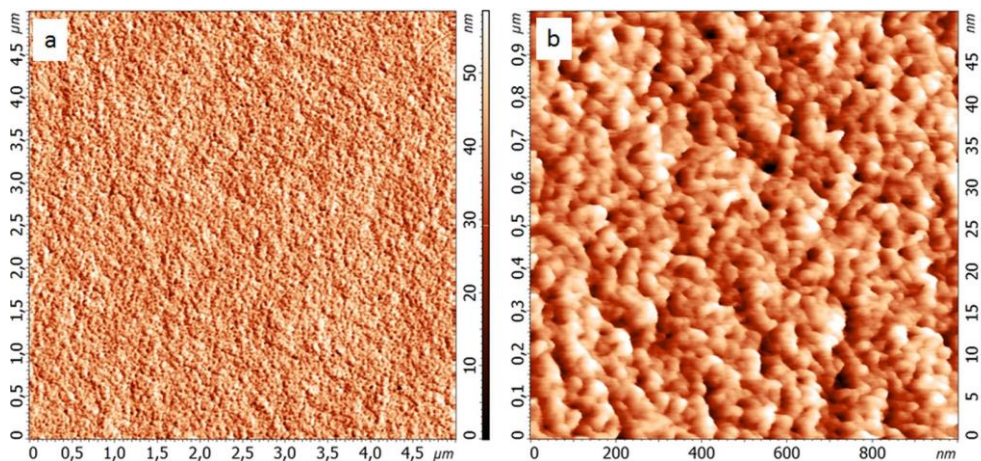


Figure 49. AFM topological images of 5PVA_4TEOS membrane on **a)** micron and **b)** submicron scale.

On the other hand, the surface of the PVA/SiO₂/3GA sample showed large domains with a relatively broad size distribution (from tens to hundreds of nanometers), see Figure 50. This confirms the presence of large particles, which were also observed by SAXS for all PVA/SiO₂/GA samples. These particles are formed by GA and silica that did not get incorporated into the polymer.

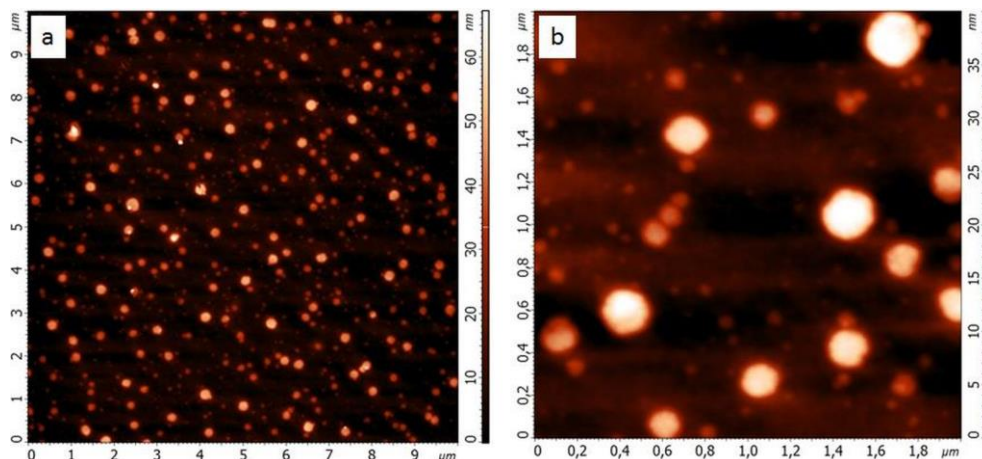


Figure 50. AFM topological images of 5PVA_1TEOS_3GA membrane on **a)** micron and **b)** submicron scale.

4.2.4. Water uptake

Figure 51 shows the effect of temperature on the water uptake properties of the PVA/SiO₂ membranes. Recently, Xie et al. [34] reported a significant decrease in the water uptake of PVA/MA/TEOS hybrid membranes from 154 to 43% when the temperature was raised from 21 to 100°C. However, our PVA/SiO₂ membranes have shown a gradual increase in W_u with the increasing temperature, as shown in Figure 51. The W_u values ranged from 16–20% at 30°C to 60–117% at 90°C. For example, 5PVA_3TEOS showed an increase of the water uptake from 18 to 117% when the membrane was heated from 30 to 90°C. The PVA/SiO₂ membranes show a good balance between the hydrophilicity and the thermal stability, as will be demonstrated in the TGA section. On the other hand, the PVA/SiO₂/GA membranes were completely dissolved when the temperature was raised above 50°C (Figure 54). This corresponds well with the fact that the molecular structure of the PVA/SiO₂/GA membranes is not effectively reinforced and that their thermal and mechanical stability is relatively poor. It was shown that the binding of PVA with TEOS and GA was not effective enough to form a stable structure, which caused an increase in hydrophilicity, but reduced the thermal stability. The excess hydrophilic nature of the PVA/SiO₂/GA membranes resulted in the dissolution of the membranes at higher temperatures.

Figure 52 shows the effect of time on the water uptake properties of the PVA/SiO₂ membranes. With increasing concentration of TEOS decrease the W_u of PVA/SiO₂ membranes while increase the membrane resistance to water (Figure 56).

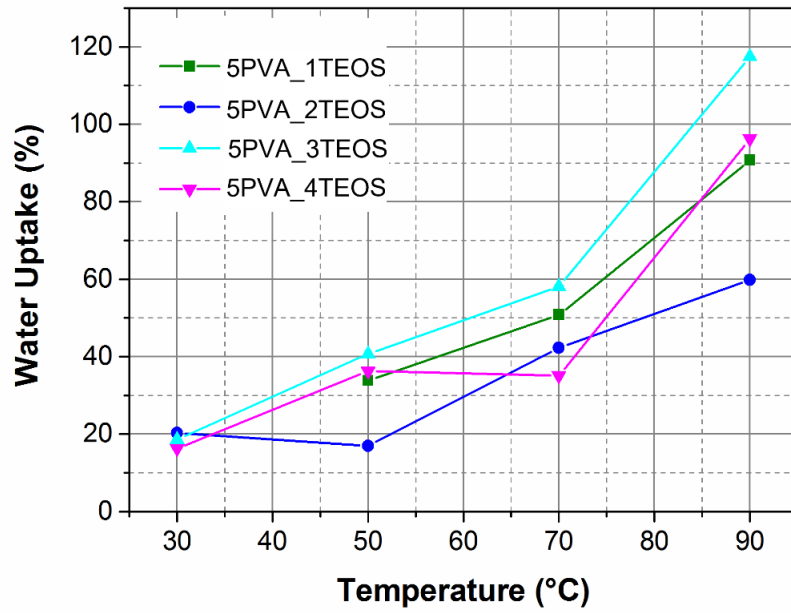


Figure 51. Water uptake properties of the PVA/SiO₂ membranes.

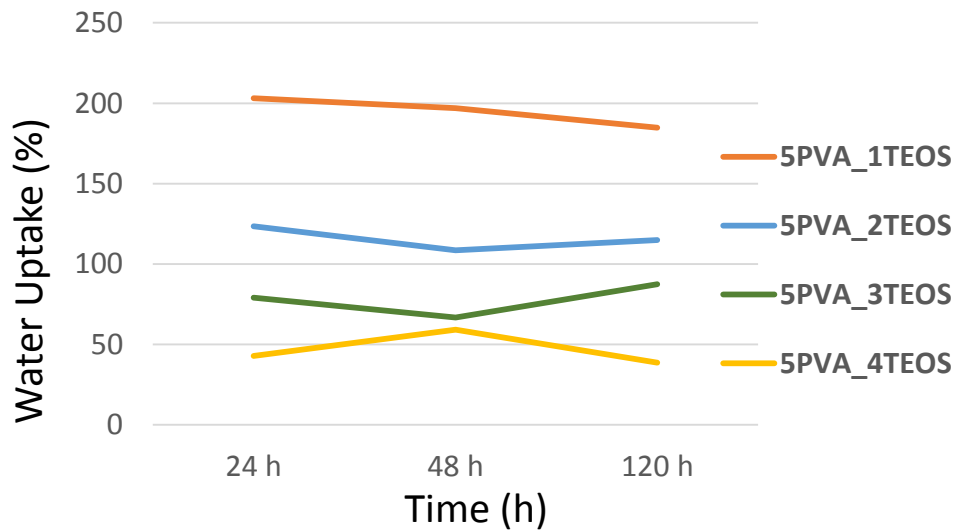


Figure 52. Water uptake of PVA/SiO₂ membranes.



Figure 53. PVA/GA membrane.

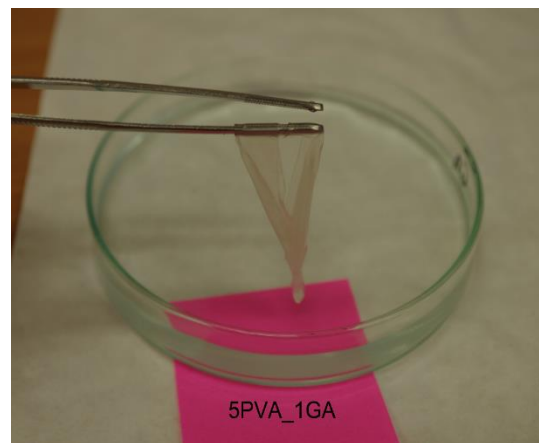


Figure 54. PVA/GA dissolved membrane.



Figure 55. PVA/SiO₂ membranes.



Figure 56. PVA/SiO₂ membranes after water uptake test.

4.2.5. Thermal analysis

The thermal degradation of pure PVA membranes showed two distinct steps in the TGA curve (Figure 57). The first step occurred between 200 and 330°C (with a sharp decrease around 260°C) with a major weight loss of 69%. The second step followed between 330 and 520°C with a weight loss of ~15%. Previous studies have shown that the decomposition of PVA begins with chain “stripping”, i.e., the elimination of water accompanied by the formation of polyene structures, as shown in Figure 18. At higher temperatures (350°C), these polyene structures are further converted to low-molecular weight aliphatic products [35–37].

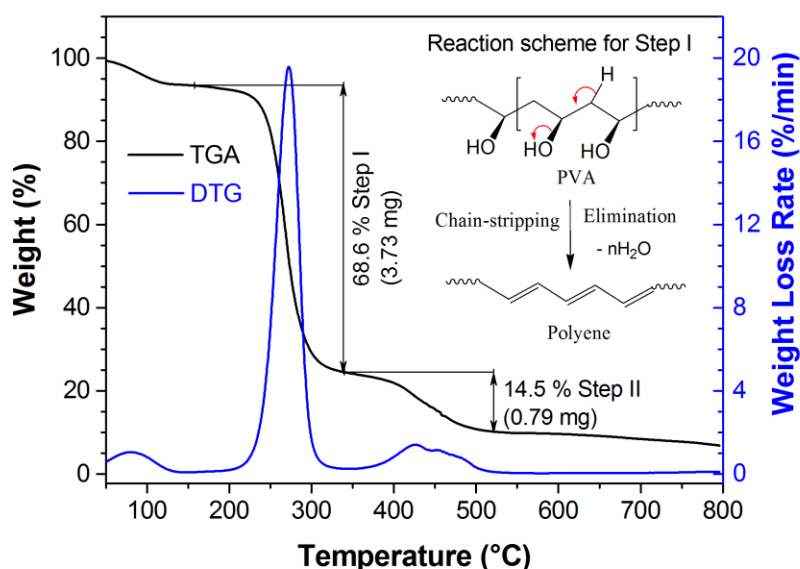


Figure 57. TGA and DTG curves of pure PVA membrane.

The presence of silica in the PVA matrix improved the thermal stability of the PVA/SiO₂ membranes (Figure 58). Furthermore, the distinct two-step degradation pattern of pure PVA did not occur in this case. Instead, a slow and gradual degradation pattern was observed for the PVA/SiO₂ membranes, which was due to their less ordered, predominantly amorphous structure. Although it is difficult to define a clear initial decomposition temperature from the TGA curves due to the continuous weight loss, it was still possible to distinguish two weight loss stages. The first stage occurred in the temperature range from 50 to about 450°C with the maximum weight loss of ~70% observed for 5PVA_1TEOS and the minimum weight loss of ~35% for 5PVA_4TEOS. For the 2TEOS, 3TEOS, and 4TEOS samples, the first stage continuously passed into the second stage corresponding to the chain degradation. The char yield values of the PVA/SiO₂ membranes increased with the increasing silica loading, with the maximum char yield of 46% observed for the 5PVA_4TEOS membrane.

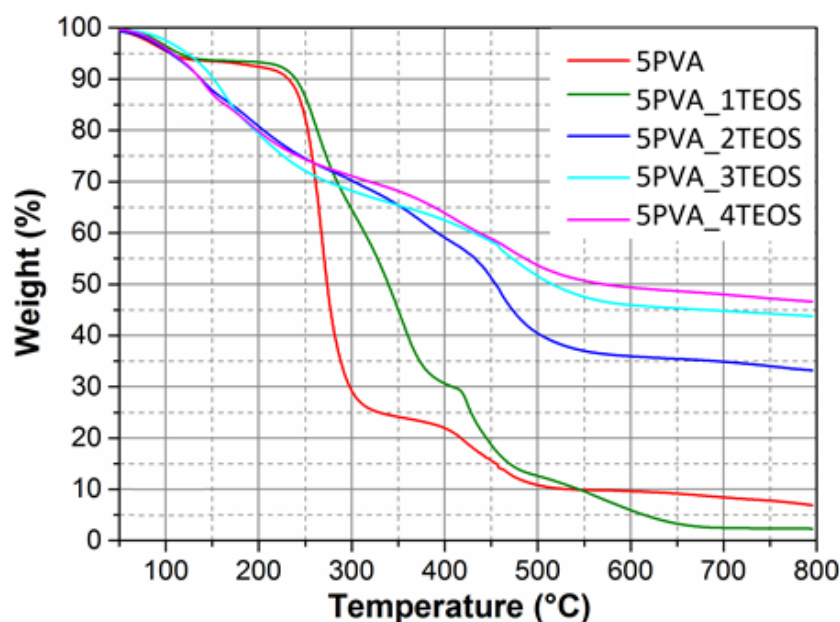


Figure 58. TGA thermograms of PVA/SiO₂ membranes.

The earlier onset of the weight loss of samples 5PVA_2TEOS, 3TEOS, and 4TEOS in comparison with pure PVA suggests that the chain stripping process starts at a lower temperature, which means that at the beginning, water can cleave off more easily from the polymer chains in these samples than in the case of pure PVA. This was ascribed to the lower crystallinity going hand in hand with a disturbed regularity of hydrogen bonding in contrast with the regular hydrogen bonding between the PVA chains in the crystallites of pure PVA. The lower crystallinity is caused by the incorporation of small silica nanoparticles which are homogeneously distributed throughout the PVA matrix, as discussed above in the SAXS/WAXS and AFM sections. However, further thermal degradation is slowed down due to the strong

chemical bonding between the silica nanoparticles with a high surface area and PVA via its OH groups (Scheme 2). Some reports also suggested the migration of silica nanoparticles to the surface to form SiO₂/PVA char, which acts as a heating barrier and protects the PVA matrix inside [38, 39]. On the basis of the TGA analyses, it can thus be concluded that the nanoscale deposition of thermally stable silica has effectively enhanced the overall thermal stability of the PVA/SiO₂ membranes.

The difference in the degradation processes of the PVA and PVA/SiO₂ membranes was clearly seen in derivative thermogravimetric (DTG) curves (Figure 59). There are two obvious degradation peaks of pure PVA, one sharp peak at 268°C and a broad peak above 350°C. The significant change in the shape of the degradation peaks of the PVA/SiO₂ membranes was evident. The main degradation peak of PVA (at 268°C) was not observed for the PVA/SiO₂ membranes, whereas two minor peaks with lower intensities were observed at ~150 and ~450°C. In the PVA/SiO₂ membranes, the elimination reaction spans over a wide temperature range and starts sooner, as discussed above. The first peak obviously corresponds to the fast onset of the elimination reactions in the PVA/SiO₂ membranes. However, the second peak, corresponding to the second degradation stage, shifted to higher temperatures with respect to pure PVA, exhibiting enhancement in the thermal stability. During this stage, the elimination reactions are accompanied by several chain-scission reactions, cyclization, and side reactions. Peng and Kong [38] identified the degradation products as low-molecular weight polyenes, acetaldehyde, benzenoid derivatives, furan, acetone, and acetic acid. It can be observed that the second peak is superimposed on a background originating from the first degradation stage. The overlap of the two stages can be better observed from the integral dependencies (TGA).

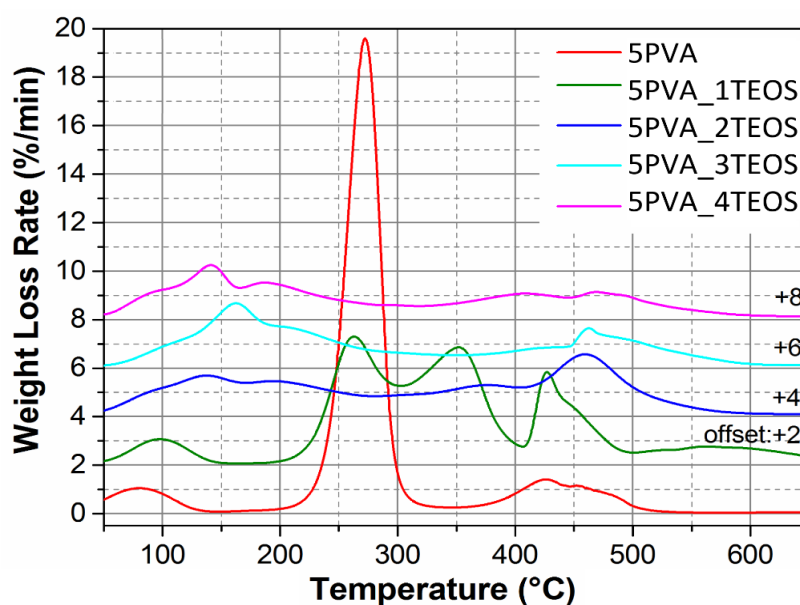


Figure 59. DTG curves of pure PVA/SiO₂ membranes.

The degradation behaviour of the PVA/SiO₂/GA membranes was similar to that of the pure PVA membranes (Figures 60, 61). In other words, the incorporation of GA only had a small influence on the membrane thermal stability. The membranes exhibited a weight loss of about 70% in the first stage (50–350°C), with a further loss of 25% in the second stage as shown in Figure 60. In this case, GA and TEOS did not bind effectively with the PVA network, which lead to the formation of bigger particles (confirmed by SAXS and AFM) instead of the small nanoparticles formed in the PVA/SiO₂ samples. Therefore, the thermal stability did not increase upon silica addition, contrary to the PVA/SiO₂ membranes.

The only significant change in the TGA curves of PVA/SiO₂/GA compared to pure PVA was the broader first stage of the weight loss corresponding to the elimination reactions. This correlates very well with the decrease in crystallinity of the PVA/SiO₂/GA membranes in comparison with pure PVA, which was proved by WAXS and Raman spectroscopy (see Figures 41 and 46). However, the first weight loss stage of PVA/SiO₂/GA is not that broad as in the case of PVA/SiO₂, which reflects the fact that the crystallinity of the PVA/SiO₂ membranes is lower than that of the corresponding PVA/SiO₂/GA membranes (compare the WAXS spectra in Figures 45-47 and the Raman spectra in Figures 40, 41). Thus, the width of the temperature range of the first decomposition stage reflects very well the crystallinity of the samples: the most crystalline PVA showed the fastest decomposition, followed by the less ordered PVA/SiO₂/GA samples with a slower decomposition, and finally by the most amorphous PVA/SiO₂ samples.

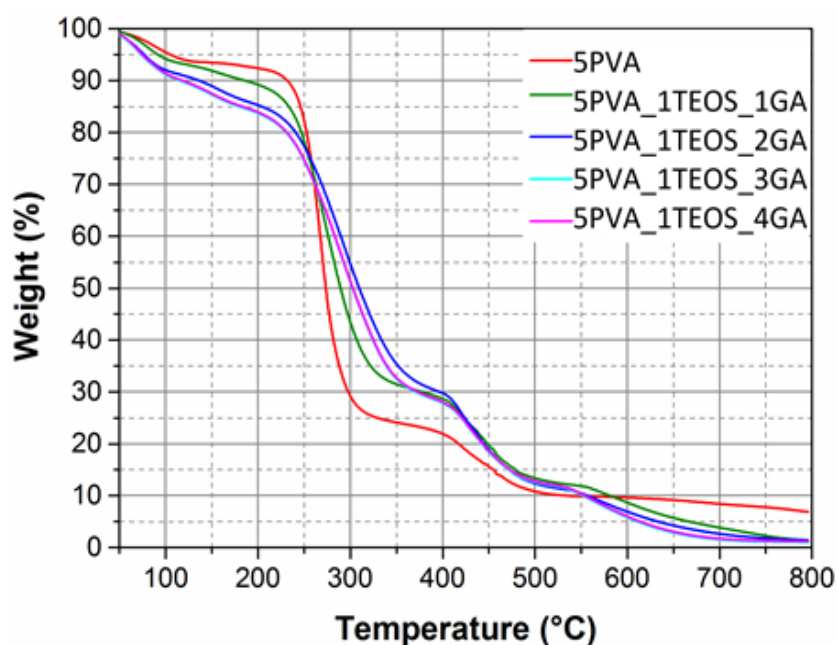


Figure 60. TGA thermograms of a PVA/SiO₂/GA membranes.

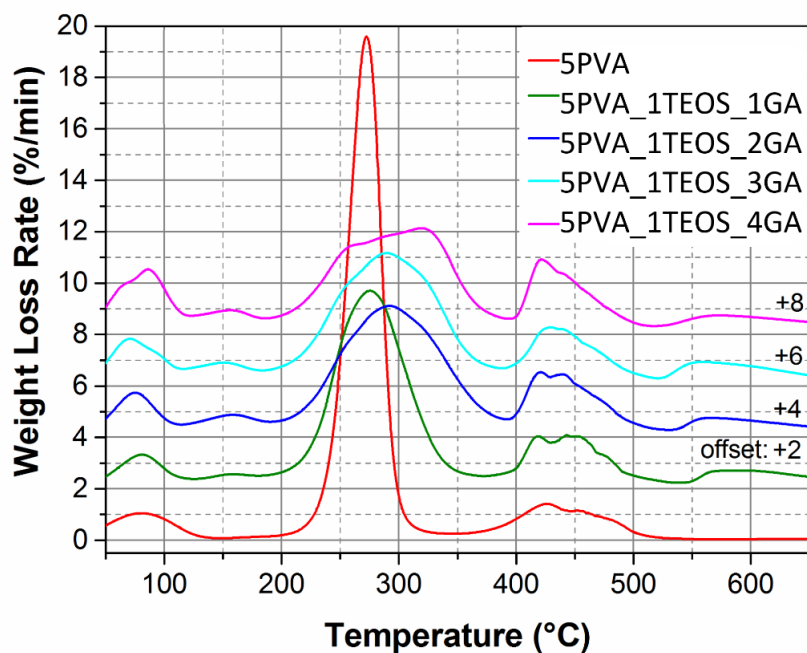


Figure 61. DTG curves of pure PVA/SiO₂/GA membranes.

DSC profiles of PVA and PVA/SiO₂ are shown in Figure 62. PVA exhibited a clear melting transition (T_m) at 223°C, whereas T_m of the PVA/SiO₂ membranes ranged from 176 to 204°C, i.e., were lower than that of the pure PVA membrane. The melting peaks of the PVA/SiO₂ membranes decreased in intensity and shifted to lower temperatures with increasing silica loading. This decline is clearly seen for 5PVA_1TEOS, but as the silica loading increases, the endothermic melting peak becomes broader and totally vanishes for the 5PVA_3TEOS and 5PVA_4TEOS membranes. Both the decrease of T_m and the broadening of the melting peak can be attributed to the reduced crystallinity due to the incorporated SiO₂ nanoparticles. Bin et al. reported this kind of behaviour for PVA–VGCF and PVA–MWNT composites [40].

The DSC profiles of the PVA/SiO₂/GA membranes (Fig. 63) showed a similar melting transition as the pure PVA membrane with only a small decrease in T_m . This is in agreement with the smaller decrease in crystallinity compared to the PVA/SiO₂ samples. The increase in GA concentration had a relatively small effect on the endothermic transition of the PVA/SiO₂/GA membranes. This correlates well with the already discussed fact that the influence of GA concentration on the crystallinity of the PVA/SiO₂/GA membranes is not that strong as in the case of the PVA/SiO₂ membranes.

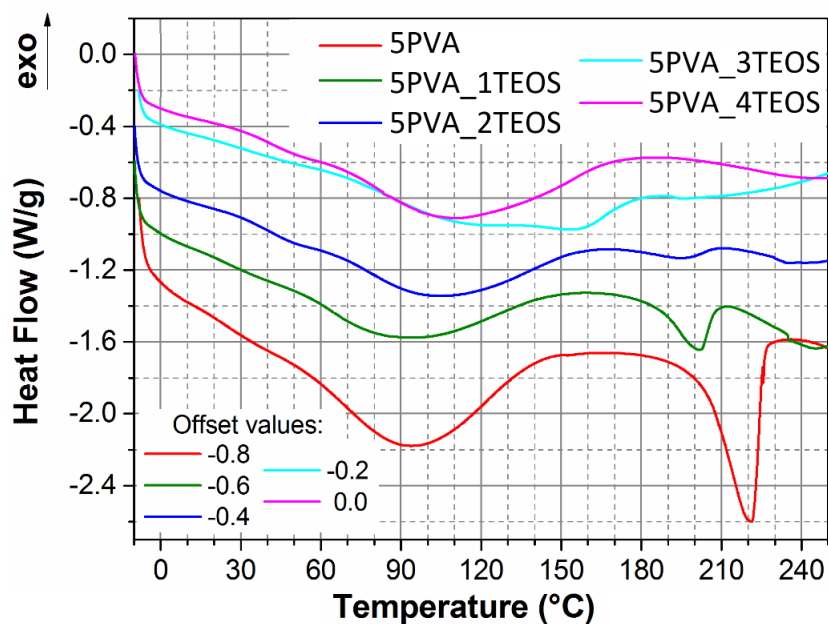


Figure 62. DSC scans of PVA/SiO₂ membranes.

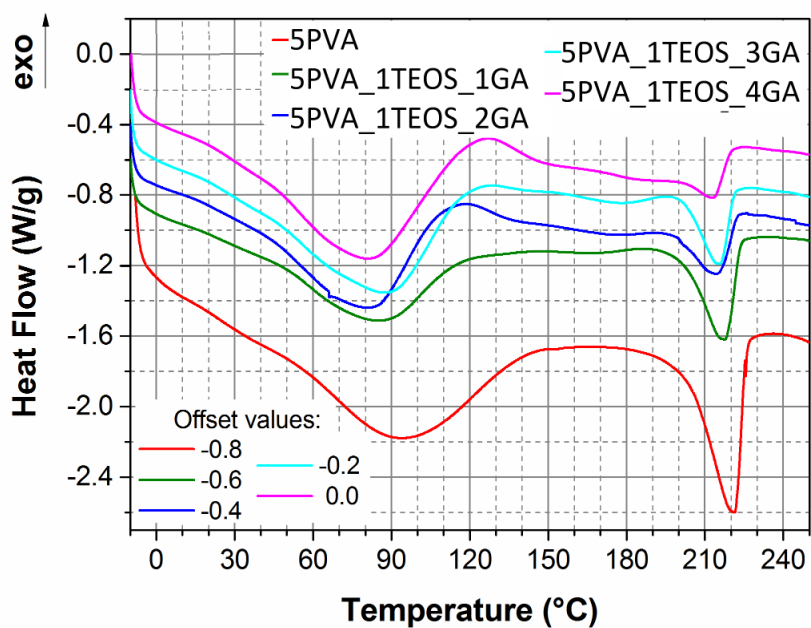


Figure 63. DSC scans of PVA/SiO₂/GA membranes.

4.2.6. Dynamic mechanical analysis

DMA analysis was performed to investigate the thermomechanical properties of the nanocomposite membranes. The temperature dependence of the storage modulus (E') was measured in the range from 30 to 250°C. At higher temperatures (< 200°C), where the material enters the rubbery phase, the storage modulus is referred to as rubbery modulus, E_R .

In the case of PVA/SiO₂ membranes, E' increased with the increasing silica loading as shown in Figure 64. The membranes displayed a higher E_0 in the initial stages from 30 to 70°C,

followed by a flat mid-region between 70 and 120°C. A subsequent increase in E' was observed at higher temperatures (200°C) for the 5PVA_2TEOS, 3TEOS, and 4TEOS samples. The inset graph in Figure 64 shows a zoom of the plot for higher temperatures, i.e., the dependencies of rubbery modulus, E_R versus temperature for the PVA/SiO₂ membranes. Depending on the silica loading, E_R values ranged from 17 to 1015 MPa at 250°C. 5PVA_4TEOS exhibited the highest E_R value of 1015 MPa and 5PVA_1TEOS displayed the lowest E_R of 17 MPa. The E_R value of pure PVA was 6 MPa at 250°C. We can thus conclude that the silica loading clearly improved the mechanical strength of the membranes.

On the other hand, the presence of GA has shown an adverse effect on the PVA/SiO₂/GA membrane strength (Figure 65). The inset graph in Figure 65 shows a detail of the plot for higher temperatures. These membranes followed a reverse trend, i.e., the 5PVA_1TEOS_1GA membrane exhibited the highest E_R of 28 MPa at 250°C and the other membranes showed a decrease of E_R with the increasing GA concentration down to 15 MPa in the case of 5PVA_1TEOS_4GA. This can be explained based on our previous conclusions. In the PVA/SiO₂ membranes, the silica incorporates into the membrane structure in the form of small nanoparticles and binds with the PVA polymer, whereas in the presence of GA, larger separated particles of GA and silica were observed. The presence of these larger nanoparticles resulted in the inferior thermo-mechanical stability of these membranes.

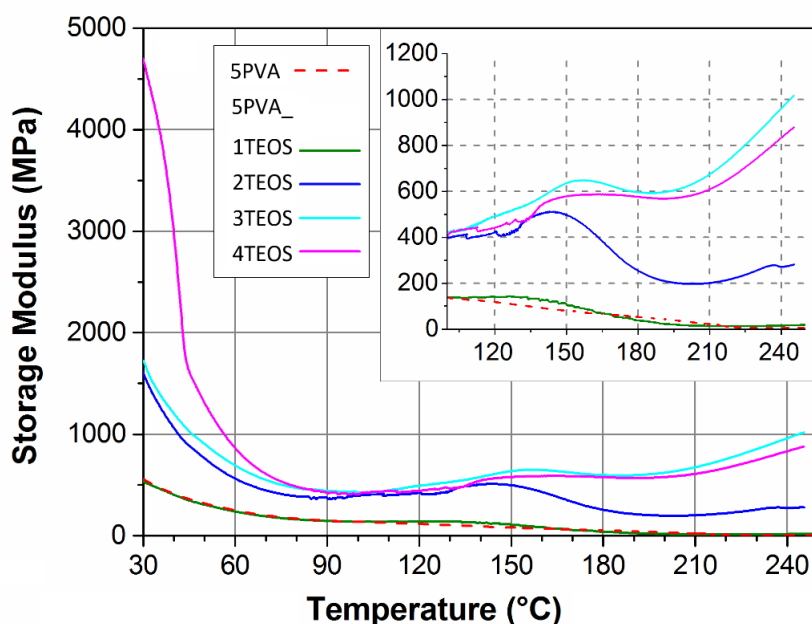


Figure 64. DMA curves of PVA/SiO₂ membranes.

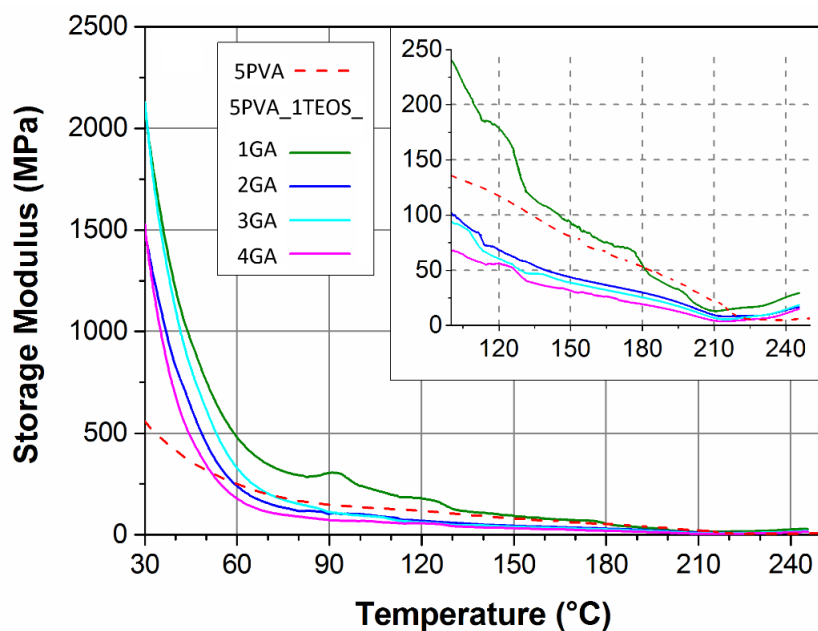


Figure 65. DMA curves of PVA/SiO₂/GA membranes.

4.3. PVA/SSA/SiO₂ membranes

Membranes with different contents of silica and SSA were characterized by FT-IR, rheometer ARES G2, thermogravimetric analysis (TGA), dynamic mechanical analysis (DMA), ion conductivity and water uptake experiments. The effect of silica and SSA incorporation on the properties and morphology of the nanocomposite membranes was systematically investigated.

4.3.1. FT-IR

Figure 66 shows the FT-IR spectra of the 5PVA and 5PVA_0.5SSA_5TEOS membranes. It was reported that the absorption band of ester ($-\text{COO}-$) appeared at $1730\text{--}1735\text{ cm}^{-1}$. This results indicate the spectral changes are an evidence of a crosslinking by the esterification between $-\text{OH}$ in PVA and $-\text{COOH}$ in SSA. The absorption band at 2369 cm^{-1} indicate the presence of sulfonic acid group, which is formed by the introduction of SSA [41]. The band at approximately 1040 cm^{-1} is assigned to stretching vibrations of Si-O-Si . The absorption band, at 900 cm^{-1} can be attributed to the stretching vibration of Si-OH or Si-O- groups. A broad absorption band, situated between $3,000$ and $3,600\text{ cm}^{-1}$, are assigned to O-H stretching and O-H bending vibrations, respectively [42].

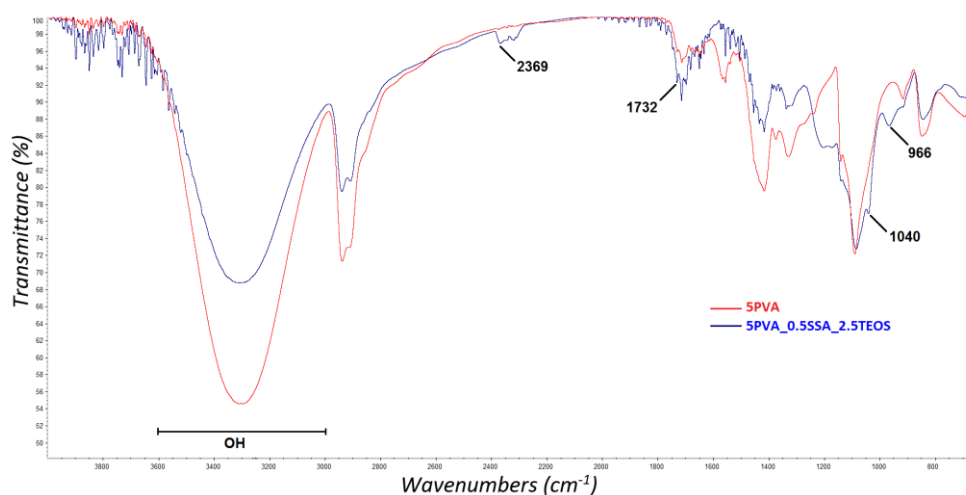


Figure 66. FT-IR spectra of composite PVA membranes.

4.3.2. Rheology

The viscosity of the polymer solution plays a key role, which not only helps to fabricate membranes of specific thickness, but also prevents the formation of pinholes and membrane delamination. Therefore, the understanding of the rheological properties of casting solutions is important for preparing appropriate membranes for fuel cells. In this study we have prepared conducting membranes based on PVA, TEOS and SSA at various stoichiometric ratios and investigated the rheological properties.

The viscosity of the pure PVA solution changed after the incorporation of SSA (Figure 67). At low SSA content, the viscosity was initially increased due to the interaction between the acid groups of SSA and PVA. However, the viscosity was reduced slightly when the SSA loading percentage exceeded 0.5 wt%. The slight reduction in our observed viscosity can be explained by the limited dispersion behaviour of SSA in the PVA matrix. Agglomeration of particles resulted in the reduced surface area between the SSA and PVA, and caused the decrease in viscosity. The similar situation described Chien et al. [43].

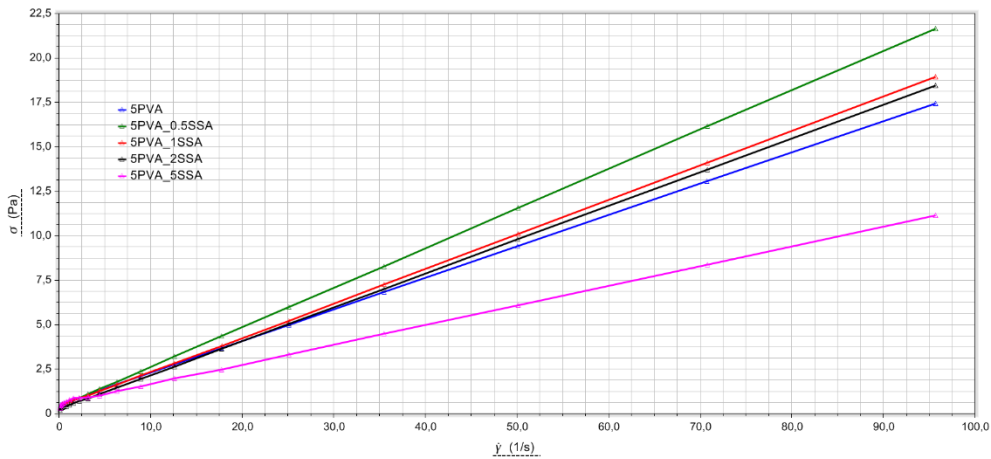


Figure 67. Rheological spectra of pure PVA solution and different SSA loadings of PVA/SSA solutions.

4.3.3. TGA

Figure 68 shows thermogram of composite PVA_TEOS membranes. Thermal stability increase with increasing content of SiO₂, which means higher crosslinking extents for the composite membrane 1TEOS, 2TEOS, 5TEOS and for 10TEOS, respectively.

Figure 69 shows thermogram of composite PVA_SSA membranes. At temperature around 300°C, the highest thermal stability was seen for 5PVA_0.5SSA membrane. This results correspond with rheological properties of PVA_SSA solutions (Figure 67) and show the maximum dispersion of SSA in the PVA matrix for SSA loading 0.5 wt%.

Thermal properties of mixed composite PVA_SSA_TEOS membranes are shown in Figure 70. The increase in thermal properties was seen for membranes with 0.5 wt% of SSA and with 1 or 2.5 wt% of TEOS.

The comparison of all types of composites can be seen in Figure 71. Combination of SSA and SiO₂ crosslinking components into PVA matrix shows good thermal properties of prepared membranes.

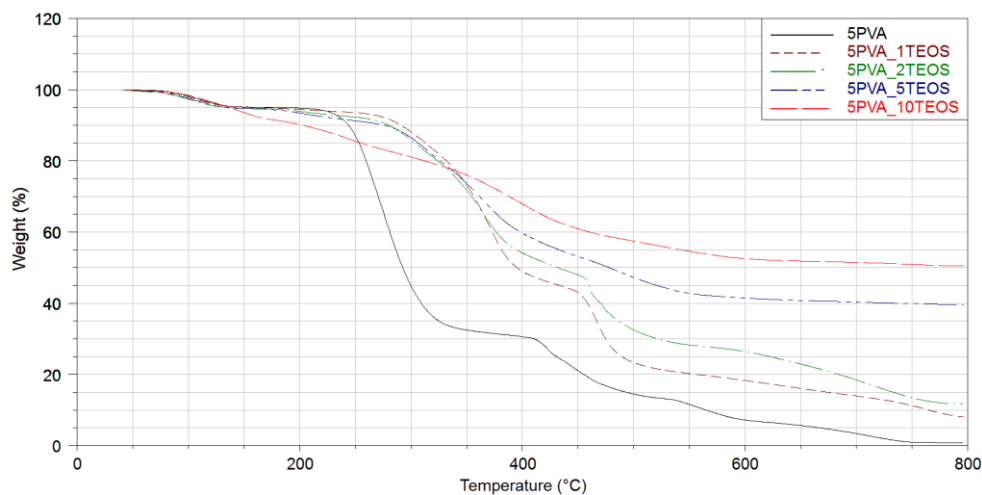


Figure 68. TG thermograms of composite PVA_TEOS membranes.

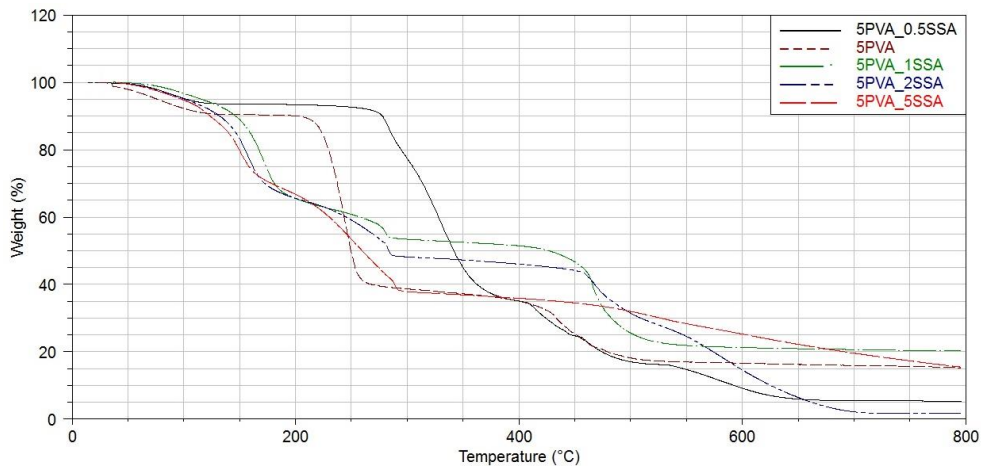


Figure 69. TG thermograms of composite PVA_SSA membranes.

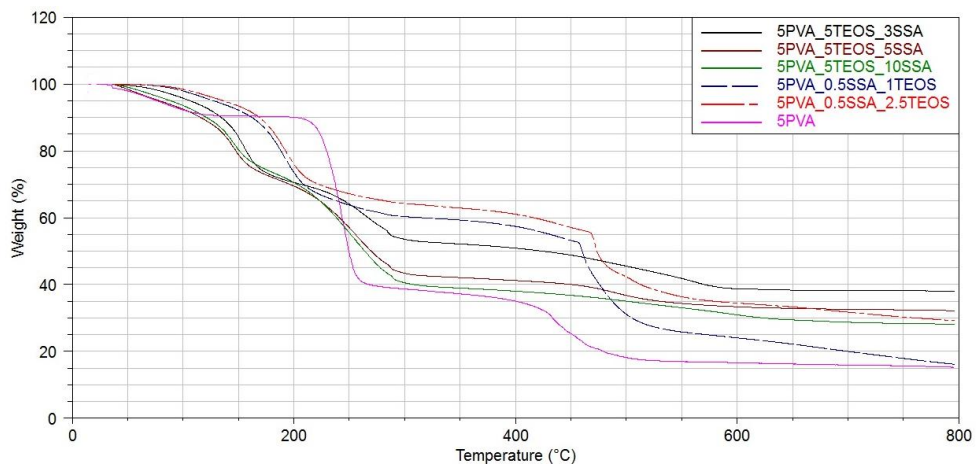


Figure 70. TG thermograms of composite PVA_SSA_TEOS membranes.

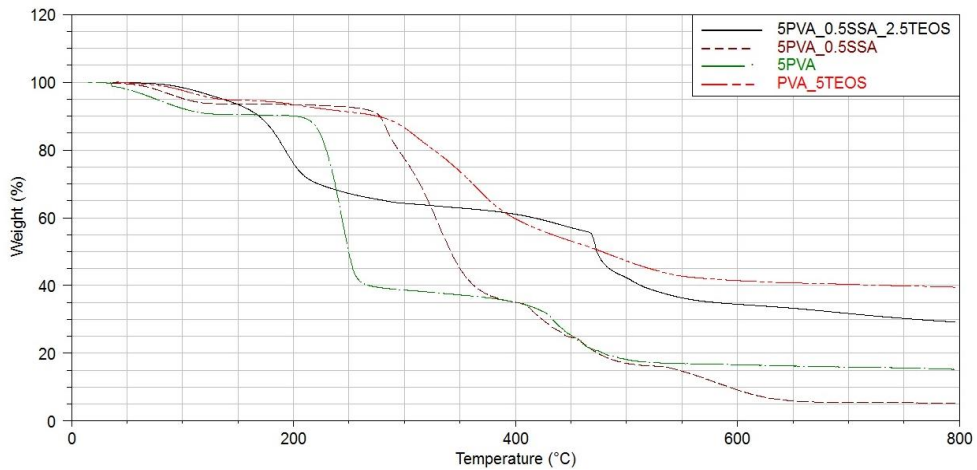


Figure 71. TG thermograms of composite PVA_SSA_TEOS membranes.

4.3.4. DMA

DMA analysis shows dependence of the storage modulus (E') on temperature. For membranes crosslinking with SiO_2 , E_R increased with the increasing silica loading as shown in Figure 72. The membranes displayed a higher E_R in the initial stages from 30 to 70°C, followed by a flat mid-region between 70 and 100°C.

In the case of PVA_SSA membranes, E' decreased with the increasing SSA loading as shown in Figure 73, except membrane 5PVA_0.5SSA, which due to the maximum crosslinking, shows higher value of E' . The decrease of E_R with increasing temperature is similar as for PVA_TEOS membranes.

Mixed PVA_SSA_TEOS membranes show very low value of E' compared to pure PVA and PVA_TEOS membranes (Figure 74).

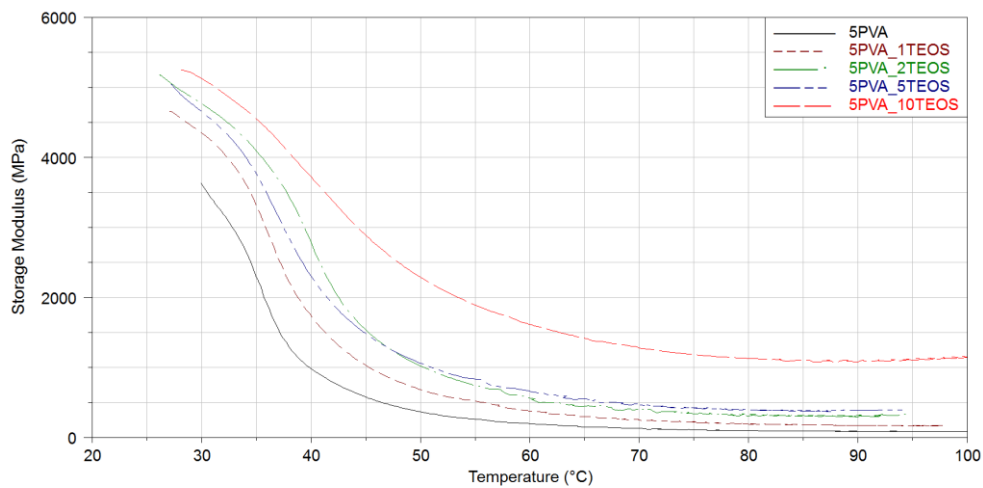


Figure 72. DMA of composite PVA_TEOS membranes.

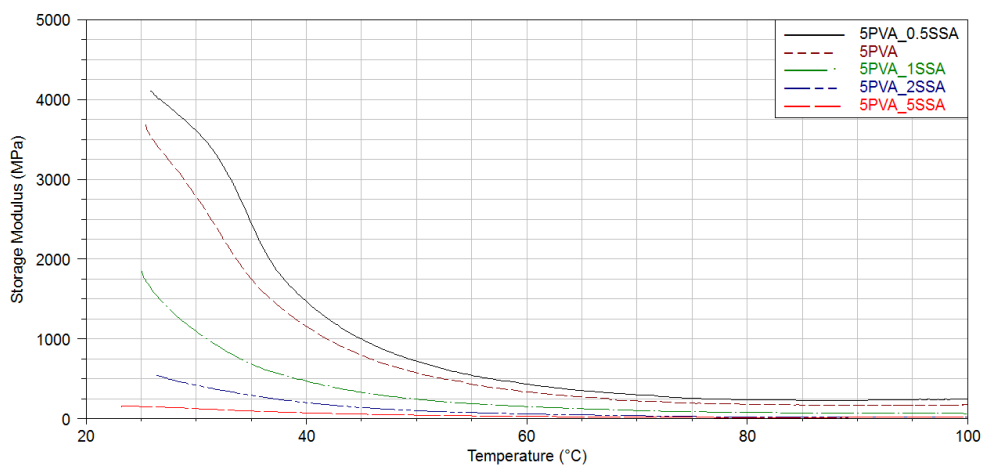


Figure 73. DMA of composite PVA_SSA membranes.

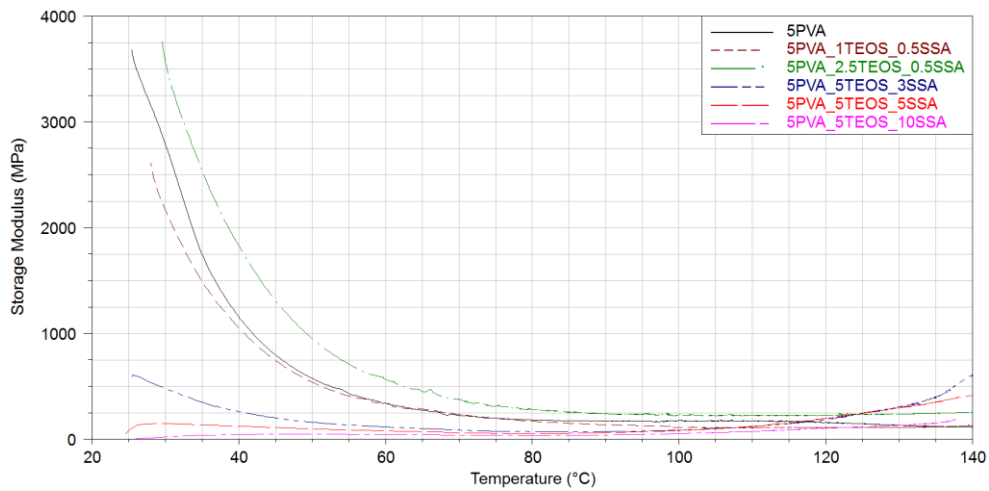


Figure 74. DMA of composite PVA_TEOS membranes.

4.3.5. Water uptake

The W_u was calculated using the equation 1. Figure 75 shows the decreasing ability of PVA composite membranes to absorb water depending on increasing SiO_2 content in the membrane matrix. Thanks to SiO_2 crosslinking, the membrane loses its ability to absorb water, and also increases the resistance of membranes to the aquatic environment. The pure PVA membrane is dissolved in water within minutes, while the composite PVA_ SiO_2 membranes are water insoluble.

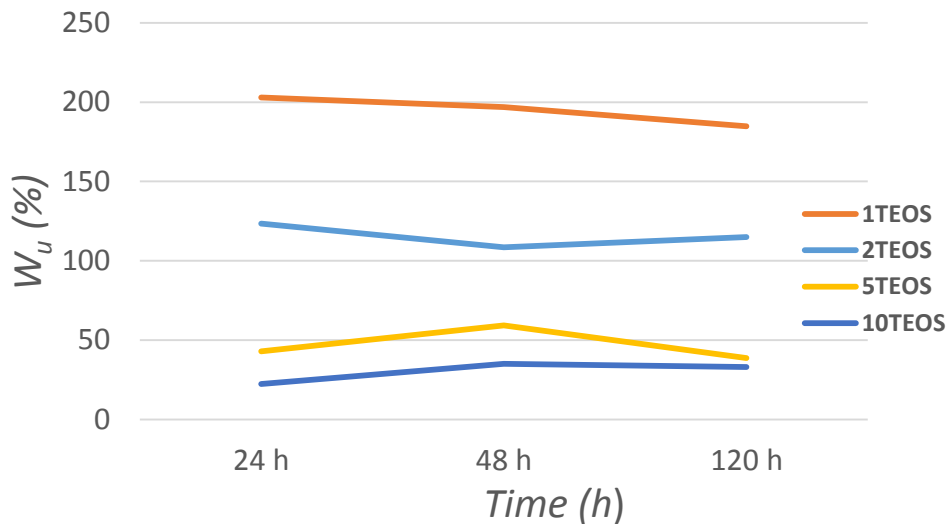


Figure 75. Water uptake of composite PVA_TEOS membranes.

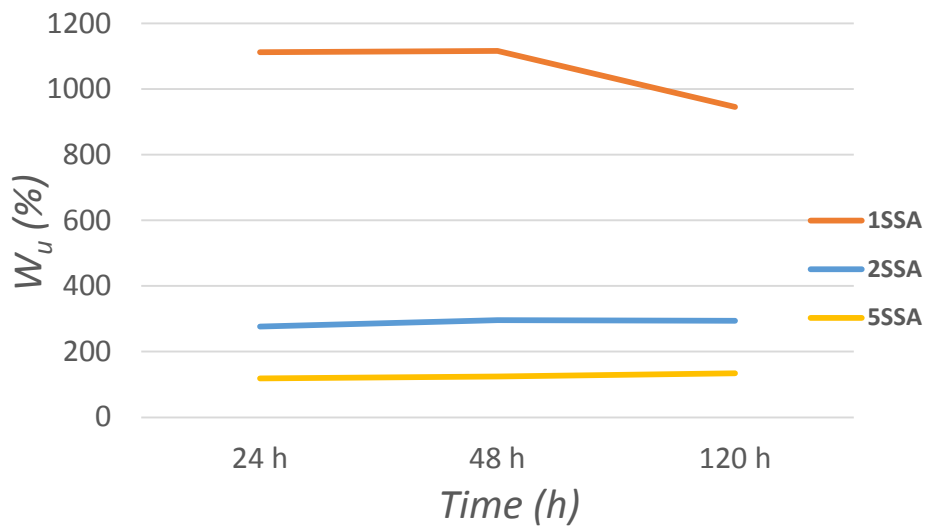


Figure 76. Water uptake of composite PVA_SSA membranes.

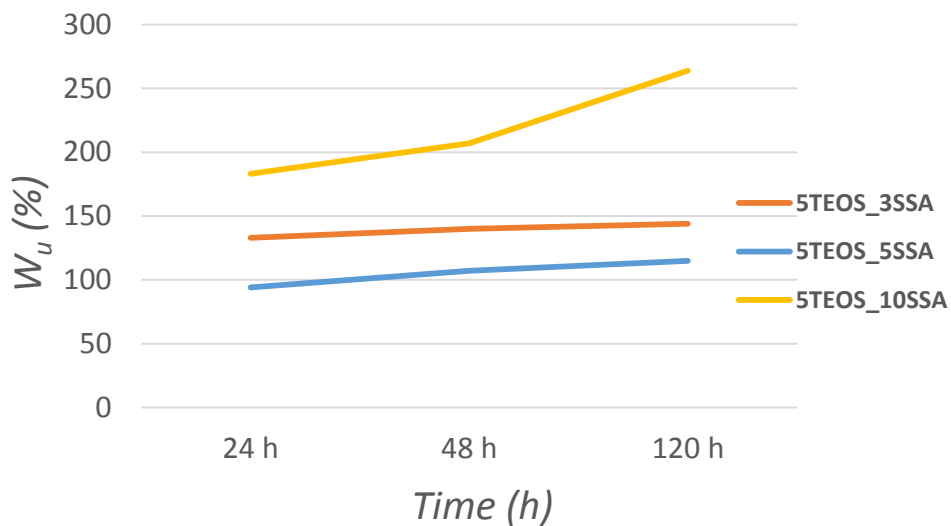


Figure 77. Water uptake of composite PVA_SSA_TEOS membranes.

4.3.6. Ion conductivity

The ionic conductivities of membranes have been determined. In case of dry composites the conductivity significantly increased with SSA loading (Figure 78). Nevertheless, dry composites exhibit very low ionic conductivity compared with Nafion 212 membranes (Table 11).

After wetting of the membranes (immersion in water for 10 seconds) the ion conductivity has increased significantly (Figure 79).

Table 11. Ion conductivity of PVA composite membranes.		
Membranes	Ion conductivity ($\text{mS}\cdot\text{cm}^{-1}$)	
	Dry	Wet
5PVA	0,0060	0,4000
5PVA_0.5SSA	0,0030	1,9600
5PVA_1SSA	0,0645	10,0141
5PVA_2SSA	0,1040	96,8667
5PVA_5SSA	2,1838	90,4289
5PVA_10SSA	1,6187	38,4652
5PVA_1TEOS	0,0369	0,1090
5PVA_2TEOS	0,0762	0,2690
5PVA_5TEOS	0,0333	0,0178
5PVA_10TEOS	0,1320	0,1530
5PVA_0.5SSA_1TEOS	0,0120	1,8734
5PVA_0.5SSA_2.5TEOS	0,0110	0,0327
5PVA_3SSA_5TEOS	0,6207	6,2067
5PVA_5SSA_5TEOS	3,2939	32,9390
5PVA_10SSA_5TEOS	10,9046	26,8886
Nafion 212	3,4300	4,7100

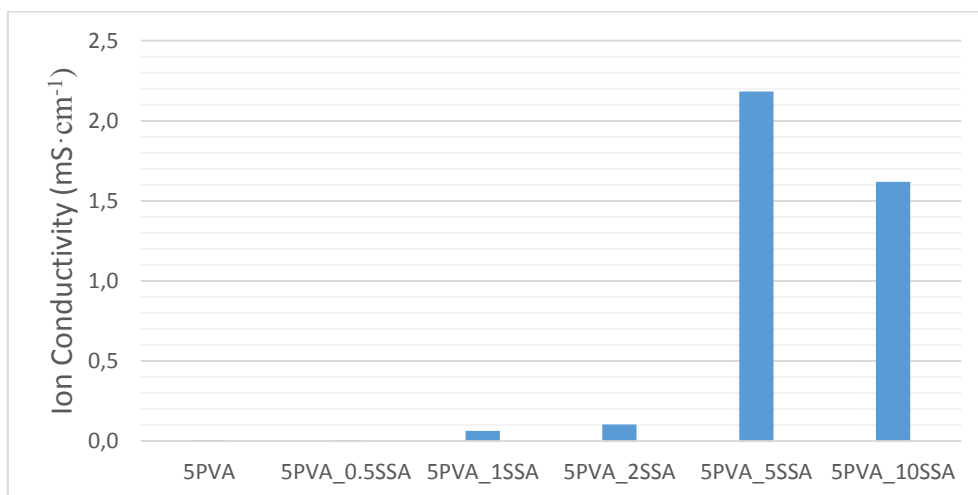


Figure 78. Ion conductivity of composite dry PVA_SSA membranes.

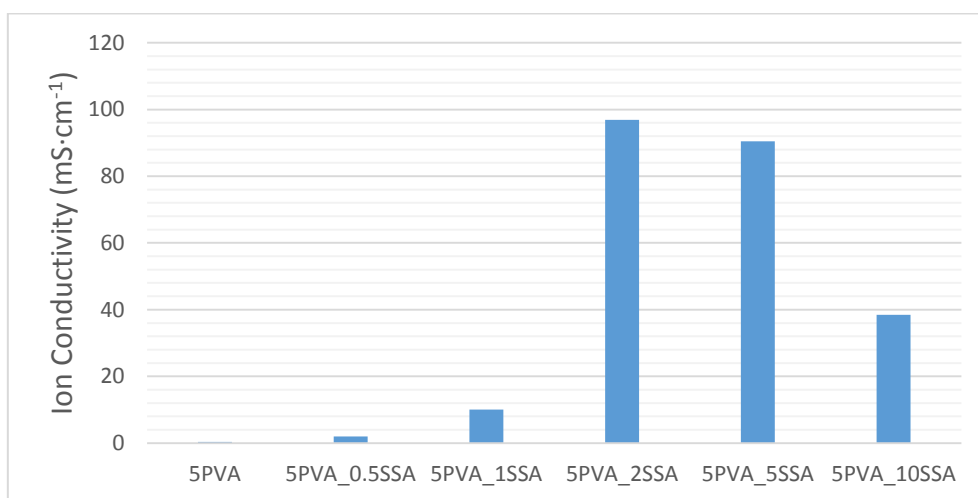


Figure 79. Ion conductivity of composite wet PVA_SSA membranes.

For PVA_TEOS membranes the increase of ion conductivity after wetting is insignificant (Figure 80).

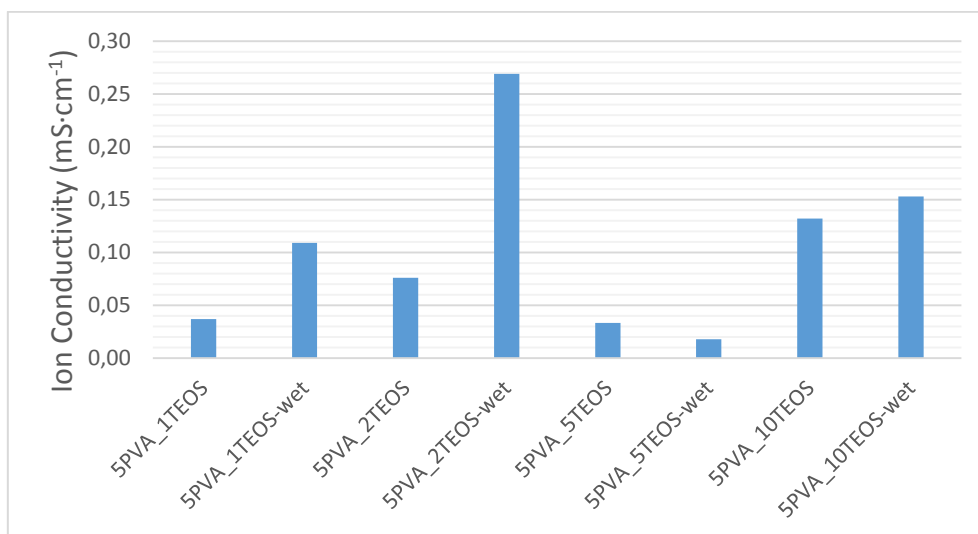


Figure 80. Ion conductivity of composite PVA_TEOS membranes.

Because PVA_SSA membranes aren't stable in water, the combination of SSA and TEOS seems to be ideal for preparation of composite PVA membranes. Swelling PVA_SSA_TEOS membranes exhibit comparable (or higher) ion conductivity with Nafion 212 (Figure 81), (Table 11).

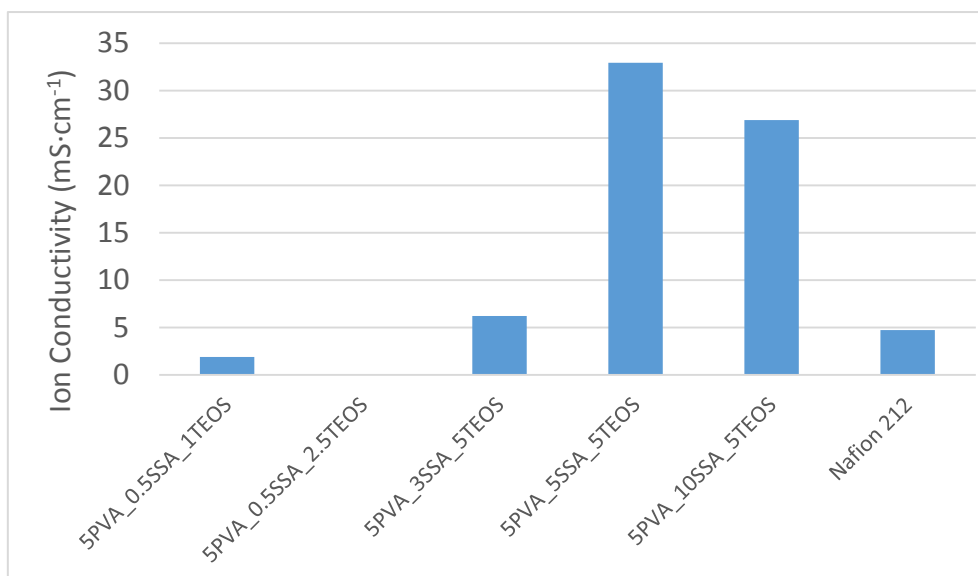


Figure 81. Ion conductivity of composite PVA_SSA_TEOS membranes and Nafion 212.

4.4. Summary

We successfully prepared Nafion-PFA composite membranes using *in situ* acid-catalyzed polymerization method. The influence of the PFA content on the water uptake, water vapour uptake, ionic conductivity, thermal and mechanical stability was investigated. The impregnation of PFA changed the physicochemical properties of composites, owing to the interaction with the Nafion. Consequently, the membranes with high PFA loading exhibited better thermal and mechanical properties. Whereas, membranes with a small amount PFA loading have shown better electrical and water uptake properties. Particularly, NF24 exhibited the best performance in terms of water vapour uptake, conductivity and thermo-mechanical stability from all modified membranes and pure Nafion 115, respectively.

We successfully prepared PVA-based nanocomposite membranes with various silica and GA loading (PVA_SiO₂ and PVA_SiO₂_GA) via the solution casting method. Membranes with and without GA displayed considerably different characteristic features. SAXS/WAXS, AFM and Raman spectroscopy confirmed the incorporation of fine silica nanoparticles (~1 nm) into the PVA_SiO₂ membranes. These membranes showed a significant improvement in the water uptake, thermal stability, and mechanical strength compared to the pure PVA and PVA_SiO₂_GA membranes. The 5PVA_3TEOS membrane with high silica loading exhibited the best thermo-mechanical stability with E_R of 1015 MPa (at 250°C, DMA). In the case of PVA_SiO₂_GA membranes, GA preferably reacted with TEOS forming submicron particles (~25 nm) contrary to PVA_SiO₂ membranes, which reduced the thermal stability of these membranes. The comparison of structural and thermo-mechanical characteristics of the PVA_SiO₂ and PVA_SiO₂_GA membranes indicates that the homogeneous incorporation of small silica nanoparticles (~1 nm) played a crucial role in improving the properties of the PVA_SiO₂ membranes. These membranes are both hydrophilic and thermally stable, which are important criteria for the application of PVA-based membranes. Furthermore, they are produced without any cross-linking agent such as GA, which makes the process simpler and cost-effective.

Studies of PVA_SSA membranes show increase of ion conductivity of composites due to incorporation of SSA particles to PVA matrix. Conductivity of wet membranes can be compared with commercially used Nafion membrane. Nafion is the world's most widely used membrane for fuel cells. The best thermo-mechanical properties exhibits 5PVA_0.5SSA membrane. However, the stability of PVA_SSA membranes in water isn't high. The combination of SSA and SiO₂ crosslinking agents shows as suitable solution for preparation of

new composite membranes for fuel cells. The results of this study can be useful for further research of PVA based composite membranes.

4.5. Literature

1. Liu, J., Wang, H., Cheng, S., & Chan, K. Y. (2005). Nafion–polyfurfuryl alcohol nanocomposite membranes for direct methanol fuel cells. *Journal of Membrane Science*, 246(1), 95-101.
2. Ludvigsson, M., Lindgren, J., & Tegenfeldt, J. (2000). FTIR study of water in cast Nafion films. *Electrochimica Acta*, 45(14), 2267-2271.
3. Vishwanatham, S., & Haldar, N. (2008). Furfuryl alcohol as corrosion inhibitor for N80 steel in hydrochloric acid. *Corrosion Science*, 50(11), 2999-3004.
4. Shindo, A., & Izumino, K. (1994). Structural variation during pyrolysis of furfuryl alcohol and furfural-furfuryl alcohol resins. *Carbon*, 32(7), 1233-1243.
5. González, R., Figueroa, J. M., & González, H. (2002). Furfuryl alcohol polymerisation by iodine in methylene chloride. *European Polymer Journal*, 38(2), 287-297.
6. Sakintuna, B., & Yürüm, Y. (2006). Preparation and characterization of mesoporous carbons using a Turkish natural zeolitic template/furfuryl alcohol system. *Microporous and mesoporous materials*, 93(1), 304-312.
7. Elliott, J. A., Wu, D., Paddison, S. J., & Moore, R. B. (2011). A unified morphological description of Nafion membranes from SAXS and mesoscale simulations. *Soft Matter*, 7(15), 6820-6827.
8. Arico, A. S., Creti, P., Antonucci, P. L., & Antonucci, V. (1998). Comparison of Ethanol and Methanol Oxidation in a Liquid-Feed Solid Polymer Electrolyte Fuel Cell at High Temperature. *Electrochemical and Solid-State Letters*, 1(2), 66-68.
9. Deng, Q., Wilkie, C. A., Moore, R. B., & Mauritz, K. A. (1998). TGA–FTi. r. investigation of the thermal degradation of Nafion® and Nafion®/[silicon oxide]-based nanocomposites. *Polymer*, 39(24), 5961-5972.
10. Guigo, N., Mija, A., Zavaglia, R., Vincent, L., & Sbirrazzuoli, N. (2009). New insights on the thermal degradation pathways of neat poly (furfuryl alcohol) and poly (furfuryl alcohol)/SiO₂ hybrid materials. *Polymer Degradation and Stability*, 94(6), 908-913.
11. Jiang, S., Yan, Y., & Gavalas, G. R. (1995). Temporary carbon barriers in the preparation of H₂-permselective silica membranes. *Journal of membrane science*, 103(3), 211-218.
12. Song, C., Wang, T., Jiang, H., Wang, X., Cao, Y., & Qiu, J. (2010). Gas separation performance of C/CMS membranes derived from poly (furfuryl alcohol) (PFA) with different chemical structure. *Journal of Membrane Science*, 361(1), 22-27.
13. Men, X. H., Zhang, Z. Z., Song, H. J., Wang, K., & Jiang, W. (2008). Functionalization of carbon nanotubes to improve the tribological properties of poly (furfuryl alcohol) composite coatings. *Composites science and technology*, 68(3), 1042-1049.
14. Song, C., Wang, T., Wang, X., Qiu, J., & Cao, Y. (2008). Preparation and gas separation properties of poly (furfuryl alcohol)-based C/CMS composite membranes. *Separation and purification technology*, 58(3), 412-418.
15. Jalani, N. H., Dunn, K., & Datta, R. (2005). Synthesis and characterization of Nafion®-MO₂ (M= Zr, Si, Ti) nanocomposite membranes for higher temperature PEM fuel cells. *Electrochimica Acta*, 51(3), 553-560.
16. Majsztrik, P. W., Satterfield, M. B., Bocarsly, A. B., & Benziger, J. B. (2007). Water sorption, desorption and transport in Nafion membranes. *Journal of Membrane Science*, 301(1), 93-106.

17. Jalani, N. H., & Datta, R. (2005). The effect of equivalent weight, temperature, cationic forms, sorbates, and nanoinorganic additives on the sorption behavior of Nafion®. *Journal of membrane science*, 264(1), 167-175.
18. Li, L., & Zhang, Y. (2008). Chemical modification of Nafion membrane with 3, 4-ethylenedioxythiophene for direct methanol fuel cell application. *Journal of Power Sources*, 175(1), 256-260.
19. Men, X. H., Zhang, Z. Z., Song, H. J., Wang, K., & Jiang, W. (2008). Fabrication of superhydrophobic surfaces with poly (furfuryl alcohol)/multi-walled carbon nanotubes composites. *Applied surface science*, 254(9), 2563-2568.
20. Jiang, R., Kunz, H. R., & Fenton, J. M. (2006). Composite silica/Nafion® membranes prepared by tetraethylorthosilicate sol-gel reaction and solution casting for direct methanol fuel cells. *Journal of Membrane Science*, 272(1), 116-124.
21. Shao, Z. G., Xu, H., Li, M., & Hsing, I. M. (2006). Hybrid Nafion-inorganic oxides membrane doped with heteropolyacids for high temperature operation of proton exchange membrane fuel cell. *Solid State Ionics*, 177(7), 779-785.
22. Klotzbach, T., Watt, M., Ansari, Y., & Minter, S. D. (2006). Effects of hydrophobic modification of chitosan and Nafion on transport properties, ion-exchange capacities, and enzyme immobilization. *Journal of Membrane Science*, 282(1), 276-283.
23. Soboleva, T., Xie, Z., Shi, Z., Tsang, E., Navessin, T., & Holdcroft, S. (2008). Investigation of the through-plane impedance technique for evaluation of anisotropy of proton conducting polymer membranes. *Journal of Electroanalytical Chemistry*, 622(2), 145-152.
24. Martinelli, A., Matic, A., Jacobsson, P., Börjesson, L., Navarra, M. A., Fericola, A. & Scrosati, B. (2006). Structural analysis of PVA-based proton conducting membranes. *Solid State Ionics*, 177(26), 2431-2435.
25. Yang, C. C., Li, Y. J., & Liou, T. H. (2011). Preparation of novel poly (vinyl alcohol)/SiO₂ nanocomposite membranes by a sol-gel process and their application on alkaline DMFCs. *Desalination*, 276(1), 366-372.
26. Alessi, A., Agnello, S., Buscarino, G., & Gelardi, F. M. (2013). Raman and IR investigation of silica nanoparticles structure. *Journal of Non-Crystalline Solids*, 362, 20-24.
27. Yang, C. C., Lin, C. T., & Chiu, S. J. (2008). Preparation of the PVA/HAP composite polymer membrane for alkaline DMFC application. *Desalination*, 233(1-3), 137-146.
28. Hema, M., Selvasekarapandian, S., Hirankumar, G., Sakunthala, A., Arunkumar, D., & Nithya, H. (2010). Laser Raman and ac impedance spectroscopic studies of PVA: NH₄NO₃ polymer electrolyte. *Spectrochimica Acta Part A: Molecular and Biomolecular Spectroscopy*, 75(1), 474-478.
29. Assender, H. E., & Windle, A. H. (1998). Crystallinity in poly (vinyl alcohol). 1. An X-ray diffraction study of atactic PVOH. *Polymer*, 39(18), 4295-4302.
30. Guirguis, O. W., & Moselhey, M. T. (2012). Thermal and structural studies of poly (vinyl alcohol) and hydroxypropyl cellulose blends. *Natural Science*, 4(1), 57.
31. Hassan, C., & Peppas, N. (2000). Structure and applications of poly (vinyl alcohol) hydrogels produced by conventional crosslinking or by freezing/thawing methods. *Biopolymers· PVA Hydrogels, Anionic Polymerisation Nanocomposites*, 37-65.
32. Ilavsky, J., & Jemian, P. R. (2009). Irena: tool suite for modeling and analysis of small-angle scattering. *Journal of Applied Crystallography*, 42(2), 347-353.
33. Mansur, H. S., Oréfice, R. L., & Mansur, A. A. (2004). Characterization of poly (vinyl alcohol)/poly (ethylene glycol) hydrogels and PVA-derived hybrids by small-angle X-ray scattering and FTIR spectroscopy. *Polymer*, 45(21), 7193-7202.

34. Xie, Z., Hoang, M., Ng, D., Doherty, C., Hill, A., & Gray, S. (2014). Effect of heat treatment on pervaporation separation of aqueous salt solution using hybrid PVA/MA/TEOS membrane. *Separation and Purification Technology*, 127, 10-17.
35. Tsuchiya, Y., & Sumi, K. (1969). Thermal decomposition products of poly (vinyl alcohol). *Journal of Polymer Science Part A: Polymer Chemistry*, 7(11), 3151-3158.
36. Gilman, J. W., VanderHart, D. L., & Kashiwagi, T. (1994, August). Fire and polymers II: materials and test for hazard prevention. In *ACS Symposium Series* (Vol. 599, pp. 21-26).
37. Alexy, P., Bakoš, D., Crkoňová, G., Kolomaznik, K., & Kršiak, M. (2001, June). Blends of polyvinylalcohol with collagen hydrolysate: Thermal degradation and processing properties. In *Macromolecular Symposia* (Vol. 170, No. 1, pp. 41-50). WILEY-VCH Verlag GmbH.
38. Peng, Z., & Kong, L. X. (2007). A thermal degradation mechanism of polyvinyl alcohol/silica nanocomposites. *Polymer Degradation and Stability*, 92(6), 1061-1071.
39. Vyazovkin, S., & Sbirrazzuoli, N. (1999). Kinetic methods to study isothermal and nonisothermal epoxy-anhydride cure. *Macromolecular Chemistry and Physics*, 200(10), 2294-2303.
40. Bin, Y., Mine, M., Koganemaru, A., Jiang, X., & Matsuo, M. (2006). Morphology and mechanical and electrical properties of oriented PVA-VGCF and PVA-MWNT composites. *Polymer*, 47(4), 1308-1317.
41. Rhim, J. W., Park, H. B., Lee, C. S., Jun, J. H., Kim, D. S., & Lee, Y. M. (2004). Crosslinked poly (vinyl alcohol) membranes containing sulfonic acid group: proton and methanol transport through membranes. *Journal of Membrane Science*, 238(1), 143-151.
42. Katumba, G., Mwakikunga, B. W., & Mothibinyane, T. R. (2008). FTIR and Raman spectroscopy of carbon nanoparticles in SiO₂, ZnO and NiO matrices. *Nanoscale Research Letters*, 3(11), 421.
43. Chien, H. C., Tsai, L. D., Huang, C. P., Kang, C. Y., Lin, J. N., & Chang, F. C. (2013). Sulfonated graphene oxide/Nafion composite membranes for high-performance direct methanol fuel cells. *international journal of hydrogen energy*, 38(31), 13792-13801.

5. Conclusion

The main objectives of the dissertation were the questionnaire survey of selected students of the University of West Bohemia in Pilsen focusing on knowledge of renewable energy sources, especially fuel cells, preparation of laboratory tasks for subject Physical practice that is taught at the Department of Mathematics, Physics and Technical Education, at the Faculty of Pedagogy and preparation of new composite proton exchange membranes suitable for use especially in fuel cells.

For the accurate design of learning objects it is necessary to estimate the level of knowledge of students for whom the given learning object is intended. Whereas the college students come from different types of schools, the level of acquired knowledge may be significantly different. It is difficult for the teacher to find a suitable compromise, when the learning object is not too detailed or too superficial. For these and other reasons, a questionnaire survey was conducted to monitor the level of acquiring the basic concepts of renewable energies, such as fuel cells.

The results of the questionnaire survey show that the overall level of acquisition of knowledge and phenomena associated with fuel cells is for university students quite satisfactory. Higher success has been achieved by students in technical study programs. For a more accurate interpretation of the measured data, it would be advisable to repeat the questionnaire survey on a larger group of students.

Preparing of laboratory exercises which would be focused on renewable energy issues, can help students to get to know the issue better. One of the objectives of this work was the preparation of the laboratory exercise, which was focused on measuring of the rheological properties of solutions for the preparation of polymeric PVA membranes for fuel cells. Students performed measurements on the Ares G2 rheometer, which is located at the Department of Engineering of Special Materials at NTC in Pilsen. There are several other laboratory exercises and bachelor's or master's theses focused on fuel cell issues are carried out in the ISM.

The aim of this work was also the preparation of new composite membranes for fuel cells. The developed membranes in some properties exceed the Nafion membranes, which represent a standard for properties of PEM. The obtained knowledge about the properties and characterization of polymer membranes can be helpful in creating others laboratory exercises for physical practice or in choosing topics of bachelor's and master's theses for students of natural sciences.

Considering of the increasing up-to-date topic of renewable resources, it is necessary to include information about this issue in teaching, not only through laboratory exercises.

Appendix 1 – Questionnaire in Czech

Věk:

Ročník:

Fakulta:

Obor:

1. Jako palivo pro vznětový motor se používá:

- a) uhlí
- b) benzín
- c) nafta
- d) metanol

2. Palivový článek:

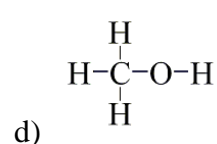
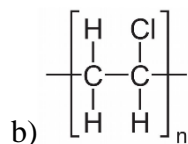
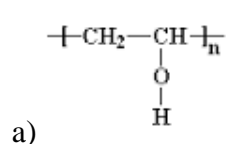
- a) převádí elektrickou energii na chemickou
- b) využívá tuhá paliva
- c) převádí chemickou energii na elektrickou
- d) je druh perpetuum mobile

3. PEMFC je označení pro:

- a) palivové články s alkalickým elektrolytem
- b) palivové články s kyselinou fosforečnou
- c) palivové články s polymerní membránou
- d) palivové články s tuhými oxidy

4. Uveďte palivo, které se využívá v palivových člancích:

5. Polyvinylalkohol má strukturní vzorec:



6. Nafion je membrána vyráběná na základě:

- e) polyvinylalkoholu
- f) polysulfonu
- g) kyseliny chlorovodíkové
- h) polytetrafluorethylenu

7. Palivový článek **není** tvořen:

- e) anodou
- f) katodou
- g) membránou či elektrolytem
- h) zapalovací svíčkou

8. Palivový článek **není** tvořen:

- i) anodou
- j) katodou
- k) membránou či elektrolytem
- l) zapalovací svíčkou

9. Funkcí membrány ve vodíkovém palivovém článku je:

- e) propouštět protony
- f) propouštět elektrony
- g) propouštět plyn
- h) nepropouštět protony

10. Teflon je zkratka pro:

- e) polyvinylalkohol
- f) polytetrafluorethylen
- g) polyethylentereftalát
- h) polyethylenglykol

11. Reologie je věda, která se zabývá:

- e) magnetickými jevy
- f) elektrickými jevy
- g) chemickou reaktivitou látek
- h) zkoumáním a modelováním deformačních vlastností látek

12. Termogravimetrie:

- e) zkoumá deformaci materiálu v závislosti na mechanickém namáhání
- f) zkoumá změnu hmotnosti v závislosti na tepelném namáhání
- g) zkoumá nasákavost materiálu
- h) zabývá se měřením teploty

Appendix 2 – Questionnaire in English

Age:

Year of study:

Faculty:

Field of study:

1. As fuel for the diesel engine is used:

- e) coal
- f) gasoline
- g) diesel
- h) methanol

2. Fuel cell:

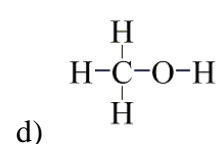
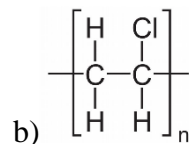
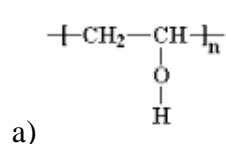
- e) converts electrical energy to chemical
- f) use solid fuels
- g) converts chemical energy to electrical
- h) is a kind of perpetuum mobile

3. PEMFC is stands for:

- e) fuel cells with alkaline electrolyte
- f) fuel cells with phosphoric acid
- g) fuel cells with polymeric membrane
- h) fuel cells with solid oxide

4. Provide the fuel that is used in fuel cells:

5. Polyvinylalcohol has the structural formula:



6. Nafion is membrane produced on the basis of:

- i) polyvinylalcohol
- j) polysulfone
- k) hydrochloric acid
- l) polytetrafluorethylene

7. Polymerization is a chemical reaction in which:
- e) from polymers are formed monomers
 - f) from small molecules formed high molecular substances
 - g) from alcohol is formed acid
 - h) is formed ester and water
8. The fuel cell **is not** formed by:
- m) anode
 - n) cathode
 - o) membrane or electrolyte
 - p) spark plug
9. Functions of the membrane in a hydrogen fuel cell is:
- i) transmit protons
 - j) transmit electrons
 - k) transmit gas
 - l) not transmit protons
10. Teflon is stands for:
- i) polyvinylalcohol
 - j) polytetrafluorethylene
 - k) polyethylenterephthalate
 - l) polyethylenglycol
11. Rheology is the science that deals:
- i) magnetic phenomena
 - j) electrical phenomena
 - k) the chemical reactivity of substances
 - l) investigation and modelling of deformation properties of substances
12. Thermogravimetry:
- i) examine the deformation of the material in dependence on the mechanical stress
 - j) examine the weight change according to the thermal changes
 - k) examine the water absorption of material
 - l) deal with measuring of temperature

Měření reologických vlastností roztoků pro přípravu modifikovaných poly(vinyl alkohol) (PVA) kompozitních membrán pomocí rotačního reometru ARES-G2.

Teoretický úvod

Hydrofilní PVA membrány jsou používány v mnoha aplikacích, v poslední době byly široce využívány také jako polymerní elektrolytické membrány (PEM) pro palivové články. Na vytvoření kvalitní membrány se podílí mnoho parametrů, jako jsou vlastnosti roztoku pro přípravu membrány litím, podmínky přípravy (teplota, relativní vlhkost, čas), reakční složky atd. Viskozita polymerního roztoku hraje klíčovou roli nejen při přípravě membrány specifické tloušťky, ale rovněž zabraňuje tvorbě bublin a praskání membrány. Porozumění reologickým vlastnostem polymerních roztoků je důležité pro přípravu membrán vhodných pro využití v palivových článcích [1].

Reologie zkoumá, jak se za působení mechanických vlivů mění a přetvářejí pevné látky nebo také, jak tečou a proudí kapaliny a plyny. Reologie je velice rozsáhlý obor, který zasahuje do celé řady jiných vědních disciplín (stavebnictví, strojírenství, hutnictví, sklářství, potravinářství, chemie, geologie, medicína, doprava, kosmetika, atd.)

Kapaliny jsou látky, které se účinkem i malé vnější síly trvale deformují – tečou. Rychlost toku kapaliny je tím větší, čím větší je vnější síla a čím menší jsou vnitřní síly, které působí proti toku. Vnitřní síly (vnitřní tření) vznikají v kapalině jako důsledek tepelného pohybu a mezimolekulárních přitažlivých sil. Při malých rychlostech proudění (laminární proudění) se tok kapalin uskutečňuje jako smyková deformace, která charakterizuje změnu materiálu při smykovém (tečném) napětí. Při laminárním proudění reálné tekutiny vzniká v důsledku mezimolekulárních sil ve stykové ploše dvou vrstev pohybujících se různou rychlostí v tečné napětí τ , jímž se snaží rychlejší vrstva urychlovat vrstvu pomalejší a ta naopak zpomalovat vrstvu rychlejší. Podle Newtona je toto tečné napětí přímo úměrné gradientu rychlosti

$$\frac{dv}{dy}$$

tj. přírůstku rychlosti dv mezi dvěma přiléhajícími vrstvami dělenému vzdáleností vrstev dy . Platí:

$$\tau = \eta \frac{dv}{dy},$$

kde konstanta úměrnosti η se nazývá dynamická viskozita.

Dynamická viskozita je látkovou charakteristikou, jejíž hodnota závisí na teplotě a tlaku. U plynů s teplotou roste, u kapalin naopak klesá [2-3].

Úkolem reologie je experimentální stanovení funkční závislosti mezi tečným napětím a gradientem rychlosti pro daný vzorek kapaliny, tzn. závislosti zdánlivé viskozity na tečném napětí nebo gradientu rychlosti.

K měření viskozity se běžně používají průtokové, pádové a rotační reometry.

U rotačních reometrů je vzorek podrobován smyku mezi dvěma definovanými plochami. Jedna plocha (rotor) se otáčí konstantní úhlovou rychlostí. Vnitřním třením kapaliny se otáčivý moment přenáší na druhou desku (převodník), kde se může měřit například stočení vlákna, na kterém je druhá deska zavěšena, nebo se otáčivý moment měří elektronicky.

Mezi nejběžnější typy rotačních reometrů patří typ složený ze dvou souosých válců, mezi kterými je měřená kapalina, typ složený z desky a kužele nebo dvou rovnoběžných desek (Obrázek 1).

Vztah mezi smykovým napětím τ a momentem síly M je pro uspořádání kužel – deska s poloměrem podstavy kužele R dán rovnicí

$$\tau = \frac{3M}{2\pi R^3}$$

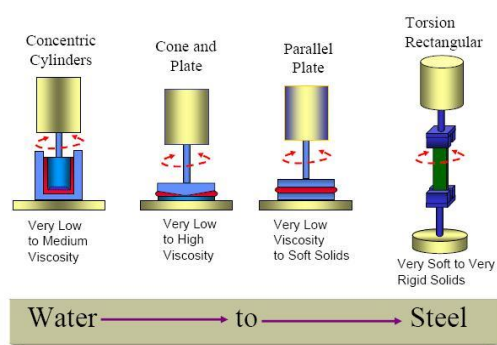
a pro gradient rychlosti platí

$$D = \frac{\omega}{\alpha},$$

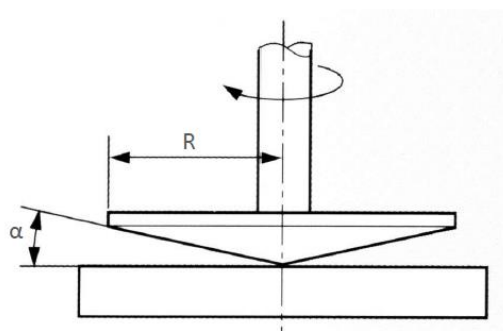
kde α je úhel zkosení v radiánech odpovídající štěrbině mezi deskou a kuželem (Obrázek 2).

Tokovou rovnicí neneutonských kapalin lze tedy tímto reometrem určovat přímo z naměřených závislostí momentu síly na úhlové rychlosti:

$$\eta = \frac{\tau}{D} = \frac{3M \cdot \alpha}{2\pi \cdot R \cdot \omega^3} = K \frac{M}{\omega}.$$



Obrázek 1. Typy geometrií [4].



Obrázek 2. Geometrie kužel-deska [5].

Měřicí metody

K měření využijeme rotační reometr ARES-G2 od TA Instruments. Toto zařízení se skládá s rotoru, který pohybuje se vzorkem a převodníku, který sleduje odezvu vzorku na jeho namáhání. Pro měření reologických vlastností polymerních PVA roztoků použijeme geometrie deska-kužel o průměru patice $d = 25$ mm a úhlu zkosení $\alpha = 2,3^\circ$. Pro každý vzorek provedeme měření jako závislost napětí na smykové rychlosti v rozmezí od $0,1$ do 100 s^{-1} a na úhlové rychlosti v rozmezí od 1 do $100 \text{ rad}\cdot\text{s}^{-1}$.

Úkoly měření

- 1) K manipulaci se vzorky, kolonou a dalším vybavením vždy používejte nitrilové rukavice.
- 2) Za dozoru vyučujícího připevněte patice (deska a kužel) do geometrií. Pro dotažení použijte imbusový klíč příslušné velikosti.
- 3) Zkontrolujte, zda je vypnutý rotor a vložte spodní geometrii (deska) a dotáhněte pomocí šroubu.
- 4) Zkontrolujte, zda je převodník nastaven na vysoký rozsah (high) a opatrně vložte horní geometrii (kužel) a dotáhněte pomocí šroubu.
- 5) Na spodní geometrii umístěte příslušné množství vzorku.
- 6) Nastavte vzdálenost mezi geometriemi tak, aby vzorek vyplňoval souvisle celý prostor mezi paticemi.
- 7) Nastavte experiment dle instrukcí vyučujícího.
- 8) Vyhodnoťte obdržaná data pomocí softwaru Trios.

Diskuse

Cílem měření je určit rozdíl viskozity u jednotlivých kompozitních PVA roztoků. Rozdíl mezi jejich viskozitami může přinést dodatečnou informaci o jejich vnitřní struktuře. PVA roztoky se modifikují různými látkami, aby výsledná membrána získala lepší vlastnosti. Zejména se jedná o větší mechanickou a tepelnou odolnost a lepší elektrické vlastnosti membrány [6].

Tvorba záznamu měření

Záznam měření musí obsahovat grafické zpracování výsledků.

Do záznamu o měření zpracujte následující otázky:

- 1) Uveďte, co se děje s viskozitou vzorku vlivem zvyšující se koncentrace přidané látky do PVA roztoku.
- 2) Pomocí zdroje [6] diskutujte, jak se mění vnitřní struktura roztoku vlivem koncentrace přidané látky.
- 3) Proč se pro měření polymerních roztoků používají geometrie deska-kužel. Jaké jiné typy geometrií by byly pro tyto roztoky vhodné?
- 4) Diskutujte a odhadněte možné chyby měření.

- 5) Popište rozdíl mezi newtonskými a neneutonskými kapalinami a uveďte alespoň čtyři příklady neneutonských kapalin.

Literatura

- [1] LARMINIE James, DICKS Andrew. Fuel Cell Systems Explained. 2nd ed. John Wiley & Sons Ltd, England: West Sussex, ©2003. ISBN 0-470-84857-X
- [2] MACOSKO Christopher W. Rheology: Principles, measurements and application. John Wiley & Sons, Inc, Canada, ©1994. ISBN 1-56081-579-5
- [3] HOLZAPFEL Gerhard A. Nonlinear solid mechanics: A continuum approach for engineering. John Wiley & Sons Ltd, England: West Sussex, ©2000. ISBN 0-471-82304-X
- [4] Instruments T. Rheology: Theory and Applications. 2010.
- [5] PragoLab. Seminář reologie. 2015
- [6] Chien, Hung-Chung, et al 2013 *J. Hydr. En.* **38** 13792

Measurement of the rheological properties of solutions for the preparation of modified poly (vinyl alcohol) (PVA) composite membranes using a rotary rheometer ARES-G2.

Introduction

Hydrophilic PVA membranes are used in many applications, but lately they have been widely utilized as polymer electrolyte membrane (PEM) for fuel cells. In order to design a good membrane many parameters are involved, such as the properties of casting solution, preparation conditions (temperature, relative humidity and time), reactants etc. The viscosity of the polymer solution plays a key role, which not only helps to fabricate membranes of specific thickness, but also prevents the formation of pinholes and membrane delamination. Therefore, the understanding of the rheological properties of casting solutions is important for preparing appropriate membranes for fuel cells [1].

Rheology examines how the influence of mechanical stress changes and transforms solids or also how liquids and gases flow. Rheology is a very broad field that extends into many other disciplines (civil engineering, mechanical engineering, metallurgy, glass, food, chemistry, geology, medicine, transportation, cosmetics etc.)

Liquids are substances which effect even a small external force permanently deformed - flow. The flow rate of the liquid is greater, the greater is the external force and the smaller are the internal forces that counteracts the flow. Internal forces (internal friction) are formed in the liquid as a result of thermal movement and intermolecular attractive forces. At low velocities of flow (laminar flow), the flow of fluid takes place as shear deformation, which characterizes the change of the material under shear (tangential) tension. At laminar flow of a real fluid is formed due to the intermolecular forces in the contact area of two layers moving at different speeds v the shear stress τ . According to Newton, the shear stress is directly proportional to the velocity gradient

$$\frac{dv}{dy}$$

i.e. increase of speed dv between two layers divided by the distance dy .

The following applies:

$$\tau = \eta \frac{dv}{dy},$$

where the proportionality constant η is called the dynamic viscosity.

Dynamic viscosity is characteristic of the material, it depends on temperature and pressure. For gases with a temperature is increasing, the case of liquids is decreasing [2-3].

The task of rheology is the experimental determination of the functional dependence between the shear stress and velocity gradient for the liquid sample, ie. dependence of viscosity on shear stress or velocity gradient.

The viscosity measurements are commonly used flow, falling and rotational rheometers.

For rotary rheometers sample is subjected to shear between two defined planes. One plate (rotor) rotating at constant angular velocity. Due to the internal friction of the fluid the torque transmitted to the second plate (transducer), where is torque measured electronically.

The most common types of rotary rheometers include the type composed of two coaxial cylinders between them is measured liquid, the type composed of a plate and cone or two parallel plates (Figure 1).

The relationship between shear stress τ and torque M is for ordering cone - plate with a base radius of the cone R given by equation

$$\tau = \frac{3M}{2\pi R^3}$$

and for the velocity gradient applies

$$D = \frac{\omega}{\alpha},$$

where α is the skew angle in radians corresponding to slot between the plate and the cone (Figure 2).

Flow equation non-Newtonian fluids is determined by rheometer directly from the measured dependence torque to angular velocity:

$$\eta = \frac{\tau}{D} = \frac{3M \cdot \alpha}{2\pi \cdot R \cdot \omega^3} = K \frac{M}{\omega}$$

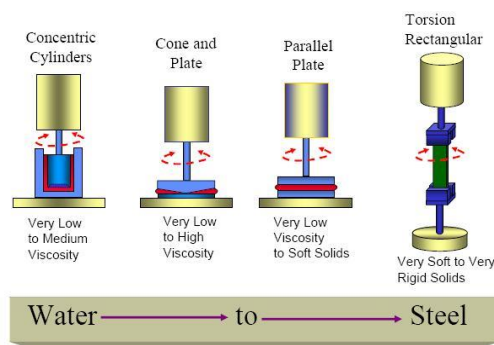


Figure 1. Geometry types [4].

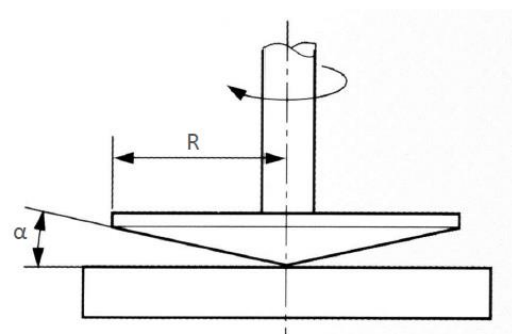


Figure 2. Cone and plate geometries [5].

Measurement methods

For the measurement we use rotational rheometer ARES-G2 from TA Instruments. This device consists of a rotor which moves with the sample and transducer, which monitors the response of the sample to the stress. For measuring the rheological properties of polymer PVA solutions we use cone-plate geometry with a diameter $d = 25$ mm and a skew angle $\alpha = 2.3^\circ$. For each sample, we perform the stress versus shear rate measurement in the range of 0.1 to 100 s^{-1} and the stress versus angular velocity in the range from 1 to $100 \text{ rad} \cdot \text{s}^{-1}$.

Tasks

- 1) For manipulation with samples, column and other equipment always use nitrile gloves.
- 2) For any supervision attach the plates (plate and cone) to geometries. For tightening use hexagon key of the appropriate size.
- 3) Make sure the rotor is turned off and insert the bottom geometry (plate) and tighten with the screw.
- 4) Make sure that the converter is set to a high range (high) and carefully insert the upper geometry (cone) and tighten with the screw.
- 5) Place on the bottom geometry the appropriate amount of sample.
- 6) Set the distance between the geometries so that the sample continuously fills the entire space between the plates.
- 7) Set the experiment according to the instructions of the teacher.
- 8) Evaluate received data using software Trios.

Discussion

The aim of measurement is to determine the difference in viscosity of different PVA composite solutions. The difference between their viscosities can provide additional information about their internal structure. PVA solutions are modified with various substances to obtain membrane with better properties. Especially the higher mechanical and thermal stability and better electrical properties of the membranes [6].

Creating measurement record

The protocol of measurement must contain a graphics processing results.

To the protocol process the following questions:

- 1) Identify what is happening with the viscosity of the sample due to increasing concentrations of substances added to the PVA solution.
- 2) Use literature [6] discuss how to change the internal structure of the solution due to the concentration of the additives.
- 3) Why is for the measurement of polymer solutions using cone and plane geometries. What other geometry types would be suitable for these solutions?
- 4) Discuss and assess possible measurement errors.
- 5) Describe the difference between Newtonian and non-Newtonian fluids and give at least four examples of non-Newtonian fluids.

Literature

- [1] LARMINIE James, DICKS Andrew. Fuel Cell Systems Explained. 2nd ed. John Wiley & Sons Ltd, England: West Sussex, ©2003. ISBN 0-470-84857-X
- [2] MACOSKO Christopher W. Rheology: Principles, measurements and application. John Wiley & Sons, Inc, Canada, ©1994. ISBN 1-56081-579-5
- [3] HOLZAPFEL Gerhard A. Nonlinear solid mechanics: A continuum approach for engineering. John Wiley & Sons Ltd, England: West Sussex, ©2000. ISBN 0-471-82304-X
- [4] Instruments T. Rheology: Theory and Applications. 2010.
- [5] PragoLab. Seminář reologie. 2015
- [6] Chien, Hung-Chung, et al 2013 *J. Hydr. En.* **38** 13792

Appendix 5 – Publications

1. Remiš, T. (2017, January). Rheological properties of poly (vinyl alcohol)(PVA) derived composite membranes for fuel cells. In *Journal of Physics: Conference Series* (Vol. 790, No. 1, p. 012027). IOP Publishing.
2. Tomáš, M., Remiš, T.: Role polymerních membrán v obnovitelných zdrojích energie. *PMFA* 62 (2), 2017, 121-128
3. Remiš, T., Dodda, J. M., Tomáš, M., Novotný, P., Bělský, P. (2016). Influence of polyfurfuryl alcohol (PFA) loading on the properties of Nafion composite membranes. *Journal of Macromolecular Science, Part A*, 53(12): 757-767.
4. Dodda, J. M., Remiš, T., Tomáš, M., Novotný, P. (2016). Effect of alternation of polyamide selective layers in the formation and performance of thin-film composite membranes. *Desalination and Water Treatment*, 57(19): 8720-8729.
5. Dodda, J. M., Bělský, P., Chmelař, J., Remiš, T., Smolná, K., Tomáš, M., Kadlec, J. (2015). Comparative study of PVA/SiO₂ and PVA/SiO₂/glutaraldehyde (GA) nanocomposite membranes prepared by single-step solution casting method. *Journal of materials science*, 50(19): 6477-6490.
6. Dodda, J. M., Remiš, T., Tomáš, M., Novotný, P. (2015). Thermal Cycloimidization Study of Polyimides and Poly (amide imide) s Synthesized from Low-Temperature Solution Polymerization. *Journal of Macromolecular Science, Part B*, 54(6): 629-648.